KATHOLIEKE UNIVERSITEIT LEUVEN
FACULTEIT INGENIEURSWETENSCHAPPEN
DEPARTEMENT WERKTUIGKUNDE
Kasteelpark Arenberg 1, B-3001 Leuven, Belgium

FACULTEIT BIO-INGENIEURSWETENSCHAPPEN
DEPARTEMENT BIOSYSTEMEN
Kasteelpark Arenberg 30, B-3001 Leuven, Belgium

ASSESSMENT AND IMPROVEMENT OF THE LOW-FREQUENCY VIBRATIONAL COMFORT ON AGRICULTURAL MACHINERY BY OPTIMIZED CABIN SUSPENSION

Promotoren:
Prof. dr. ir. H. Ramon
Prof. dr. ir. W. Desmet

Proefschrift voorgedragen
tot het behalen van het
doctoraat in de
ingenieurswetenschappen

door

Koen DEPREZ

April 2009

KATHOLIEKE UNIVERSITEIT LEUVEN
FACULTEIT INGENIEURSWETENSCHAPPEN
DEPARTEMENT WERKTUIGKUNDE
Kasteelpark Arenberg 1, B-3001 Leuven, Belgium

FACULTEIT BIO-INGENIEURSWETENSCHAPPEN
DEPARTEMENT BIOSYSTEMEN
Kasteelpark Arenberg 30, B-3001 Leuven, Belgium

ASSESSMENT AND IMPROVEMENT OF THE LOW-FREQUENCY VIBRATIONAL COMFORT ON AGRICULTURAL MACHINERY BY OPTIMIZED CABIN SUSPENSION

Examencommissie:
Prof. dr. ir. P. Van Houtte, voorzitter
Prof. dr. ir. H. Ramon, promotor
Prof. dr. ir. W. Desmet, promotor
Prof. dr. ir. J. De Baerdemaeker
Prof. dr. ir. A. de Boer, Universiteit Twente
Prof. dr. ir. P. Sas
Prof. dr. ir. J. Swevers
dr. ir. J. Anthonis, LMS International
dr. ir. I. Hostens, Agoria

Proefschrift voorgedragen
tot het behalen van het
doctoraat in de
ingenieurswetenschappen

door

Koen DEPREZ

UDC 631.3 April 2009

‘If more of us valued food and cheer and song above hoarded gold, it would be a merrier world.’

J. R. R. Tolkien, The Hobbit

D/2009/7515/42
ISBN 978-94-6018-059-0
UDC 631.3

Voorwoord

Een doctoraat maken is altijd een strijd. Gelukkig zijn er heel veel mensen die je tijdens dit gevecht op een of andere manier steunen. Bij het begin van dit boekje is het dan ook heel gepast om deze mensen te bedanken.

In het laatste jaar burgerlijk ingenieur kregen Marnix en ik de kans om ons eindwerk tussen de spuitbomen af te leggen in het labo voor landbouwwerktuigkunde. Het was de ideale opdracht voor twee industrieel ingenieurs die vooral het praktische nut van iets wilden zien, zonder al te veel in de theorie te blijven plakken. Na ons eindwerk, onder het promotorschap van prof. Herman Ramon, kregen we de kans om op het labo te blijven. Marnix had zijn hart echter al in Duitsland verloren, maar ik wou wel eens de cabinetrillingen onder handen nemen. Ik wil mijn promotor Herman Ramon bedanken voor de kansen die hij mij heeft gegeven en voor de vrijheid die je kreeg op het labo om je ten volle te ontplooien.

Ook mij andere promotor, prof. Wim Desmet, wil ik hartelijk danken om het promotorschap op zich te nemen. Ik was er één van bij de landbouw, maar dat maakte geen verschil. We hadden samen aan een project gewerkt en er een tijdens enkele nachtelijke uren samen één geschreven en dat maakte de drempel naar het PMA een stuk lager.

De andere leden van de doctoraatsjury , prof. Paul Van Houtte, prof. Josse De Baerdemaeker, prof. Jan Swevers, prof. Andre de Boer, prof. Paul Sas, dr. Jan Antonis en dr. Ivo Hostens, wil ik bedanken voor het lezen van het proefschrift en het geven van waardevolle opmerkingen. Daarvan wil ik er twee extra bedanken: Jan Anthonis en Josse De Baerdemaeker. Ik denk niet dat dit werk er zou gekomen zijn zonder jou, Jan. Dankzij jouw advies en aanporren ben ik er finaal geraakt. Ik heb een zalige tijd doorgebracht op het labo. De sfeer die er heerste was heel aangenaam en dit heeft veel te maken met zijn baas, Josse. Ik

hoop dat er nog nu en dan eens in het warmst van de zomer met wat labomankracht ijs wordt gemaakt.

Eigenlijk wil ik alle collega's van het labo danken. Toch wil ik er hier enkele met naam en toenaam vernoemen. Eerst en vooral zijn er mijn bureaugenoten: Dimitrios, Jan, Stijn, Cédric, Danny, Rene en Flies. De sfeer was altijd goed en helpende handen en geesten waren altijd in de buurt. Koen en Mieke moet ik bedanken voor de gezellige dinertjes. Volgens mij is het de volgende keer zeker aan Koen. Ik mag zeker ook "Das Bingo Verein"niet vergeten. Mireille, Els, Sandra, Pal en Veerle, we komen misschien niet zoveel meer samen als toen, maar het was en is altijd fijn om met jullie samen te zitten. Christel, Petula en Dirk, wil ik bedanken voor de ondersteuning. Jullie zorgden ervoor dat alles op tijd geregeld werd of het nu administratieve rompslomp was of het lassen van een kader.

Naast de mensen uit het labo wil ik ook enkele andere Leuvengangers bedanken die meer voor aangename tijden buiten het labo zorgend: Annemie, Iris, Katleen, Marie, Pieter, Ann en Ghil. Als de nood hoog was, dan kon er altijd stoom worden afgeblazen bij jullie. En zonder dat ze het misschien besteffen, ben ik heel wat judomaten dankbaar dat ik iedere week de kans kreeg om, als het nodig was, de frustraties van mij af te kloppen.

Het thuisfront is natuurlijk ook heel belangrijk. Pa en ma, ik denk dat ik heel gelukkig mag zijn met mijn moderne ouders. Mijn zus en ik kregen alle mogelijkheden om te studeren wat we graag wilden en hoewel jullie niet wisten wat ik in Leuven allemaal deed, hebben jullie er wel vertouwen in gehad dat alles wel op zijn pootjes terecht zou komen.

De laatste jaren is er een tweede thuisfront bijgekomen met schoonouders,schoonzussen en suikerwafels, maar vooral met Ingrid en Gwen. Ingrid, ik hoop dat de nachtelijke uurtjes werk nu eindelijk voorbij zullen zijn en dat jij en Gwen me niet meer zullen moeten delen met mijn doctoraat. Bedankt voor alles, ik kon me in mijn leven geen betere twee vrouwen wensen!

Koen Deprez, April 2009

Abstract

This work aims at the improvement of the low-frequency vibrational comfort on mobile agricultural machines. Assessment of the comfort situation on a combine harvester shows that the European action and limit values for low-frequency vibrational comfort are violated for several working conditions of the machine. The frequently used rubber cabin mounts have a deteriorating effect on the comfort of the operator in the low-frequency region.

Two alternative cabin mounts are designed consisting of hydraulic and pneumatic components. Non-linear parametric models based on first principles are derived and verified experimentally. Optimization of the model parameters is performed with respect to the objective comfort values effective root means square and vibration dose value. Alternatively the deviation for an ideal frequency response function is also proposed as goal to be minimized.

A six degree of freedom linear model of the cab suspension is derived. By incorporating linearized models of the cab mounts, predictions can be made of the resulting comfort values for the different working conditions. These predictions are verified by evaluation of the physical cabin suspension system on a hydraulic test rig. In-situ measured vibration signals are reproduced by the rig enabling the evaluation of the suspension under controlled lab conditions.

Beknopte Samenvatting

In dit proefschrift wordt het laagfrequent trillingscomfort op mobiele landbouwmachines aangepakt. Een evaluatie van het comfort op een maaidorser toont aan dat Europese actie- en limietwaardes voor dit laagfrequent trillingscomfort worden overschreden bij verschillende werkomstandigheden van de machine. De rubberen trillingsisolatoren die als cabineophanging worden gebruikt, hebben een negatief effect op het comfort van de bestuurder.

Twee alternatieve trillingsisolatoren opgebouwd uit hydraulische en pneumatische componenten worden ontwikkeld. De niet-lineaire parametrische modellen van deze trillingisolatoren zijn gebaseerd op fysische wetmatigheden. De correctheid van de modellen wordt experimenteel geverifieerd. Optimalisatie van de parameters in de modellen gebeurt vanuit het oogpunt een zo goed mogelijk comfortgedrag te realiseren. Optimalisatiecriteria worden zowel in het tijdsdomein als in het frequentiedomein gespecificeerd.

Gelineariseerde versies van de modellen van de isolatoren worden verwerkt in een model van de cabineophanging. Deze laat toe om het comfortgedrag van de nieuwe ophanging onder verschillende werkomstandigheden te voorspellen. Toetsing van deze voorspelling gebeurt met behulp van een hydraulische schudstand die in staat is opgemeten trillingssignalen te reproduceren. Dit laat toe om onder gecontroleerde labomstandigheden een evaluatie te doen van de cabineophanging bij verschillende werkomstandigheden van de machine.

Table of contents

List of Figures

List of Tables

Symbols

Variables

Chapters 2&3

$\sum$	:	combined VDV or effRMS values	
$\hat{x}$	:	average of x	
x_m	:	measured x value	
λ	:	transmissibility	
ω/ω_n	:	normalized frequency	
ζ	:	damping ratio	
H_1	:	FRF-estimator: response error minimized	
H_2	:	FRF-estimator: excitation error minimized	
H_{EV}	:	FRF-estimator: errors-in-variables	
$H(j\omega)$	:	frequency response function	
N, M	:	number of periods	
$W_{ij}(s)$	:	frequency weighing filter	
$X(j\omega)$	:	fourier coefficients of the periodic excitations	
$Y(j\omega)$	:	fourier coefficients of the steady-state response of a system	
$n_{xy}(j\omega)$	:	contribution of noise to fourier coefficients of excitation/response	
x	:	longitudinal or driving direction	
y	:	lateral direction	
z	:	vertical direction	
Δ_{static}	:	static deflection	$[m]$
ω_n	:	natural undamped frequency	$[rad/s]$
F	:	force input	$[N]$
RMS_{total}	:	multi-axial Root Mean Square	$[m/s^2]$
T_s	:	measurement period	$[s]$

VDV_{comb}	:	combined Vibration Dose Value	$[m/s^{1.75}]$
VDV_{total}	:	multi-axial Vibration Dose Value	$[m/s^{1.75}]$
VDV_{xyzs}	:	Vibration Dose Value on the seat in x/y/z direction	$[m/s^{1.75}]$
VDV_{xb}	:	Vibration Dose Value in the x direction on the backrest	$[m/s^{1.75}]$
a_{xyzw}	:	frequency weighted acceleration in x,y and z direction	$[m/s^2]$
a_{max}	:	maximum peak acceleration	$[m/s^2]$
a_w	:	frequency weighted acceleration	$[m/s^2]$
c_s	:	seat suspension damping coefficient	$[Ns/m]$
c_{tb}	:	tire/suspension damping coefficient	$[Ns/m]$
g	:	gravitational acceleration	$[N]$
k_{tb}	:	tire/suspension stiffness	$[N/m]$
k_s	:	seat suspension stiffness	$[N/m]$
m_{bw}	:	sprung/unsprung mass	$[kg]$
m_s	:	mass of the seat enlarged with portion of the mass of the driver	$[kg]$
z_{gwb}	:	ground/wheel/body displacement	$[m]$
z_s	:	seat displacement	$[m]$
$\ddot{z}_b$	:	body acceleration	$[m/s^2]$

Chapter 4

dx	:	infinitesimal change of x	
$\frac{d}{dt}$	:	time derivative	
Ω	:	ratio of natural frequencies	
κ	:	ratio of specific heats	
A_B	:	ordinate of point B	
D	:	constant	
s	:	Laplace varable	
Φ	:	work done by the system	$[J]$
ρ_i	:	fluid density i	$[kg/m^3]$
ρ_{i0}	:	initial density i	$[kg/m^3]$
A	:	surface of the air spring	$[m^2]$
A_c	:	effective area at 10 mm below design height	$[cm^3]$

A_e	:	effective area at 10 mm above design height	$[cm^3]$
C_p	:	specific heat at constant pressure	$[J/kgK]$
C_v	:	specific heat at constant volume	$[J/kgK]$
E	:	total internal energy inside the control volume	$[J]$
F	:	force	$[N]$
F_C	:	Coulomb friction	$[N]$
F_s	:	static friction	$[N]$
F_v	:	viscous friction	$[Ns/m]$
F_W	:	friction force	$[N]$
K	:	spring rate of an air spring	$[kN/m]$
P_g	:	pressure at design height of an air spring	$[Bar]$
Q_h	:	heat flow to the control volume	$[J]$
R	:	specific gas constant	$[J/kgK]$
R_F	:	linear flow resistance	$[sPa/kg]$
S	:	surface of the valve opening	$[m^2]$
S_{cyl}	:	surface of the piston	$[m^2]$
S_{rod}	:	surface of the rod	$[m^2]$
T	:	temperature	$[K]$
V	:	volume	$[m^3]$
V_c	:	internal volume at 10 mm below design height	$[cm^3]$
V_d	:	internal volume at design height	$[cm^3]$
V_e	:	internal volume at 10 mm above design height	$[cm^3]$
V_{i0}	:	initial volume i	$[m^3]$
f_B	:	abscissa of point B	$[Hz]$
f_S	:	natural frequency of the air spring	$[Hz]$
f_{SA}	:	natural frequency of the air spring combined with the auxiliary volume	$[Hz]$
g	:	gravitational acceleration	$[N]$
h	:	height of the spring	$[m]$
h	:	enthalpy of the fluid	$[J/kg]$
$\acute{h}$	:	total energy per unit of mass	$[J/kg]$
k	:	spring stiffness	$[N/m]$
k_S	:	spring stiffness of the air spring	$[N/m]$
k_{SA}	:	spring stiffness of the air spring combined with the auxiliary volume	$[N/m]$

m	:	mass	$[kg]$
$\dot{m}$	:	mass flow	$[kg/s]$
p_i	:	pressure i	$[Pa]$
p_{i0}	:	initial pressure i	$[Pa]$
u	:	internal energy	$[J/kg]$
v	:	fluid velocity	$[m/s]$
x, y	:	position	$[m]$
$\dot{x}, \dot{y}$	:	velocity	$[m/s]$
$\dot{x}_s$	:	empirical parameter	$[m/s]$
$\ddot{y}$	:	acceleration	$[m/s^2]$
z	:	elevation	$[m]$

Chapter 5

λ_{ij}	:	cosine of the angle between directions i and j	
i^T	:	transpose of matrix i	
C_i	:	damping matrix	
D	:	constant	
K_i	:	stiffness matrix	
M_i	:	mass matrix	
P, Q, R	:	frame linked to support	
X, Y, Z	:	cabin frame	
X_0, Y_0, Z_0	:	fixed inertial frame	
q	:	output matrix	
w	:	input matrix	
$\ddot{i}$	:	acceleration in i direction	$[m/s^2, rad/s^2]$
i_{out}	:	displacement of/ rotation about i of the cabin frame	$[m, rad]$
i_{in}	:	displacement of/ rotation about i of the inertial frame	$[m, rad]$
α	:	rotation about the x axis	$[rad]$
β	:	rotation about the y axis	$[rad]$
δ	:	angle	$[rad]$
γ	:	rotation about the z axis	$[rad]$
I_{ij}	:	moment/product of inertia	$[kgm^2]$
F_i	:	force in i direction	$[N]$
M_i	:	moment about i direction	$[Nm]$

a_i	:	distance between support and center of gravity of the cabin in the i direction	$[m]$
c_{ij}	:	damping relation between force in the i direction and velocity in the j direction	$[Ns/m]$
k_{ij}	:	spring stiffness relation between force in the i direction and displacement in the j direction	$[N/m]$
k^t	:	torsional stiffness	$[Nm/rad]$
x	:	displacement in longitudinal or driving direction	$[m]$
y	:	displacement in lateral direction	$[m]$
z	:	displacement in vertical direction	$[m]$

Chapter 6&7

$\mathbb{R}$	:	set of all real numbers	
A_k	:	desired magnitude at frequency line k	
B_k	:	measured magnitude at frequency line k	
$DIFF$	:	deviation from ideal FRF	
$Drives$	:	FFT of the drive signals	
K	:	number of frequency lines	
N	:	number of measurements	
$Targets$	:	FFT of the target signals	
W_k	:	weighing factor at frequency line k	
i	:	index	
$f(x)$	:	objective function	
$minf(x)$	:	minimum of function f(x)	
l	:	lower bound of x	
u	:	upper bound of x	
x	:	parameter vector	
S	:	surface of the valve	$[m^2]$
V_i	:	volume of the accumulator	$[m^3]$
e	:	error between target and response	$[m/s^2]$
i	:	index	
p_i	:	pressure i	$[Pa]$
r	:	response acceleration	$[m/s^2]$
t	:	target acceleration	$[m/s^2]$

Appendices

$\mathbb{R}$	:	set of all real numbers	
$\varnothing$	:	empty set	
A_1, A_2	:	coefficient matrix	
D	:	subset	
K	:	Lipschitz constant	
T	:	objective function	
(X, B)	:	coordinates of the intersection	
Z	:	solution matrix	
a_i, b_i	:	endpoints of interval i	
b_1, b_2, c	:	coefficient vector	
$f(c_i)$	:	function evaluated in the middle of interval i	
$f(x)$	:	objective function	
$f(x')$	:	function evaluated in x'	
$minf(x)$	:	minimum of function f(x)	
$g(y, x)$	:	inequalities in x and y	
$h(y, x)$	:	equalities in x and y	
i, j	:	index	
l	:	lower bound of x	
m_1	:	number of equality constraints	
m_2	:	number of inequality constraints	
n	:	number of equations	
u	:	upper bound of x	
x	:	parameter vector	
x'	:	parameter vector	
y	:	binary variable vector	
β	:	damping constant of the passive part	$[Ns/m]$
β_{SA}	:	damping constant of the semi-active part	$[Ns/m]$
F_D	:	damping force	$[Ns/m]$
$\dot{x}$	:	input velocity	$[m/s]$
$\dot{y}$	:	output velocity	$[m/s]$

Abbreviations

BS	:	British Standards Institution
DOF	:	Degrees Of Freedom
EA	:	Evolutionary Algorithm

$ETFE$	:	Empirical Transfer Function Estimate	
FRF	:	Frequency Response Function	
$GAOT$	:	Genetic Algorithm OpTimization	
ISO	:	International Organization for Standardization	
LBP	:	Low Back Pain	
LQG	:	Linear Quadratic Gaussian control	
LQR	:	Linear Quadratic Regulator	
$MINLP$	:	Mixed-Integer NonLinear Programming	
$MIMO$	:	Multiple Input, Multiple Output	
MIP	:	Mixed-Integer Programming	
NP	:	Nondeterministic Polynomial time	
PI	:	Proportional Integral control	
PID	:	Proportional Integral and Derivative control	
PSD	:	Power Spectral Density	
RMS	:	Root Mean Square	
SA	:	Simulated Annealing	
$SISO$	:	Single Input, Single Output	
TWR	:	Time Waveform Replication monitor	
WBV	:	Whole-Body Vibration	
VDV	:	Vibration Dose Value	$[m/s^{1.75}]$
$effRMS$	:	Root Mean Square of frequency weighted signal	$[m/s^2]$

Ontwikkeling van een geoptimaliseerde cabineophanging voor het verbeteren van het laagfrequent trillingscomfort op mobiele landbouwvoertuigen

I Inleiding

Overal op onze wereldbol worden alle levende wezens blootgesteld aan verschillende vormen van trillingen. Sommige zijn aangenaam zoals iemand de hand schudden of op een kermisattractie zitten. Andere zijn heel onprettig, denk maar aan de mensen die moeten werken met een pneumatische hamer of die dicht bij een luchthaven wonen. Dit proefschrift concentreert zich op een onaangenaam effect, namelijk de blootstelling aan algehele lichaamstrillingen van de bestuurders van mobiele landbouwmachines. De doelstelling van dit werk is het verbeteren van het comfort door de ontwikkeling van een geoptimaliseerde cabineophanging.

II Comfort op mobiele landbouwmachines

II.1 Laagfrequent trillingscomfort

Lage rugpijn wordt beschouwd als een van de belangrijkste medische klachten in de geïndustrialiseerde wereld. De oorzaak van deze klachten is heel moeilijk te achterhalen omdat heel veel factoren een rol spelen: anatomische, industriële en omgevingsfactoren. Van alle factoren die van belang zijn, wordt aangenomen dat algehele lichaamstrillingen de belangrijkste, met het werk gerelateerde risicofactor is. Ze worden veroorzaakt door het trillen van het oppervlak waarop een lichaam zit, ligt of staat. Het gaat meestal om trillingen tussen de 0.5 en 100 Hz met amplitudes van 0.01 tot 10 m/s^2. Deze algehele lichaamstrillingen zijn vooral te vinden bij verschillende transportmiddelen: trein, auto, vrachtwagens, tractoren, graafmachines, ... Ondanks de vele epidemiologische studies is tot op heden nog geen direct verband gevonden tussen de hoeveelheid trillingen waaraan iemand wordt blootgesteld en de zwaarte van de rugklachten. Algemeen wordt echter wel aanvaard dat een vermindering van algehele lichaamstrillingen een positief effect op het voorkomen van lage rugpijn heeft. Onderzoek toont ook aan dat mensen die in de landbouwsector actief zijn, gemiddeld aan hogere dosissen algehele lichaamstrillingen worden blootgesteld. Het trillingsniveau bij tractoren en mobiele landbouwmachines ligt gevoelig hoger dan bij doorsnee wegtransport.

Meten hoe comfortabel een bestuurder zich voelt in een bepaald voertuig, is vrij complex omdat comfort afhangt van heel veel verschillende factoren. Naast trillingen heeft wat men ziet, hoort of ruikt een invloed op het comfortgevoel en zal bijvoorbeeld een volle of lege maag ook een effect hebben. In dit proefschrift wordt alleen rekening gehouden met het laagfrequent trillingscomfort en worden meetstandaarden (ISO2631 en BS6841) enkel als vergelijkingsbasis gebruikt om de effectiviteit van de cabineophanging te checken. De objectieve comfortwaardes, "effective root mean square"(effRMS) en "vibration dose value"(VDV) worden hier gebruikt. Het zijn ook deze waardes die de Europese richtlijn over de blootstelling aan trillingen hanteert. Deze richtlijn legt de dagelijkse limietwaarde vast op een effRMS van 1.15 m/s^2 en een VDV van 21 $m/s^{1.75}$. Deze waardes worden gemeten ter hoogte van de zetel en mogen binnen een arbeidsperiode van 8 uur niet overschreden worden. Vanaf een effRMS van 0.5 m/s^2 en een VDV van 9.1 $m/s^{1.75}$, de zogenaamde actiewaardes, moet een plan voor de

verbetering van de werkomstandigheden worden opgesteld. Om niet uit de markt te worden geconcurreerd, zullen producenten van mobiele landbouwmachines inspanningen moeten leveren om deze actiewaardes te vermijden.

II.2 Comfortverbeterende ophangingen bij mobiele landbouwmachines

Bij mobiele landbouwmachines zijn er ruwweg vier plaatsen waar ingegrepen kan worden om het comfort van de bestuurder te verbeteren: de banden, de wielophanging, de cabine en de zetel. Alle landbouwmachines zijn uitgerust met lage druk banden die als laagdoorlaat filter fungeren voor de oneffenheden van de weg of het veld. In veel gevallen is dit de enige ophanging die aanwezig is op mobiele landbouwvoertuigen. Om hier een sterke comfortverbetering te realiseren zouden de banden 5 tot 10 keer meer trillingsenergie moeten absorberen. Dit zou ze nog groter en zachter maken, wat dan nefaste gevolgen heeft voor de levensduur van de banden omdat de rolweerstand verhoogt.

Op gebied van wielophangingen, ook wel primaire ophanging genoemd, zijn de meest geavanceerde systemen terug te vinden in de automobielsector. De ophanging is daar verantwoordelijk voor zowel comfort als veiligheid. De veren en dempers hebben echter een beperkte ruimte (slag) waarbinnen dit gerealiseerd moet worden, daarom ruimen de zuiver passieve systemen hier plaats voor semiactieve en actieve varianten.

99% van de landbouwtractoren hebben geen primaire ophanging en bij mobiele landbouwmachines zoals aardappelrooiers of maaidorsers wordt deze niet toegepast. De oorzaken zijn vooral het gevaar voor verlies aan stabiliteit bij het werken op een hellend veld, het grote verlies aan energie door dissipatie in de dempers en de complexiteit en kostprijs voor het realiseren van een primaire ophanging bij deze zware machines. Bij landbouwtractoren is er wel een trend naar het gebruik van een voorasophanging bij de "high-end"modellen. Tractoren met zowel voor- als achterasophanging zij uitzonderlijk. Deze worden vooral voor transportdoeleinden ingezet. De nood aan hogere productiecapaciteit zullen er echter voor zorgen dat bij mobiele landbouwmachines primaire ophangingen ook hun intrede zullen doen.

De zetel is de eerste secundaire ophanging die bij trucks, tractoren en mobiele landbouwvoertuigen wordt gebruikt. In de meeste gevallen

bestaat die uit een pneumatisch geveerd en hydraulisch gedempt systeem. Recente trend is wel naar het gebruik voor een semiactieve variant van deze passieve ophanging. Ook actieve zetelophangingen verschijnen op de markt.

Wat betreft cabineophangingen, de tweede secundaire ophanging, moet een onderscheid gemaakt worden tussen cabineophangingen die bestaan uit rubberen blokken en laagfrequente twee- of vierpunts mechanische ophangingen. Deze laatste worden vooral bij landbouwtractoren toegepast, terwijl mobiele landbouwmachines vooral van het eerste type cabineophanging gebruik maken. Het voordeel van een cabineophanging ten opzichte van een goedwerkende zetelophanging is dat er bij de zetel een faseverschil ontstaat tussen de beweging van het zitvlak en de beweging van de voeten, wat leidt tot een groot discomfort. Gebruik maken van een stijve of geen zetelophanging en een adequate cabineophanging is een veel betere optie en heeft het voordeel dat niet alleen de trillingen in de verticale richting kunnen worden aangepakt, maar ook trillingen in de andere.

Onderzoek naar het toepassen van een laagfrequente mechanische cabineophanging op mobiele landbouwvoertuigen beperkt zich tot twee instituten: het VTT technische onderzoekscentrum van Finland en het landbouwkundige departement van de Zweedse universiteit. In Finland beperkte het onderzoek zich echter tot 2 vrijheidsgraden (rol en verticaal). In Zweden werd via genetische algoritmes een geoptimaliseerde hydropneumatische ophanging ontwikkeld, die in het verdere onderzoek ook voorzien werd van actieve componenten. Alles gebeurde louter door simulaties en zonder de resultaten te checken in een fysische opstelling. Op gebied van cabineophanging bij mobiele landbouwvoertuigen is dus nog onderzoek en ontwikkeling noodzakelijk.

III Evaluatie van het huidige comfort op mobiele landbouwvoertuigen

III.1 De maaidorser

Al het onderzoek wordt verricht op een New Holland CX 820 maaidorser, uitgerust met lage druk banden en een pneumatisch geveerde zetel. Er is geen primaire ophanging, wat standaard is bij mobiele landbouwmachines. Aangezien alle mobiele landbouwmachines zich pakweg hetzelfde gedragen wat betreft trillingen, zijn de con-

clusies die hier getrokken worden overdraagbaar naar andere mobiele landbouwvoertuigen. Naast trillingen die afkomstig zijn van het rijden op het veld of de weg zijn ook heel wat trillingen afkomstig van bewegende onderdelen in de machine. Die geven aanleiding tot trillingen op specifieke frequenties. Modale analyse toont aan dat met betrekking tot laagfrequente trillingen, de cabine als een rigid body mag worden beschouwd.

III.2 Eigenschappen van de inkomende trillingen

Een eerste stap in de evaluatie van de huidige comfortsituatie op de maaidorser is het bepalen van de eigenschappen van de trillingen waaraan de cabineophanging wordt blootgesteld. Daarvoor worden de trillingen gemeten op de dragende structuur van de maaidorser waar de cabine op is bevestigd. Dit wordt gedaan onder diverse omstandigheden: stationaire toestanden, tijdens het oogsten en tijdens transport tussen twee velden. Achttien frequent in de praktijk voorkomende toestanden worden hier opgemeten en geanalyseerd. Analyse in het frequentiedomein toont aan dat bij stationaire regimes van de machine het gemiddelde trillingsniveau vrij laag is en dat specifieke frequentiepieken, overeenkomend met de bewegende onderdelen in de reinigingssectoren van de maaidorser, duidelijk zichtbaar zijn. Het gemiddelde trillingsniveau stijgt met 30 dB als stationaire condities vergeleken worden met een oogstconditie. Bij de oogstcondities wordt ook de invloed van het veld zichtbaar door het ontstaan van een verhoogd trillingsniveau rond 2 Hz, onafhankelijk van de snelheid, en een snelheidsafhankelijke verhoging van het trillingsniveau. Dit effect is nog explicieter zichtbaar bij de transportcondities. Om uit deze data af te leiden welke condities nu het meest oncomfortabel zijn, wordt gebruik gemaakt van de effRMS en VDV waardes. Deze tonen aan dat de comfortcondities behoorlijk slecht zijn, vooral in de verticale richting en bij transport op de weg.

III.3 Evaluatie van de cabineophanging

Als diezelfde objectieve comfort waardes worden uitgerekend in de cabine, dan is er een significante verhoging van de comfortwaardes, wat dus voor een minder comfortabele situatie zorgt. De rubberen blokken die nu de ophanging uitmaken, zijn hiervoor verantwoordelijk. Deze zorgen in het laagfrequente gebied voor een versterking van de

trillingen. Er moet dus naar alternatieve trillingsisolatoren worden gezocht.

IV Ontwikkeling van trillingsisolatoren voor de cabine

IV.1 Introductie

Trillingsreductie met een tweede orde massa-veer-dempersysteem is maar mogelijk vanaf $\sqrt{2}$ keer de eigenfrequentie van het systeem. Om adequate trillingsisolatoren te vinden, zullen hier systemen gezocht moeten worden met een eigenfrequentie rond 1 à 1.5 Hz omdat de eerste serieuze piek in het spectrum van de inkomende trillingen bij 2 Hz ligt. Om deze lage eigenfrequentie te realiseren kan gebruik gemaakt worden van luchtveren of van een systeem met accumulatoren.

IV.2 De hydropneumatische ophanging

Deze hydropneumatische ophanging bestaat uit een hydraulische, dubbelwerkende cilinder met lage wrijving die aan beide zijden verbonden wordt met een accumulator. Deze accumulatoren moeten voor de verende werking zorgen terwijl een klep in de verbinding tussen de cilinder en één van de accu's zorgt voor de demping. Door gebruik te maken van enkele fysische wetten die onder andere het gedrag van de stikstof in de accu's en de wrijving van de zuiger in de cilinder beschrijven, kan een model worden opgesteld van dit systeem. Metingen tonen aan dat het niet-lineaire model nauw aansluit bij het werkelijke gedrag van een gebouwde opstelling. Dit systeem beschikt over de vereiste lage eigenfrequentie en een lage versterking van deze eigenfrequentie, maar is vrij duur in vergelijking met de rubberen elementen. Het is ook niet in te bouwen in het huidige ontwerp van de maaidorser en er zijn 6 dergelijke systemen vereist voor een volledige cabineophanging.

IV.3 De pneumatische ophanging

Het hydropneumatische systeem schiet tekort op gebied van inbouwmogelijkheden en kostprijs. Daarom wordt in het pneumatische systeem gewerkt met een luchtbalg, de *Firestone Airmount 1M1A-1*, die een inbouwhoogte van 75 mm heeft en een veel lagere kostprijs. Deze luchtbalg heeft een natuurlijke eigenfrequentie van 2.8 Hz, wat veel

te hoog is om als isolator te kunnen fungeren. Daarom wordt deze balg gekoppeld met een expansievolume om de eigenfrequentie ervan te verlagen. Een klep in het verbindingsstuk tussen de balg en het expansievolume zorgt voor de demping in het systeem.

Het model wordt afgeleid door gebruik te maken van thermodynamica van open systemen, de balg te beschouwen als cilindrisch en de lucht als een ideaal gas voor te stellen. Dit levert na enig rekenwerk de niet-lineaire vergelijking op van dit systeem. Indien de doorstroomopening van de klep klein wordt genomen, dan heeft dit systeem een natuurlijke eigenfrequentie die overeenkomt met die van de balg. Als de doorstroomopening groot wordt genomen, dan is de eigenfrequentie die van een balg met dezelfde oppervlakte als de gebruikte balg maar met een volume gelijk aan de som van het volume van de balg en van het expansievat. Dit resulteert in een veel lagere eigenfrequentie.

Alle instellingen van de klep leveren een systeem op dat qua amplitudeverloop in het frequentiedomein door één voor alle grafieken gemeenschappelijk punt loopt. Dit is gelegen tussen de eigenfrequentie van de balg en die van de balg in combinatie met het expansievat. De amplitude van dit punt wordt kleiner naar mate de afstand tussen beide eigenfrequenties vergroot. Een groot expansievolume geeft dus aanleiding tot een lage versterking. Met een goede instelling van de klep is het mogelijk om de natuurlijke eigenfrequentie op dit gemeenschappelijke punt te leggen, wat ervoor zorgt dat de versterking op eigenfrequentie wordt geminimaliseerd. Een linearisatie van dit systeem levert een derde orde systeem op en een wiskundige formulering van het gemeenschappelijke punt op de grafiek van de amplitudes.

Metingen op een testopstelling tonen aan dat er een goede overeenstemming is tussen het model en de werkelijkheid. Enkel de eigenfrequentie van de balg, gecombineerd met het expansievolume ligt iets hoger dan voorspeld door het model omdat de invloed van het rubber van de balg werd verwaarloosd. Wegens de inbouwmogelijkheden van het systeem, de relatief lage kostprijs en het goede gedrag in het laagfrequente trillingsgebied, zullen deze elementen gebruikt worden in de verdere ontwikkeling van de cabineophanging.

V Ontwikkeling van een cabinemodel met meerdere vrijheidsgraden

Analyse van de trillingen waaraan een cabine wordt blootgesteld, toont aan dat het wenselijk is om in meerdere vrijheidsgraden tot trillingsreductie te komen. Een lineaire model wordt hier opgebouwd om het effect van de nieuwe trillingsisolatoren op de zes vrijheidsgraden van de cabine te voorspellen.

V.1 Theoretisch model

De cabine wordt als stijf verondersteld en door middel van de wet van Newton worden de bewegingen vastgelegd. De krachten en momenten die aangrijpen op de cabine ontstaan in de trillingsisolatoren. Door positie- en snelheidsverschillen tussen de eindpunten van deze elementen ontstaan de veer- en demperkrachten. Een luchtbalg heeft echter niet enkel veer- en demperkarakteristieken in één richting. Ook de torsie-eigenschappen van het rubber moeten in rekening worden gebracht.

V.2 Validatie

Het valideren van het model gebeurt aan de hand van een testopstelling. Die bestaat uit een ijzeren plaat die door middel van vier luchtbalgen wordt ondersteund. Die balgen staan onder een hoek van 45° met de verticale om toe te laten om in 6 vrijheidsgraden voor trillingsreductie te zorgen. Het model is in staat om de eigenfrequenties van de zes "rigid body"modes nauwkeurig te voorspellen. Tijdens de validatie werd wel duidelijk dat het gebruik van luchtbalgen onder een helling tot instabiliteit kan leiden. Daarom worden de luchtbalgen in de uiteindelijke opstelling verticaal geplaatst.

V.3 Praktische implementatie van het lineaire model

In het meerdere vrijheidsgraden model wordt het lineaire model van de pneumatische trillingsisolatoren ingebracht. De massa-, dempings- en stijfheidsmatrices worden aangepast. Met behulp van dit model worden er voorspellingen gedaan van de comfortwaardes voor de nieuwe ophanging.

VI Optimalisatie van niet-lineaire ophangingen

VI.1 Opstellen van de procedure

Dit werk stelt een optimalisatieprocedure voor die gebruik maakt van opgemeten trillingssignalen, met als voordeel dat niet-lineaire modellen ook kunnen worden geoptimaliseerd. Zo wordt een reële bedrijfstoestand gecreëerd waarbij het model in de optimalisatie net zo gaat reageren als in de werkelijkheid. Als functies om te minimaliseren worden de objectieve comfortwaardes gebruikt, maar ook een formulering die de afwijking van de ideale frequentie response functie beschrijft. Er wordt een globale optimalisatietechniek gebruikt omdat de functie heel veel lokale minima heeft.

VI.2 Toepassing op de hydropneumatische isolator

Deze procedure toepassen op het model van een hydropneumatische element levert, afhankelijk van het inputsignaal en afhankelijk van het gebruik van de comfortwaardes of van de formulering met de frequentie respons functie, verschillende optimale resultaten op. De comfortwaardes zorgen voor systemen met een lage eigenfrequentie. Trage schommelingen leveren namelijk weinig versnellingen op, maar kunnen leiden tot een gevoel van zeeziekte. Bij het gebruiken van de frequentie response functie kan dit vermeden worden.

VII Evaluatie van de cabineophanging

VII.1 Het evaluatieplatform

Voor de evaluatie van de pneumatische cabineophanging wordt gebruik gemaakt van een zes assige schudtafel. Deze hydraulische schudtafel wordt door middel van Time Waveform Replication Monitor software zo aangestuurd dat de trillingen, opgemeten tijdens de verschillende werkcondities voor de maaidorser, kunnen worden nagebootst. Dit heeft als voordeel dat de ophanging in een labo kan worden getest i.p.v. gebruikt te moeten maken van heel dure testen met een echte machine. Het evaluatieplatform is in staat om heel nauwkeurig de trillingen tijdens het oogsten na te bootsen. Voor de trillingen bij het transport op de weg zijn de trillingen in de verticale richting vrij

accuraat. De trillingen in het horizontale vlak zijn een stuk minder nauwkeurig, maar voldoen nog aan de eisen. De oorzaak voor het verschil in nauwkeurigheid heeft met de configuratie van de schudtafel te maken.

VII.2 Evaluatie van de ophanging

Voor de evaluatie van de ophanging wordt deze opgebouwd op de schudtafel. De verschillende trillingen worden aangelegd en een meting van het verschil tussen de aangelegde trillingen en de trillingen in de cabine geven de efficiëntie van de ophanging aan.

Voor alle vrijheidsgraden, wordt een verbetering van het comfort gerealiseerd. In sommige gevallen zelfs boven de 50 %. Hoewel de luchtbalgen vertikaal werden gemonteerd, is de verbetering in het horizontale vlak, toch vrij goed. Tijdens het oogsten en transport bij relatief lage snelheden worden de actiewaardes vermeden. Enkel bij transport op hoge snelheden blijven de verticale trillingen boven het actieniveau van de Europese Commissie. Dit heeft vooral te maken met de beperkte slag van de balgen, waardoor frequent de eindbuffers worden aangestoten. Dit zorgt voor bijkomende trillingen. Hierbij moet worden opgemerkt dat hier enkel naar de cabineophanging wordt gekeken en dat de zetelophanging in verticale richting ook nog voor een reductie van trillingen kan zorgen.

VIII Conclusies en verder werk

Dit werk heeft een commercieel bruikbare cabineophanging ontwikkeld om het laagfrequent trillingscomfort op mobiele landbouwvoertuigen te verbeteren. Een maaidorser werd als studieobject gebruikt en aangezien alle mobiele landbouwvoertuigen ongeveer een gelijkaardig gedrag vertonen in het laagfrequent trillingsgebied, zijn de resultaten overdraagbaar.

De ophanging maakt gebruik van luchtbalgen, die vrij goedkoop zijn en in het huidige design de plaats van de rubberen isolatoren kunnen innemen. Om de eigenfrequentie van de balg te verlagen, wordt die gekoppeld aan een expansievat. Om de demping te verhogen, wordt een klep in het verbindingstuk tussen balg en vat geplaatst. Er wordt een verbetering van de objectieve comfortwaardes gerealiseerd tot 50 %. Enkel wat de verticale richting tijdens het transport bij hoge snelhe-

den betreft, worden de actiewaardes van de Europese Commissie nog overschreden. Dit omdat de balgen maar een beperkte slag hadden.

Omdat de ophanging enkel op een hydraulische schudtafel is geëvalueerd, is het realiseren van de ophanging op een echte machine één van de nog uit te voeren taken. Het probleem van de beperkte slag van de balgen moet ook worden aangepakt. Dit kan door een primaire ophanging te voorzien, maar een goede optimalisatie van zetel en cabine samen kan ook een stap in de goede richting zijn.

Chapter 1

Introduction

The world is a vibrating one and every living creature gets exposed to many forms of vibrations in its every day life. Some of those are a nuisance, ask it to persons living near an airport or having to work every day with a pneumatic hammer. Others have a devastating effect like the earthquake in the eastern part of Sichuan, China, in May 2008 causing nearly 90,000 deaths. But vibrations can also be pleasant like a handshake as a means of expressing friendship or be a source of excitement at the fairground, on surf-boards or in motor racing [56]. Good effects of vibrations are also used by physiotherapists to help clear the lungs of their patients and to train muscles for maximal strength and flexibility in sports [74].

This research concentrates upon an unwanted effect of vibration, the exposure to whole body vibration on mobile agricultural machinery. The main objective of this thesis is *the development of a cabin suspension system to improve the vibrational comfort on mobile agricultural machinery.* In this work a combine harvester is used as a case study.

The following section states the research objective of this thesis while section 1.2 points out the main contributions of this work and section 1.3 gives an overview of the different chapters. This introductory chapter finishes with a list of published results in international journals and proceedings of international conferences.

1.1 Objective for this Research

Based on measurements performed by others and in this thesis it is clear that the comfort situation on large mobile agricultural machines is rather poor. European directive [5] on the minimum health and safety requirements regarding the exposure of workers to risks arising from physical agents (vibration), put certain limit and action values for the daily exposure to vibrations forward. Following this directive it is problematic to operate the harvester under investigation, a New Holland CX820 combine, for longer periods in the field. Knowing that during harvesting time these machines operate more than 12 hours a day, the main objective of this research is to drastically reduce the whole body vibrations the operator is exposed to.

The large mass of the machine and the necessary operating conditions make it very difficult to apply a primary suspension, making secondary cab and seat suspensions the only available means to improve the comfort. Seat suspension systems have already been investigated, commercial systems are available and are used on mobile agricultural machines. Concerning cab suspension systems, some investigations have been made but no proven concepts were shown and no commercial solutions are available for large mobile machinery. Therefore this thesis will investigate possible cab suspension systems and prove their effectiveness under real conditions.

To make a new suspension concept commercially viable, it should be relatively cheap and it would be favorable if it would fit in the same space that is provided for the currently used rubber mounts. In that way the changes to the cabin and the supporting structure are minor which makes the new suspension interchangeable with the current solution.

1.2 Main Contributions

The main contribution of this thesis is the development and evaluation of a commercially viable cab suspension for large mobile agricultural machinery. In the process of development other contributions were made:

- A summary of the research performed in the area of low frequency vibrational comfort and the generally acknowledged methods to measure this comfort.

- An overview of the suspension systems used on agricultural machinery to improve drivers' comfort, with an emphasis on the cab suspension developments.
- A comfort analysis on a New Holland CX820 combine harvester by performing measurements and evaluation in time and frequency domain.
- The development of a non-linear white box model of a hydropneumatic suspension element using thermodynamic laws, incorporating stick-slip behavior.
- The development of a non-linear white box model describing the behavior of an air spring connected to an auxiliary reservoir using thermodynamic laws of open systems.
- A multi dimensional cab suspension model able to predict the behavior of new designs.
- An optimization procedure using in-situ measurements to find the optimal behavior of non-linear suspension systems.
- The evaluation of the pneumatic cab suspension under real conditions, using an electro-hydraulic shaker and Time Waveform Replication monitor.

1.3 Chapter by chapter overview

1.3.1 Chapter 2 - Comfort on mobile agricultural machines

This chapter gives an overview of the literature on low frequency vibrational comfort and describes the tools used to evaluate the vibrational comfort as studied in this thesis. The comfort improving suspension systems used on mobile agricultural machines are presented with special attention for the former research done on cab suspension systems.

1.3.2 Chapter 3 - Assessment of the vibrational comfort

Due to the fact that all mobile agricultural machines suffer form the same issues of low frequency vibrational discomfort occur and that their behavior regarding vibrations is very similar, all research in this thesis

is performed on a combine harvester. To set realistic goals for the suspension system under development, the low frequency behavior of the combine harvester is monitored under various conditions. Frequency and time domain analysis are performed on the data and the current cab suspension system of rubber blocks is evaluated.

1.3.3 Chapter 4 - Development of vibration reducing cab mounts

Two vibration reducing cab mounts are developed in this chapter, a hydro-pneumatic and a pneumatic cab mount. Analytic models of both devices are derived and checked with real physical setups. A model based on first principles shows good resemblance for both the hydro-pneumatic cab mount and the pneumatic cab mount.

1.3.4 Chapter 5 - Design of a multi dimensional cab suspension

Based on the pneumatic cab mount a multi dimensional cab suspension is designed. A model is made that predicts the natural frequencies of the six rigid body modes of the cabin. This model is used to simulate the behavior of the new suspension design under real conditions. A prediction is made of the comfort values this suspension will attain.

1.3.5 Chapter 6 - Optimization of non-linear suspension models

This chapter explains an optimization method that uses in-situ measurements to optimize non-linear models. The method makes it possible to set objectives in time and frequency domain. The method is applied to the non-linear analytic model of a hydro-pneumatic suspension element.

1.3.6 Chapter 7 - Evaluation of the cab suspension

The final stage in the development of a cab suspension system is the evaluation of the proposed solutions. For that purpose an evaluation platform is set up using a six degree of freedom electro-hydraulic shaker driven by Time Waveform Replicator software to reproduce measured

in-situ vibration signals. On this platform the pneumatic suspension system is evaluated.

1.3.7 Chapter 8 - General conclusions and future perspectives

This final chapter summaries the main contributions of this thesis and proposes some future research.

1.3.8 Appendix A - Global optimization

This appendix gives an overview of some of the available global optimization tools and gives a thorough description of DIRECT, a branch and bound technique used in the optimization chapter of this thesis.

1.3.9 Appendix B - Semi-active suspension

This second appendix describes the use of semi-active control on the hydro-pneumatic suspension system.

1.4 Publications

During the study several results have been published in journals and have been presented at international conferences. A list of publications is given below.

1.4.1 International journals

K. Deprez, J. Anthonis, H. Ramon, H Van Brussel. Development of a Slow Active Suspension for Stabilising the Roll of Spray Booms. Part 1: Hybrid Modelling. *Biosystems Engineering*, 81(2), pp.185-191, 2002.

K. Deprez, J. Anthonis, H. Ramon, H Van Brussel. Development of a Slow Active Suspension for Stabilising the Roll of Spray Booms. Part 2: Controller Design. *Biosystems Engineering*, 81(3), pp.273-279, 2002.

J. Anthonis, K. Deprez, H. Ramon. Design and evaluation of a low power portable test rig for vibration test on mobile agricultural machinery. *Transactions of the ASAE*, 45(1), pp 5-12, 2002.

H. Ramon, J. Anthonis, E. Vrindts, R. Delen, J. Reumers, D. Moshou, K. Deprez, J. De Baerdemaeker, F. Feyaerts, L. Van Gool, R. De Winne, R. Van den Bulcke. Development of a weed activated spraying machine for targeted application of herbicides. *Aspects of Applied Biology, International advances in pesticide application*, 66, pp 147-164, 2002.

K. Deprez, J. Anthonis, H. Ramon. System for vertical boom corrections on hilly fields. *Journal of Sound and Vibration*, 266(3), pp 613-624, 2003.

D. Moshou, K. Deprez, H. Ramon. Prediction of spreading processes using a supervised Self-Organizing Map. *Mathematics and Computers in Simulation*, 65(1-2), pp 77-85, 2004.

I. Hostens, K. Deprez, H. Ramon. Evolution of Passive Suspension Systems in Seats of Agricultural Machinery. *Journal of Sound and Vibration*, 276(1-2), pp 141-156, 2004.

J. De Temmerman; K. Deprez, J. Anthonis, H. Ramon, Conceptual Cab Suspension System for a Self-propelled Agricultural Machine, Part 1: Development of a Linear Mathematical Model. *Biosystems Engineering*, 89(4), pp 409-416, 2004.

J. De Temmerman; K. Deprez, I. Hostens, J. Anthonis, H. Ramon, Conceptual Cab Suspension System for a Self-propelled Agricultural MachinePart 2: Operator Comfort Optimisation. *Biosystems Engineering*, 90(3), pp 271-278, 2005.

K. Deprez, D. Moshou, H. Ramon. Comfort Improvement of Nonlinear Suspension using Global Optimization and In-situ Measurements. *Journal of Sound and Vibration*, 284(3-5), pp 1003-1014, 2005.

K. Deprez, D. Moshou, J. Anthonis, H. Ramon, J. De Baerdemaeker. Comfort Improvement of Agricultural Vehicles by Passive an Semi-Active Suspensions. *Computers and Electronics in Agriculture*, 49, pp 431-440, 2005.

K. Deprez, I. Hostens, H. Ramon. Sospensione pneumatica di cabina per machine agricole (Pneumatic cabin suspension for agricultural machinery). *Oleopneumatica*, 2, pp 96-99, 2007.

E. Peeters, K. Deprez, F. Beckers, J. De Baerdemaeker, A.E. Aubert, R. Geers. Effect of driver and driving style on the stress responses of pigs during a short journey by trailer. *Animal Welfare*, 17(2), pp 189-196, 2008.

1.4.2 Conference proceedings

J. Anthonis, K. Deprez, M. Lannoije, H. Van Brussel, H. Ramon. Mathematical modelling and comparison of several passive vertical spray boom suspensions. In *Proceedings of the IMACS/IFAC third International Symposium on Mathematical Modelling and Simulation on Agricultural and Bio-Industries*, 7-9 June, Uppsala, Sweden, 1999, 35-41.

K. Deprez, M. Lannoije, J. Anthonis, H. Ramon, H. Van Brussel. Development of a Slow Active Suspension for Stabilising the Roll of Spray Booms. In *Proceedings of the UKACC International Confrerence on CONTROL 2000*, 4-7 September, Cambridge, UK, 2000.

J. Anthonis, K. Deprez, H. Ramon. System for vertical boom corrections on hilly fields. In *Proceedings of 1st International Workshop on Sound and Vibrations in Agricultural and Biological Engineering*, 13-15 September, Leuven, Belgium, 2000.

K. Deprez, H. Ramon. Design of a passive suspension for cabins of agricultural machinery. In *Proceedings of 1st International Workshop on Sound and Vibrations in Agricultural and Biological Engineering*, 13-15 September, Leuven, Belgium, 2000.

K. Deprez, D. Moshou, I. Hostens, J. Anthonis, H. Ramon. Hardware design and optimization of a 1 DOF suspension. In *Proceedings of Fourth International Symposium on Mathematical Modelling and Simulation in Agricultural and Bio-Industries*, 12-14 June, Haifa, Israel, 2001.

J. Anthonis, K. Deprez, H. Ramon. Active Spray-Boom Stabilisation In *Proc. of VDI-MEG Tagung Landtechnik*, 9-10 November, Hannover, Germany, 2001.

K. Deprez, K. Maertens H. Ramon. Comfort improvement by passive and semi-active hydropneumatic suspension using global optimization technique. In *Proc. of American Control Conference*, 8-10 May, Anchorage, United States, 2002.

K. Maertens, J. Schoukens, K. Deprez and J. De Baerdemaeker. Development of a Smart Mass Flow Sensor based on Adaptive Notch Filtering and Frequency Domain Identification. In *Proc. of American Control Conference*, 8-10 May, Anchorage, United States, 2002.

K. Deprez, D. Moshou, H. Ramon, J. De Baerdemaeker. Comfort Improvement of Agricultural Vehicles by Passive and Semi-Active Suspensions. In *Proc. of 15th IFAC World Congress* , 21-26 July, Barcelona, Spain, 2002.

I. Hostens, K. Deprez, H. Ramon. Improved Design of Air Suspension for Seats of Mobile Agricultural Machines. In *Proceedings of the Eleventh International Congress on Sound and Vibration*, 5-8 July, St.Petersburg, Russia, 2004.

K. Deprez, I. Hostens, H. Ramon. Pneumatic cabin suspension for agricultural machinery. In *Proceedings of the Eleventh International Congress on Sound and Vibration*, 5-8 July, St.Petersburg, Russia, 2004.

K. Deprez, H. Ramon. Development of a pneumatic cabin suspension for agricultural machinery. In *Proceedings of AGENG 2004* , 12-16 September, Leuven, Belgium, 2004.

K. Deprez, I. Hostens, H. Ramon. Modelling and design of a pneumatic suspension for seats and cabins of mobile agricultural machines. In *Proceedings of ISMA2004 International Conference on Noise and Vibration Engineering* , 20-22 September, Leuven, Belgium, 2004.

Chapter 2

Comfort on Mobile Agricultural Machines

The objective of this chapter is to situate this thesis among the research done at different institutes throughout the world. The first section discusses the possible link between whole body vibrations and low back pain and describes the environmental factors that contribute to discomfort of which vibration is but only one.

For the evaluation of the effect of vibrations on the human body, several standards are available. These are discussed (section 2.1.3) together with the European directive on the minimum health and safety requirements regarding the exposure of workers to the risks arising from physical agents (vibration)(section 2.1.4).

In a second part, this chapter gives an overview on comfort improving suspension systems on agricultural machines. Effects of tires, axle suspension and seat suspension systems are presented in a general way. Regarding cabin suspension systems, a more thorough description of both commercially available systems and research at different institutes is presented.

2.1 Low frequency vibrational comfort

2.1.1 Low back pain and whole body vibration

Low back pain (LBP) is among the most common health problems in the world. Lifetime prevalence has been estimated to be 60-80% for industrialized countries and for those younger than 45 years it is the

leading cause of industrial disability. It has in that way a large impact on health care utilization, on sickness absence and disability figures and costs. In the United States, with its 290 million inhabitants, one million back injuries occur per year, 100 million work days are lost each year and LBP accounts for 20% of all work related injuries. The total cost for LBP to the United States economy is $ 90 billion a year [72, 109].

Low back pain is multifactorial in origin: anatomic, industrial and environmental factors can influence both the severity of low back complaints and the resulting disability [134]. Of all risk factors involved, only those related to the industrial environment are the ones over which the human being has some control. Epidemiologic studies suggest that whole-body vibration (WBV) is an important work-related risk factor for LBP [108].

WBV is caused by the vibration of a surface supporting the body while sitting, standing or lying down. It generally concerns frequencies between about 0.5 and 100 Hz and acceleration magnitudes between about 0.01 and 10 m/s^2 (peak) [56]. According to the findings from a national survey done in Great Britain, approximately 7.2 million men and 1.8 million women, representing respectively 35.1% and 7.9% of the working men and women in the British population, are exposed to WBV at work in a one week period. The most common sources of occupational exposure are cars, vans, forklift trucks, lorries, tractors, buses and loaders [102].

Several epidemiologic studies tried to find evidence of a clear exposure-response relationship between whole-body vibration and low back pain. Conclusion up to now is that not sufficient evidence can be found to back this up [15]. Complications arise because vibration exposures are often associated with jobs with other undesirable features: tractor drivers often twist their spines to look behind the tractor, tractor and truck drivers often lift heavy loads and jump down from high cabs, bus drivers sit for long periods,... [56, 65]. This makes it difficult to pinpoint WBV as the main cause for LBP. Nonetheless many researchers [13, 15, 16, 56, 65, 72, 109, 134] are convinced of the increased risk that exposure to WBV poses on the occurrence of LBP.

Beside LBP there are several other adverse effects of the transmission of vibrations to the human body like reduction of comfort, impairing vision and the occurrence of difficulties in controlling a vehicle or performing other tasks [133]. Very low frequency whole-body

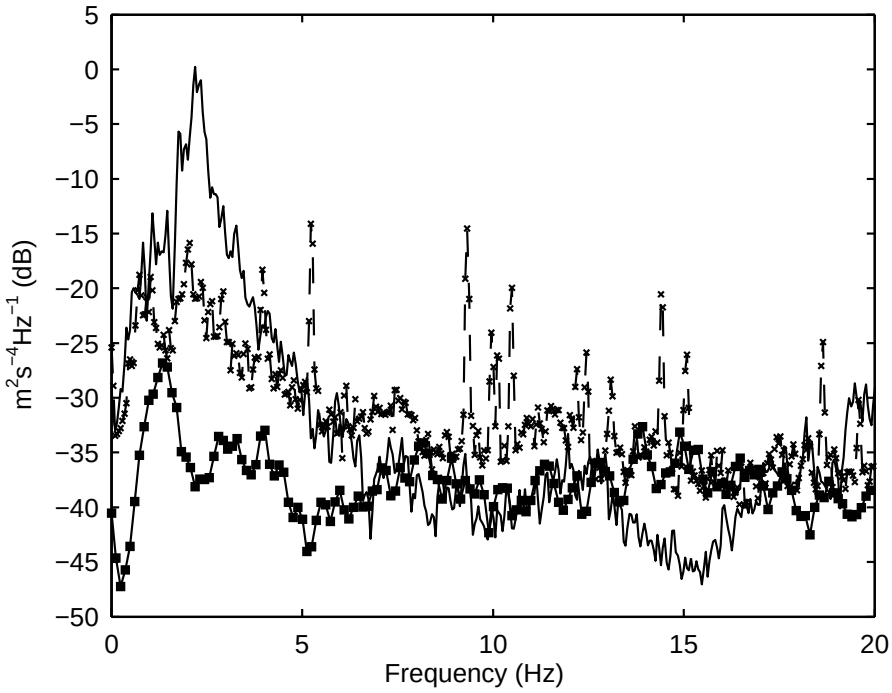

FIGURE 2.1: Power spectra of vertical acceleration on the seat of a mono-volume car on a paved road at 50 km/h (full square) and on the seat of a combine at 4 km/h in the field (dashed cross) and 20 km/h on the road (solid).

vibrations (below 1Hz) can induce kinetosis (motion sickness) affecting the performance of the operator [120]. If the vibration is very severe, which can be the case in many off-road vehicles on rough ground, impacts between the occupants and the vehicle may become a problem [99].

According to Palmer [102], farm owners and workers are among the top five professions when exposure to high levels of WBV is considered. The frequent use of tractors and harvesting machines is causing this. These machinery produce an extremely severe level of low frequency vibrations compared to other road vehicles [46, 117]. To get a good idea figure 2.1 compares the power spectral density (PSD) of the vertical vibrations measured on the seat in a combine harvester at two different

driving speeds (4 and 20 km/h) with the measurements on the seat of a car driving on road at 50 km/h.

The vibrations transmitted to the operator of such machines originate from the vehicle itself (engine, gearbox, ventilator, ...), rotating and moving elements within used implements and from the unevenness of the road or soil profile [69]. The dominant frequencies for a tractor and a combine harvester lie in the region 0.5 to 10 Hz [7, 24, 69, 84]. This is quite problematic since the most critical frequency ranges for the human spine, 4-8 Hz in the vertical direction and 0.5-2 Hz in the for and aft, and the lateral direction, lie within this band [108, 109]. As an indication the prevalence of back related problems is higher in farm owners and workers than persons not exposed to those kind of vibrations [13, 84].

2.1.2 Vibration discomfort

In order to deal with the problems concerning WBV in a structured way, consistent tools of measuring the effect of vibrations on the human body have to be used.

It has long been a goal in the automotive industry to be able to quantify objective measures of ride quality. Some of the earliest published works on the subject date back to the 1930's in the work of Jacklin [75]. It is perhaps a proof of the difficulty of the problem that investigations continue some seventy years later. Gillespie [54] describes ride quality as: "... a subjective perception, normally associated with the level of comfort experienced when travelling in a vehicle. Therefore, in its broadest sense, the perceived ride is the cumulative product of many factors. The tactile vibrations transmitted to the passenger's body through the seat, and at the hands and feet, are the factors most commonly associated with ride"[49].

What factors have to be accounted for when determining the ride quality or total comfort, are given by figure 2.2. Vibration is just one of the factors and, considered alone, cannot yield any overall prediction of a persons' total satisfaction with an environment [56].

Since the aim of this research is to look at the effect of cabin suspension systems on whole-body vibrations, a restriction to the vibrational aspect within the overall comfort is possible. But even then the list of variables to be considered is extensive (see table 2.1). This makes it still far from obvious to determine what type of damage to the human body will occur when a person is exposed to vibrations and

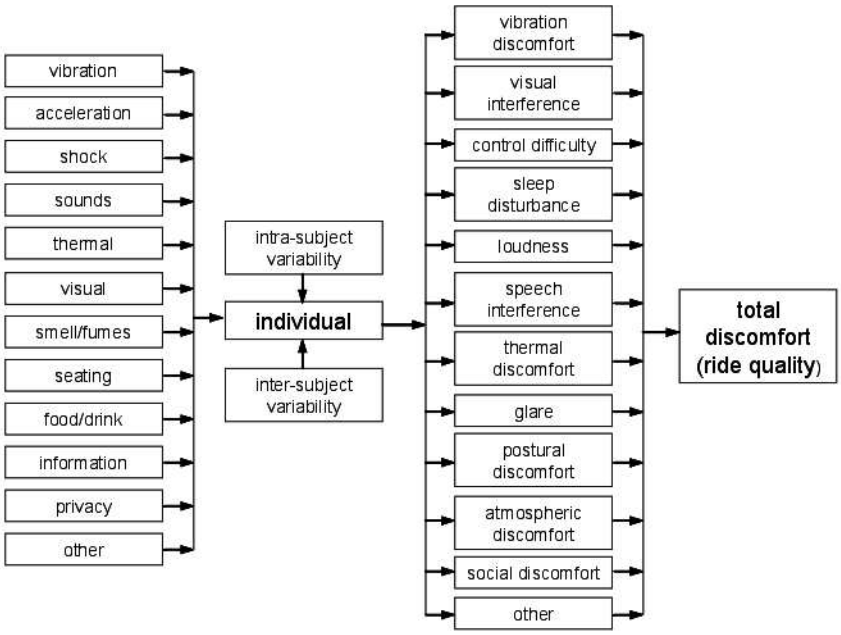

FIGURE 2.2: Factors contributing to discomfort (by Griffin [56])

what mechanisms are involved in the damage process. Several studies [31, 35, 47, 65, 76, 83, 96, 97, 99, 100, 120] have been dedicated to fully understand the behavior of the human body in a vibrating environment. Notwithstanding the effort put in by several researchers, all mechanisms involved are not yet discovered.

The believe that occupational and leisure exposures to vibration can induce injury has led to a desire to define methods of predicting the conditions which are responsible. This has resulted in various vibration standards. These standards define a method of measuring vibration (to obtain a numerical indication of the vibration), a means of evaluating the vibration (so as to obtain a measure of the vibration severity) or a means of assessing the severity (to predict the likely consequences of exposure). With uncertain knowledge of human responses to vibration, the wording of such a standard requires care: it could offer assistance in the form of clear guidance on methods without implying certainty of knowledge, or it could add to confusion. Perhaps the measurement

Extrinsic variables
Vibration variables
Vibration magnitude and combinations of magnitudes
Vibration frequency and combinations of frequencies
Vibration direction and combinations of directions
Vibration input position and combinations of positions
Vibration duration and combinations of durations
Other variables
Other stresses (noise, temperature, etc.)
Seat dynamics
Intrinsic variables
Intra-subject variability
Body posture
Body position
Body orientation (sitting, standing, recumbent)
Inter-subject variability
Body size and weight
Body dynamic response
Age
Gender
Experience, expectation and attitude, personality
Fitness

Table 2.1: Some variables associated with vibration discomfort (by Griffin [56])

and evaluation should be precisely defined but the assessment should reflect the uncertainties in knowledge [57]. It is exactly to this extent that the standards will be used in this work.

2.1.3 Measurement tools

The three human response to vibration standards of most current interest, ISO2631(1974) [1], BS6841(1987) [2] and ISO2631(1997) [3], provide several single number estimates of vibration severity called comfort values. This work uses for the one dimensional case the effective or weighted RMS (effRMS) and the vibration dose value (VDV). These values are calculated based on filtered acceleration data.

The frequency weighting filters used, combine the knowledge con-

cerning the effect of vibration on the human body to put emphasis on those frequencies that are particulary harmful and to filter out the ones of less importance. This knowledge is obtained through epidemiologic studies and shows that the sensitivity of the human body to vibration, depends greatly upon the direction of the vibration (for and aft (x), lateral (y) and vertical (z)), the orientation of the body (standing, sitting and recumbent) and the place of measurement.

The following two formulas define the weighting filters used by BS6841:

$$W_i(s) = \frac{(s + 2\pi f_3)\left(s^2 + \frac{2\pi f_5}{Q_3}s + 4\pi^2 f_5^2\right)}{\left(s^2 + \frac{2\pi f_4}{Q_2}s + 4\pi^2 f_4^2\right)\left(s^2 + \frac{2\pi f_6}{Q_4}s + 4\pi^2 f_6^2\right)} \times \frac{2\pi K f_4^2 f_6^2}{f_3 f_5^2}, \tag{2.1}$$

$$W_j(s) = \frac{(s + 2\pi f_3)}{\left(s^2 + \frac{2\pi f_4}{Q_2}s + 4\pi^2 f_4^2\right)} \times \frac{2\pi K f_4^2}{f_3}, \tag{2.2}$$

in which f_3, f_4, f_5, f_6, Q_2, Q_3, Q_4 and K are the parameters.Depending on the direction of the vibration (translation, along the three axes, or rotation, around the three axes), the orientation of the body and the place the vibration is measured, these parameters are set to specific values.

Figure 2.3 shows two examples of frequency weighting filters: $W_b(s)$ and $W_d(s)$. The first filter is based on equation 2.1 with the following parameter settings: $f_3 = 16$, $f_4 = 16$, $f_5 = 2.4$, $f_6 = 4$, $Q_2 = 0.55$, $Q_3 = 0.90$, $Q_4 = 0.95$ and $K = 0.4$. This filter is used for the vertical accelerations measured at the seat surface for a person in a seated posture. The second filter, based on equation 2.2 with $f_3 = 2$, $f_4 = 2$, $Q_2 = 0.63$ and $K = 1$, is used for the for and aft, and lateral accelerations of a seated person. It can be seen that for the vertical direction the most important region is between 4 and 8 Hz where the weight is above one, while in the for and aft and lateral direction, the frequency range of 0.5-2 Hz has the largest weight. The highest discomfort is allocated to the frequency ranges the human spine is most sensitive to. Similar filters are used by the ISO standards.

After filtering the accelerations, with the above defined frequency weighting functions, the effRMS is calculated using:

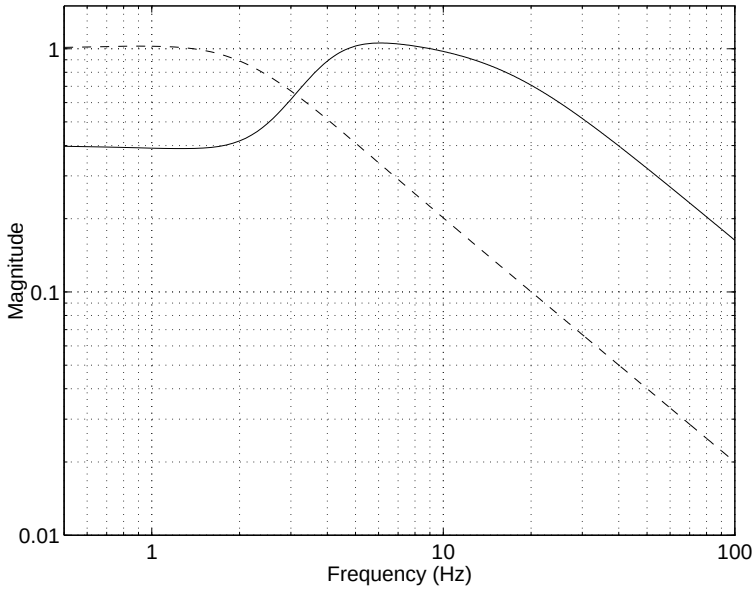

Figure 2.3: Comfort weighting filters of the BS6841 for horizontal (dashed) and vertical (solid) seat vibration

$$effRMS = \left[\frac{1}{N} \sum_{n=1}^{n=N} a_w^2 \right]^{\frac{1}{2}}, \tag{2.3}$$

with N the number of points and a_w the frequency weighted acceleration data. The unit of effRMS is m/s^2.

The VDV is given by:

$$VDV = \left[\frac{T_s}{N} \sum_{n=1}^{n=N} a_w^4 \right]^{\frac{1}{4}}, \tag{2.4}$$

with T_s the measurement period and N and a_w defined as above. The unit of VDV is $m/s^{1.75}$. The ISO2631 standard uses a complex time dependency for the effects of vibration on comfort, performance and health. The time dependency is therefore not often used. Scientific basis for it is rather weak especially for periods of exposure below one minute and above four hours. Between one minute and four hours the

effect of time can be modelled with the time function $t^{1/4}$. The formula for VDV incorporates this relationship [56].

For multi-axis vibration, different approaches are possible. The most easy to perform is the one used by ISO2631 for the evaluation of comfort on a seat. The measurements on the seat surface in x, y and z direction are combined as following:

$$RMS_{total} = \sqrt{(1.4a_{xw})^2 + (1.4a_{yw})^2 + (a_{zw})^2}, \tag{2.5}$$

with a_{xw}, a_{yw} and a_{zw} the weighted acceleration data. The unit of RMS_{total} is m/s^2. Vibrations in the horizontal plane are considered to be more harmful than vertical vibrations, therefore the x and y direction is attributed with a factor 1.4. The BS6841 also includes acceleration measurements at the backrest (chest) for a seated person and evaluates multi-axis vibration using the fourth root of the sum of the fourth powers of the VDVs. The total vibration dose value, VDV_{total}, for the environment is given by:

$$VDV_{total} = (VDV_{xs}^4 + VDV_{ys}^4 + VDV_{zs}^4 + VDV_{xb}^4)^{1/4}, \tag{2.6}$$

where VDV_{xs} is the VDV in the x-axis on the seat, VDV_{ys} is the VDV in the y-axis on the seat, VDV_{zs} is the VDV in the z-axis on the seat, and VDV_{xb} is the VDV in the x-axis on the backrest. The unit of VDV_{total} is $m/s^{1.75}$.

Which of the comfort values approaches the subjective comfort feeling the closest or which of the three standards is to be preferred, remains a difficult question. Research on automobiles by Smith *et al.* [122] points out that unweighted RMS values are as good as weighted RMS values to predict comfort. Ferris [49] states that the ISO2631 standard is not the best to predict ride quality in automobiles. On the other hand research by Fairley [46] shows that the ISO2631 standard is the best in predicting the vibration discomfort in an agricultural tractor. Griffin [57] is much in favor of the BS6841 because it provides a simpler, clearer and internally more consistent evaluation method compared with the ISO standards.

In numerous cases the RMS of the frequency weighted accelerations is a useful indicator of the severity of the vibrations. But if the vibrations are non-stationary or include a large number of shocks, the VDV is a better indicator. Determining factor in this is the crest factor given by:

$$Crestfactor = \frac{a_{max}}{effRMS}, \tag{2.7}$$

where a_{max} is the maximum peak acceleration. This factor is usually calculated from the acceleration after it has been frequency weighted according to human sensitivity to different frequencies. Typical vibration in a vehicle on a good road may have a crest factor in the approximate range 3-6, but this will increase if the measurement period includes shocks (which will mainly increase the peak value) or if the vehicle stops (which will reduce the RMS value) [56].

Besides magnitude and frequency content of the vibration, duration is also a very important factor. This aspect is covered by VDV since it incorporates a time effect in its value, this in contrast with effRMS. VDV levels in the region of 15 $m/s^{1.75}$ are considered to cause severe discomfort and levels above increase the risk of injury [2]. The following formula calculates the time needed to reach that level.

$$timetoVDV15 = \frac{15^4 \times T_{measurement}}{VDV_{measurement}{}^4}, \tag{2.8}$$

with $T_{measurement}$ the time in s that the measurement took place and $VDV_{measurement}$ the VDV for this measuring period. $TimetoVDV15$ will give the time in s to reach a VDV of 15 under the same vibrational conditions as during the measurement.

In this work the objective comfort values will only be used as a way of comparing different situations for the comfort point of view, without linking conclusions towards implications to human health. For a more thorough investigation of the human vibration comfort, more dedicated literature like Griffin's 'Handbook of Human Vibration' [56] and more resent research concerning the topic [31, 35, 65, 72, 97] can be consulted.

2.1.4 European Directive

By means of directives, the European Parliament tries to encourage improvements, especially in the working environment, to guarantee a better level of protection of the health and safety of workers, without having to impose administrative, financial and legal constraints. As a consequence no measures are taken that would hold back the creation and development of small and medium-sized undertakings.

In Directive 2002/44/EC [5], on the minimum health and safety requirements regarding the exposure of workers to the risks arising from physical agents (vibration), certain limit and action values for the daily exposure to vibrations are put forward. Every Member State has the option to maintain these minimum requirements or to adopt more favorable provisions for the protection of workers by fixing even lower values. This directive has come into force on 6 July 2005 but entitles every Member State to make use of a maximal transitional period of five years, in which under strict conditions, the limit values can be exceeded. In agriculture and forestry, an additional transitional period of four years is agreed upon.

The daily exposure limit value is set to an effRMS of 1.15 m/s^2 or a VDV of 21 $m/s^{1.75}$ over an eight-hour reference period and the daily action value is for that same eight-hour period put at an effRMS of 0.5 m/s^2 or a VDV of 9.1 $m/s^{1.75}$. The limit values cannot be violated and once the action values are exceeded, the employer has to establish and implement a program of technical and/or organizational measures intended to reduce the exposure to vibrations. One of the measures that can be taken is the choice for more appropriate work equipment that produces less vibration or has a better ergonomic design. Therefore to keep a competitive position it will be crucial for manufacturers of machinery, including agricultural machinery, to stay below the action values for an eight hours period.

To improve the comfort on agricultural machinery, several aspects can be taken into account, varying from reduction of the vibration at the source by proper maintenance and correct loading, to improvement of the cab ergonomics and seat profiles to optimize the operator posture. Another very important issue is the reduction of vibration transmission by incorporating suspension systems (vehicle, cab and seat suspension) between the operator and the source [34]. Since the design of effective suspension systems is the main issue in this work, the following section will discuss advances in this field.

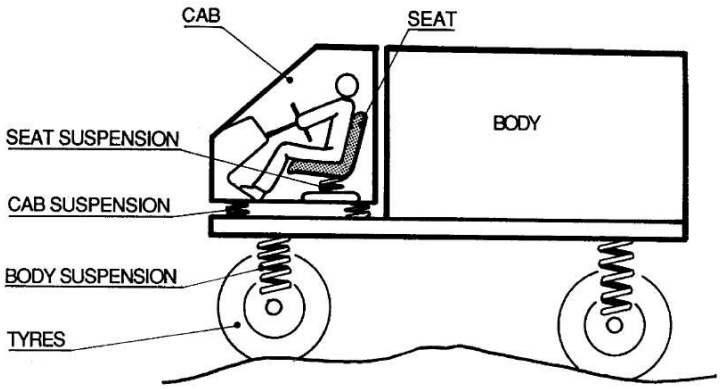

Figure 2.4: Possible positions for vehicle suspension systems (by Donati [34])

2.2 Comfort improving suspension systems on agricultural machinery

2.2.1 Introduction

The design and development of suspension systems is a topic that many engineers have touched. To give a complete overview of all possible suspension systems developed in time, would be too comprehensive for this type of work. Therefore the following sections present an overview on suspension system design together with the relevant work performed by other researchers in the same domain as this thesis.

In the transmission path between the vibration sources (road and soil undulations, translating and rotating elements within the machine itself) and the operator of the machine, there are roughly four places where an engineering solution can be introduced (see figure 2.4). To improve drivers working conditions an adequate selection of tyres, type of axle, seat and cabin suspensions is of utmost importance.

2.2.2 Tyres for optimum vibration performance

Most mobile agricultural machinery are fitted with pneumatic tyres because they act as low-pass filters by isolating the machine from small

ground surface irregularities [25]. An exception to this is off-road machines fitted with caterpillar tracks comparable to the tracks of tanks and industrial trucks which often are mounted on solid tyres to provide stability and resist puncture. Tyres are usually selected according to their rolling resistance, grip, stability, cost, influence on soil compaction, resistance to collision damage, acceptability to the driver, etc [95, 81]. The damping and stiffness parameters must be taken into account to absorb obstacle impact. However, even large tyres cannot absorb vibration energy as well as a shock absorber, so vibration builds up even on relatively smooth surfaces. Tyres are also far stiffer than a suspension system. But excessively soft tyres may induce low frequency motions, including pitching [34].

Lines et al. [86] state:"To improve their suspension properties significantly, tyres would need to absorb five to ten times more vibration energy and to be much larger and softer. Such a tyre would then also have a high rolling resistance and the heat built up in the tyre due to the rolling and the vibration would cause it to have a short life." Contrary to road vehicles, most agricultural vehicles don't have axle suspensions, with the exception of the optional front axle suspension systems on four wheel drive tractors [40, 115] and the spraying machines of e.g. Knight and Delvano. So the tyres represent the only suspension components and therefore take a central part in the dynamical behavior of these machines [24].

2.2.3 Axle suspension

Concerning axle suspension, also called primary suspension, the most advanced systems can be found in the automotive industry where the vehicle suspension of cars, busses and trucks is responsible for both the driving comfort and the safety of the passengers. The suspension systems basically consist of wishbones, a spring and a shock absorber. The task of the spring is to carry the body-mass and to isolate the body from road disturbances and therefore contributes to drive comfort. The damper contributes to both driving safety and comfort by damping the body and wheel oscillations [51]. Suspension travel or 'rattle space' is a third important issue. The current trend is towards larger tires and lower hood designs and this puts a premium on keeping the relative displacement between body and wheel as small as possible [137]. New cars are also fitted with tires with a bigger rim, making the tire stiffer and require a great deal of effort from the axle suspension to sustain

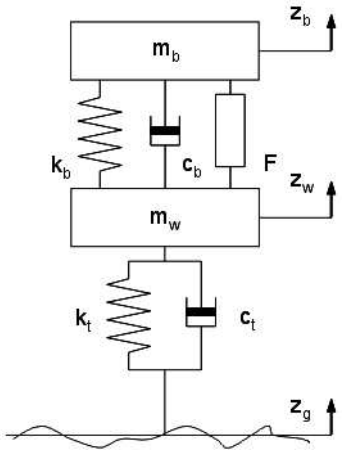

Figure 2.5: Quarter car model

the comfort in the car.

To analyze the vertical dynamics, frequently a so-called quarter-car model, shown in figure 2.5, is used. In this figure m_b represents the sprung mass (quarter of the car body mass), m_w the unsprung mass, k_t and c_t the tyre stiffness and damping coefficient, k_b and c_b the suspension stiffness and damping coefficient, z_g is the road or ground displacement, z_w the displacement of the wheel and z_b that of the car body.

Figure 2.6 shows the typical transfer function of this quarter car for the body acceleration $\ddot{z}_b$ with respect to the road excitation z_g. To improve the ride quality, it is important to decrease the resonance peak of the body, also called sprung mass, around 1Hz. In order to improve the ride stability, it is important to keep the tire in contact with the road surface and therefore to decrease the wheel hop resonance peak near 10Hz, which is the resonance frequency of the wheel also called unsprung mass.

For a given suspension spring, a better isolation of the sprung mass from road disturbances can be achieved with a soft damping. On the other hand, avoidance of wheel oscillations, which directly refers to safety as a non-bouncing wheel is the condition for transferring road-contact forces [51], is served by a hard damping. Therefore the ride quality and the drive stability are two conflicting criteria.

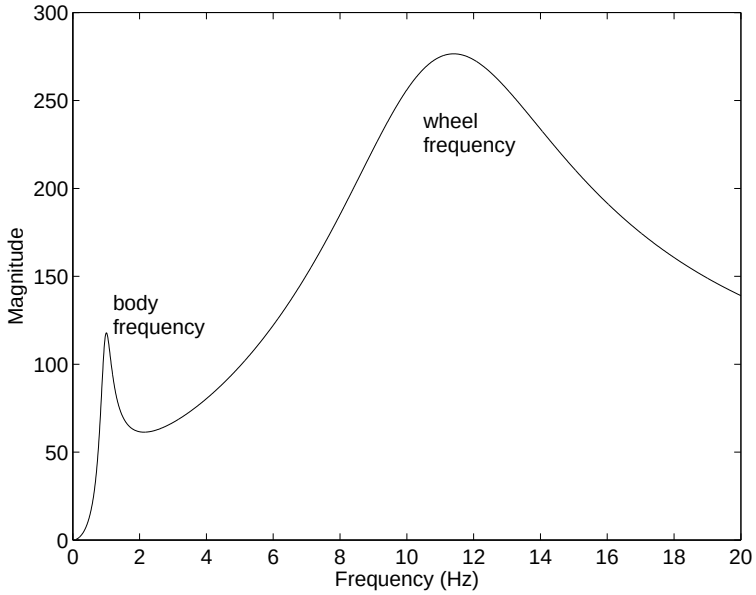

FIGURE 2.6: Frequency response magnitude for the body acceleration of a passive quarter car suspension system with road excitation as input

The available rattle space will provide an extra constraint to the system since too soft spring and damper values will result in a frequent bottoming of the suspension with a severe degradation of isolation as a consequence [41].

The fixed setting of a passive suspension system is always a compromise between comfort, safety and suspension deflection. To solve, or at least reduce the conflicts, several solutions were proposed from a stroke dependent damper [45] and nonlinear dampers [39, 38] to the introduction of semi-active [22, 51, 80, 125] and active suspensions [41, 126, 137]. Semi-active systems adapt the damping and/or the stiffness of the system to the actual demands, thus dissipating the vibration energy more quickly. Active suspension systems, in contrast to their passive and semi-active counterparts, have the possibility to put energy into the system. It makes them perform better at the expense among others of being energy consuming.

When looking at heavy road vehicles, comfort and safety remain important issues but other performance criteria gain in interest. To max-

imize the productivity of a vehicle when carrying low-density goods, it is necessary to provide the largest possible volume for payload. Since height, width and length of vehicles are usually regulated, volume is maximized by providing a low platform height. This in turn requires suspensions with minimum rattle space. The suspension system also influences the static and dynamic loading applied to the road by the tyres of the vehicle. This loading can cause significant infrastructure damage to roads and bridges. A large proportion of a heavy road vehicle's fuel consumption is used to overcome rolling resistance. Some of that arises from energy dissipation in the suspension depending on the dynamic properties of the suspension [26].

Unlike cars and trucks, most all-terrain machines have no suspension system between wheel-axles and chassis to reduce the effect of ground roughness [34]. 99 % of the world's tractors have no primary suspension [40] and axle suspension on dumpers or graders are rare. Reasons for not implementing a primary suspension are mostly loss of stability, on terrains with significant slopes and cross-slopes, loss of power due to energy consumption in dampers or simply too complicated and costly to realize [44, 128]. But the cry for comfort improvement is changing the climate. Torsio-elastic linkage suspension on a log skidder [112] or a semi-active rotary damper for a heavy armor vehicle [43] are just two of the various examples of evolution in the off-road vehicles.

On the tractor market there has been a shift from a ploughing-first tractor developed for the work on the field to a transport-first tractor that is able to pull farm trailers with loads above 3.5 *ton*. This last tractor had to be safe, stable, comfortable and speedy enough to keep up with combines and harvesters getting bigger and faster. Therefore the development of a primary suspension system was indispensable.

HST Developments Ltd., which grew out of the Engineering and Management Schools of the University of Manchester's Institute of Science and Technology, was the first to notice this shift and created the world's first fully-suspended tractor back in 1973, the Trantor. This tractor had front and rear axle suspension but also a suspension on the linkage and pick-up hitch. It took up till 1991 before some of the ideas were copied in the fully suspended JCB Fastrac and nowadays almost every constructor has front axle suspension on some of its high end models. More than 30 years after the first Trantor, every big constructor is also putting effort in the development of a fully suspended model [17, 40, 115].

Axle suspension on mobile agricultural machinery is currently 'not done'. But to meet farmer's and machinery operator's essential need for increasing overall work output with lower operating costs, higher speeds have to be realized to cut the time during harvesting but also during transport between two fields. Therefore, it is the impression of the author that also harvesters will be equipped with axle suspension within the coming years because of safety and comfort issues. In the design of an adequate primary suspension also the criteria as mentioned before e.g. fuel consumption, stability, road damage, etc. will have to be taken into account.

2.2.4 Seat suspension

(a) Car seat (b) Suspended seat

FIGURE 2.7: Photograph of a conventional car seat and a suspended seat for bus, tractor or truck

The seat suspension is one of the so called secondary suspension systems. These are means of providing the driver with a comfortable ride without requiring a soft primary suspension and consequent problems with vehicle handling, stability and static deflection. Generally there are two types of seats used in vehicles: a conventional seat and a

suspended seat (see figure 2.7) [101].

The first type is the one used in cars and has cushions made out of polyurethane foam whether or not reinforced with metal or rubber springs. For the transmission of vertical vibrations, studies show resonances in the region of 4 Hz with an amplification factor up to two or more. Only at frequencies larger than about 6 Hz conventional seats attenuate the vertical vibrations. The backrest and the seat pan exhibit three resonance frequencies below 60 Hz in the for-aft direction and a very poor attenuation level at the seat pan in this direction [110]. By tuning the foam properties, vibration attenuation could be improved but until now much of the seat design in the automotive industry is based on experience from previous designs without the benefit of a clear understanding of the properties of the foams and the seat-occupant interaction. Current research tries to fill this gap [27, 59, 82].

The second type, the suspended seat, has besides foam cushions also a separate suspension mechanism. This type of seat is used as driver seat on busses, trucks, tractors and mobile agricultural machinery. On most of the agricultural vehicles, it is the only suspension system available for vibrational comfort improvement. To allow only vertical displacements the mechanism uses a kind of scissor system which has proven to be safe, low in production costs and highly packable. A spring and damper incorporated in the system produce a substantially lower resonance frequency than can be generated with the foam alone thus improving the seat's isolation characteristics [68].

A seat suspension system works like a classical base motion model of a one degree of freedom mass-spring-damper system [127, 132] shown in figure 2.8. In this figure m_s represents the mass of the seat enlarged with a portion of the mass of the driver, k_s and c_s the seat suspension stiffness and damping coefficients, z_g the ground displacement and z_s is the displacement of the seat.

The following equation shows the transfer function of this model:

$$\frac{z_s(s)}{z_b(s)} = \frac{c_s s + k_s}{m_s s^2 + c_s s + k_s}, \tag{2.9}$$

The natural undamped frequency ω_n of the system is given by:

$$\omega_n = \sqrt{\frac{k_s}{m_s}}, \tag{2.10}$$

and can be reduced by lowering the spring stiffness k_s. Since only

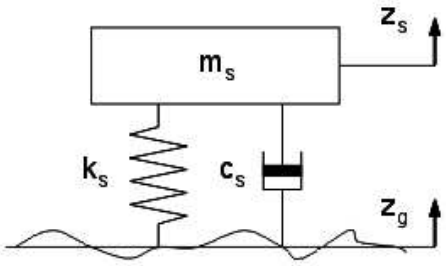

FIGURE 2.8: Simplified model of a seat suspension system

beyond $\sqrt{2}\omega_n$ the system starts attenuating considerably the vibrations, reducing the natural frequency will improve its performance. The damping in the system reduces the peak amplitude at natural frequency but, as can be seen in figure 2.9, will have a negative effect at higher frequencies [52].

In early days the suspension consisted of a mechanical spring and a hydraulic damper. Driver's height could be adjusted by changing the initial tension in the spring. The natural frequency was around 1.5 Hz since lower was not possible due to three problems. First the static deflection [131], Δ_{static} given by:

$$\Delta_{static} = \frac{g}{\omega_n^2}, \tag{2.11}$$

with g the gravitational acceleration, becomes 6 cm for a 2 Hz natural frequency. Δ_{static} becomes 25 cm for a natural frequency of 1 Hz. Total spring length in this case would be at least 0.5 m (static deflection + windings + deflection through vibration input) which makes it practically not feasible to get the spring underneath the seat.

Secondly, a lower spring stiffness would result in larger deflections. As a consequence more end-stop impacts would occur which have a very negative effect on comfort [136]. To keep the seat within the end-stroke range, higher damping would be required. This damping cancels out the advantages of the lower natural frequency (see figure 2.9).

A third problem is the Coulomb friction in the hinges and the hydraulic damper. This friction has a detrimental effect on vibrations with a low magnitude and on setting the ride height of the seat. The lower the spring stiffness, the more pronounced these phenomena be-

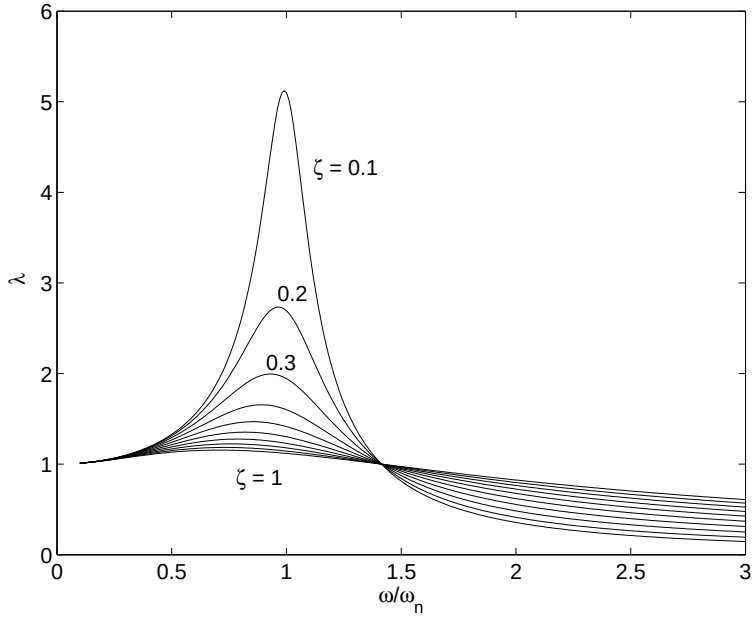

Figure 2.9: Transmissibility λ as a function of normalized frequency ω/ω_n for values of damping ratio ζ from 0.1 to 1

come [59].

In order to overcome some of those problems the most widely used seat suspension system today combines an air spring with a hydraulic damper. The air spring makes it possible to lower the natural frequency without constructional problems and the ride height can easily be set by changing the internal pressure in the spring. The non-linear characteristics of the air spring has also the advantage that a lower damping can be used without encountering problems with end-stop impacts.

Hostens et al. [68] propose an even further reduction of the spring stiffness and the use of air damping instead of hydraulic damping. A hydraulic damper has, at high frequencies, the tendency to stiffen. At high frequencies the oil has no time to pass through the orifices in the damper and due to the incompressibility of oil, the damper is almost a rigid structure through which the vibrations pass to the driver. A similar phenomenon occurs in an air damper but due to the compressibility of the air, this results in an additional spring stiffness instead of

a rigid structure.

In recent years active and semi-active applications for seat suspensions have become a topic of considerable interest [20, 37]. These seat suspensions make it possible to provide some of the ride benefits of an active primary suspension but without the cost [26]. McManus et al. [94] use a semi-active magnetorheological fluid damper to prevent end-stop impacts. This reduces the VDV levels with 40% with respect to a classical damper under the same conditions. Pantelelis & Kanarachos [103] study the effect of two active vibration control strategies: an active skyhook and a Linear Quadratic Regulator (LQR) using absolute velocity and displacement measurements. Wu & Chen [135] combine feedback and feedforward in an adaptive scheme using acceleration measurements. Also Périsse & Jézéquel [104, 105] describe the design of an active seat but use an electromechanical actuator and a model based approach to tune the proportional integral (PI) regulator. For a random excitation a reduction of 12dB in RMS value is achieved.

Now some manufacturers have an active seat suspension system available. One of the first was the John Deere Active Seat^{TM} [36]. The seat uses a hydraulic actuator in combination with an air spring. Compared to a classical pneumatic seat, this active suspension shows reductions up till 66 % in RMS acceleration when performing standardized ISO tests, but is expensive. Also Grammar has an active seat on the market.

2.2.5 Cab suspension

The cabin suspension is, besides the seat, a second secondary suspension system. A distinction should be made between cabs which are isolated from vehicles by rubber mounts and cabs fitted with low-frequency two- or four-point mechanical suspension systems. Rubber mounts between the cab and the chassis mainly isolate structurally induced vibrations at higher frequencies ($50Hz$ and higher) from entering the cab and improve in this way the acoustic comfort [19]. Only the low-frequency suspension cabs, with a natural frequency below the vehicle's dominant frequency are efficient enough to reduce the vibration transmitted to the operator. Suspension cabs can be designed to ensure isolation in all three linear axes but the main purpose is to reduce vertical movement as well as rolling and pitching [34].

Jang and Griffin [76] mention that a phase difference between seat and feet of a seated person results in more discomfort, especially below

5Hz and with low magnitudes of vibration. Seidel et al. [120] describe the effect of the relative motion between the driver and his immediate surroundings. The sensory mismatch between feeling and seeing as can be experienced even with perfect vibro-isolation of the drivers seat, can lead to kinetosis (motion sickness). This, together with the advantage that a low-frequency suspension cab is able to protect the drivers's whole-body with respect to several degrees of freedom, makes that vibration isolation through this second type of secondary suspension is to be preferred over seat suspension. The trend should even be towards elimination of the seat suspension, softer cab suspension and stiffer primary suspension (better for safety as mentioned in section 2.2.3). But this strategy is likely to result in large displacements of the cab relative to the chassis, with consequent problems for clearance and connection of driver controls [26].

Full suspension cabs are now a common feature on most articulated lorries. The standard suspension using four rubber blocks is being replaced by systems using the principal of a suspended seesaw. In this case both front mounting points of the cab are elastically fixed to the vehicle, while both rear cab mountings are replaced by mechanical or hydrodynamic suspensions. Commercial systems are already available using suspensions systems integrating an air spring and a hydraulic damper in one device. The Cabin Air Leveling Module, CALM®, made by ZF Sachs and Wabco is such a system and it even features an integrated ride-height control [138]. Even a four-point suspension system using these kind of devices is available.

Concerning off-road machinery, some research has been performed by the French INRS (l' Institut National de Recherche et de Sécurité) on the cab suspension of counterbalance trucks. Former cab suspension systems using rubber mountings were only suitable to reduce engine vibrations with frequencies above $10Hz$. The low frequency suspension system proposed in Boulanger et al. [14] and Lemerle et al. [85] uses metal compression springs and shock absorbers to attenuate vertical vibration, roll and pitch movements. Attenuation levels of 50% are achieved with this passive suspension system.

For the development of a cab suspension on mobile agricultural machines, the research concentrates itself to two institutes: VTT Technical Research Center of Finland, where Vessonen and Järviluoma performed the investigations, and the Agricultural Engineering Department of the Swedish University of Agricultural Sciences, where Hansson was the

driving force in the research.

Vessonen and Järviluoma [133] designed an active cab suspension for rubber wheeled mobile machines. To be able to reduce the amount of tests on physical prototypes, a virtual prototype of an agricultural wheeled tractor was used as a starting point. The simulation model was built up in the mechanical system simulation software ADAMS. The whole tractor was modelled based on technical drawings of the tractor manufacturer and included a rigid body model for the cabin and representative masses for driver and driver seat.

To simulate the vibration excitation coming from the ground irregularities, different tracks were modelled. One of them was the rougher track of International Standard ISO 5008 [6]. This standard specifies methods for measuring and reporting the whole body vibration to which the operator of an agricultural wheeled tractor or other field machine is exposed, when operating on a standard test track. The standard also includes the ordinates of two artificial test tracks, a $100m$ smooth track and a rougher track of $35m$. The virtual prototype was validated by comparing measured and simulated time domain vibrations while driving over the different tracks and it could be concluded that the model was realistic enough in describing the dynamic characteristics of the tractor.

This simulation model of the tractor was used to find out the relative significance of various means of vibration control. The cabin was attached to the tractor body at the four corners of the cabin. As a reference the case where the cabin of the tractor was mounted with four rubber isolators was used. For the active cabin suspension two passive vibration isolators were used for the two front corners and two active elements were used for the two rear corners. This made it only possible to improve pitch, which results in vertical movements at the driver's seat, and roll behavior of the cabin.

As control strategies different approaches were tested. Simple PID-type algorithms (proportional, integral and derivative) were found to be very laborious or even impossible to tune manually and hence, model-based control algorithms were needed. Model based predictive control algorithms and $\mathcal{H}_\infty$-control design were tried with a significant improvement in acceleration levels compared to the reference situation.

The findings deduced from the simulations were validated using a real set-up. The test bench contained two steel beams on which the tractor cabin was attached with the prototype suspension mechanism

as was used in the simulations. The beams could be swung in two directions to mimic the vertical movement and roll rotation of the tractor body. These motions were controlled according to signals, which were measured from the real tractor during test runs. As active elements two relatively cheap hydraulic elements were used in order to form an economically reasonable base for possible commercial exploitation.

The laboratory tests were carried out for one degree of freedom at the time and the results showed reasonable improvements up till $3Hz$. Due to the dynamic properties of, e.g. hydraulic valves selected for the prototype, the performance of the system was limited. Noise problems at high frequencies also form an obstruction for good behavior above $3Hz$. Vessonen and Järviluoma conclude that control systems with a certain adaptability to changes in operating conditions (difference between off-road and on the road) and automatic tuning of the control algorithm should be considered in future development work.

In the second study, Hansson [61] optimized a passive suspension system and designed an adaptive suspension controller. Four hydraulic cylinders connected in pairs to two gas accumulators provided the vertical movement of the cabin. The cylinders were placed in rubber bushings to make roll and pitching movement possible and to give the cabin even a degree of freedom in lateral, for-aft and yawing direction. The last three movements were damped using four shock absorbers.

The research of Hansson started with the modelling of this cab suspension using first principles. Non-linear dynamics of the hydraulic suspension elements, the bushings and the shock absorbers were derived and put together to get an analytic model. The model of this suspension was validated by mounting the suspension system on a hydraulic shaker and comparing model and real set-up. The signals applied to both were based on driving a tractor at different speeds on the test tracks of ISO5008. A relatively good agreement could be seen.

For the optimization of the suspension a technique based on genetic algorithms was used [62]. The input signals were again based on the ISO5008 tracks and resulted in an optimum suspension system able to reduce by approximately 40% the vector sum defined by ISO2631 [1, 3]. A travel space of $10cm$ was allowed for the hydraulic cylinders.

For the active suspension, Hansson used Linear Quadratic Gaussian control (LQG). The results achieved with this controller are rather poor, compared to those of the optimized passive suspension. The only advantage of the system, is the levelling ability of the controller,

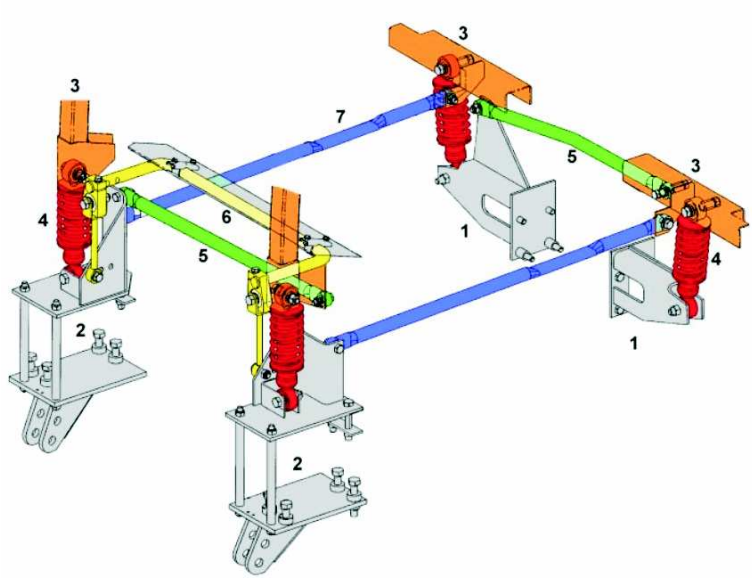

FIGURE 2.10: Renault cab suspension [115]

as the cabin is put horizontally even when the ground and the vehicle's frame are sloping.

According to Hansson the controller could be improved because it was tuned to prevent over-travel even for extreme vibration inputs and that made the controller too conservative if the vibration input levels were small. Therefore the observer and feedback gains of the LQG controller were precalculated for different levels of frame acceleration. These matrices were stored and a new, gain scheduling, controller selected the best of the stored gain matrices based on the disturbance characteristics sensed.

In [61] and [63] all results shown for the optimized passive and both active suspensions are based on simulations. Hansson states that there is 'good agreement' between the results of the simulation model and a real full-scale cab, but shows at no point real results.

Research concerning cab suspensions was concentrated on the development of systems for tractors. No records are found about investigations on cab suspension systems for other mobile agricultural machines. The commercial market reflects this imbalance since only low-frequency

cab suspensions are available on tractors. Renault (figure 2.10) was the first to develop a full suspension cab but Fendt, Deutz, Same, Steyr and others followed by developing a seesaw suspension which could simply be fitted on tractors in series production [34, 40]. The effectiveness of these developments have been demonstrated since an optimally tuned combination of cab, seat and axle suspension can reduce acceleration values up to 50% compared to a stiff vehicle [91, 119].

2.3 Conclusion

The goal of this chapter was to provide some insight in the vibrational comfort problems on agricultural machinery and to give an overview of suspension systems that up to now have been used to solve those problems.

From the first section it is clear that low back pain is common among operators of agricultural vehicles. The mechanism that lies at the origin of this problem is not clear yet, but many researchers are convinced that reduction of whole body vibration could definitely improve this situation. The dominant frequencies of vibrations transmitted to the operators of agricultural machines lie in the region 0.5 to 10 Hz. This is problematic since the most critical frequency range for the human spine is 4 to 8 Hz in the vertical direction and 0.5 to 2 Hz for both the for and aft, and the lateral direction.

Vibration standards provide objective means to evaluate the severity of the vibrations the operators are exposed to. Vibration dose value (VDV) and effective root mean square (effRMS) are commonly used single number estimates of vibration severity. They incorporate the frequency depended effect of vibrations on the human spine by applying frequency weighting filters.

European legislation uses these single number estimates to set daily exposure limit and action values. These are respectively 21 $m/s^{1.75}$ and 9.1 $m/s^{1.75}$ for the VDV and 1.15 m/s^2 and 0.5 m/s^2 for the effRMS. The European Parliament tries to encourage innovation by imposing that those limit values can not be violated in new machines and that exceeding the action values indicate that improvements to the suspensions have to be made.

The second section gave an overview of several suspension systems in the transmission path between the vibration sources and the operator. All mobile agricultural machines are fitted with pneumatic tires.

These act as low-pass filters by isolating the machine form small ground surface irregularities and are considered as the first and, in many cases, the only suspension elements on agricultural machines.

Axle or primary suspension systems are most advanced in the automotive industries where even semi-active and active suspensions are introduced to deal with the conflict between comfort and road safety. Most agricultural vehicles don't have primary suspensions, with the exception of the optional front axle suspension systems on four wheel drive tractors and some spraying machines. Reasons for not implementing primary suspensions are loss of stability on significant slopes, loss of power due to energy consumption in dampers or simply too complicated and costly to realize when having to deal with all working conditions.

Two types of so called secondary suspensions are used on agricultural machines: suspended seats and cabin suspensions. The suspended seats use a scissor system to allow only vertical displacements and incorporate spring and damper elements. Current trend there is to construct seats with a low spring stiffness. As a consequence more end-stop impacts occur, having a very negative effect on the comfort behavior. Research is performed to improve the passive designs and to use active and semi-active systems. Only a few of these new designs are commercially available.

But knowing that phase difference between seat and feet of a seated operator results in discomfort and that sensory mismatch even with a perfect vibro-isolation of the driver's seat can lead to motion sickness, points out the importance of a good cab suspension. This, together with the advantage that a cabin suspension is able to protect the drivers's whole-body with respect to several degrees of freedom, makes that vibration isolation through this second type of secondary suspension is to be preferred over seat suspension.

For a cab suspension rubber cab mounts are frequently used. These mounts mainly isolate structurally induced vibrations at higher frequencies (50 Hz and above) from entering the cab and improve the acoustic comfort. Only low-frequency cabin suspensions, with a natural frequency below the vehicles dominant frequency are efficient enough to reduce the vibration transmitted to the operator. The principal of a suspended seesaw is commonly used and can be found on articulated lorries and some agricultural tractors.

Research in the field of cab suspensions on agricultural machines is

restricted to two institutes: VTT Technical Research Center of Finland and the Agricultural Engineering Department of the Swedish University of Agricultural Sciences. The research also concentrates on cabins for tractors. In Finland an active cabin suspension was developed using two hydraulic cylinders. Different control strategies were tried out. Only two degrees of freedom (vertical and roll) could be controlled, one at the time. Validation of the system using a real cabin showed reasonable improvements only up till 3 Hz due to poor dynamic behavior of the valves used and noise problems. The Swedish approach used four hydro-pneumatic elements. Optimization of the passive suspension using genetic algorithms resulted in a 40% reduction of vibrations if 10cm travel space was allowed. Active suspensions were also tested, but all results were shown on simulations and no real cabin was used to carry out tests.

As can be seen in the last part of this chapter, work needs to be done, especially in the field of low-frequency cabin suspensions for mobile agricultural machines.

Chapter 3

Assessment of the Vibrational Comfort

To be able to solve some of the low frequency vibration problems on agricultural machines, it is important to precisely analyse the present situation. All the research has been performed on a combine harvester but because off-road machinery all behave in a similar way with respect to vibrations [34, 101], the results obtained in this thesis are transferable to other types of off-road vehicles. The basic features of the combine are described in the first section. In the second section a thorough analysis of the characteristics of the machine vibrations at the base of the cab suspension is performed. The third section investigates the effect of the current cab suspension on the transmission of vibrations to the driver.

3.1 Combine Harvester

The machine used in this research is the *New Holland CX820* shown in figure 3.1. This conventional harvester with its width and height of around $3.5m$, length of over $9m$ and a weight of approximately 16 ton, is not the biggest of the mobile agricultural machines, as potato and sugar beet harvesters go above 25 ton, but a combine harvester can be seen as a representative selfpropelled agricultural machine.

With respect to vibrations this machine is equipped with pneumatic tyres and has no axle suspension system. As cab suspension, four rubber mounts are used which have as main purpose to reduce the

Figure 3.1: Combine harvester CX820

noise produced by resonating panels of the cabin. The seat installed is a classic air suspended one with hydraulic damper and air spring. This arrangement with no primary suspension and only secondary suspension elements is somewhat the general standard among agricultural machines.

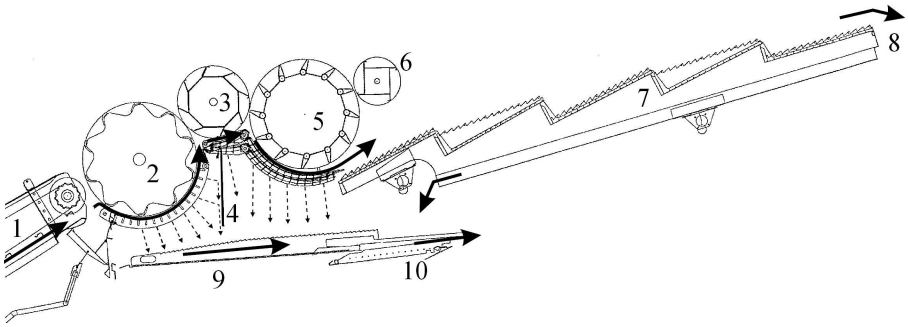

Figure 3.2: Overview of the key elements in the separation section of a conventional New Holland CX combine harvester: (1), crop elevator; (2), threshing drum; (3), *Beater*®; (4), rubber guidance flap; (5), *Rotary Separator*®; (6), straw rotor; (7), straw walkers; (8), separation loss sensors; (9), grain pan; (10), pre-sieve. [89]

Vibrations that are very specific for this machine are produced by either the elements in the header or devices in the separation and clean-

ing section of the harvester. Figures 3.2 and 3.3 give an overview of the main elements of the separation and cleaning section.

In the low frequency region, $0 - 20\ Hz$, vibrations are produced by the threshing drum with a base frequency between $11.4Hz$ at low speed and $15.5Hz$ at high speed, the cleaning fan with a base frequency at $11.7Hz$, the *Roto-Threshers*® at $12.8Hz$, the cleaning shoe (sieves in the cleaning section) at $5.1Hz$, the straw walkers at $3.7Hz$ and in the header by the horizontal knife at $9.5Hz$ and the auger at $5.9Hz$. No contribution of the motor can be found in this region since the idle speed of the engine is 1320 *rpm* or $22Hz$ and for a 6 cylinder engine the first major contribution to vibrations is situated at the third harmonic of this frequency.

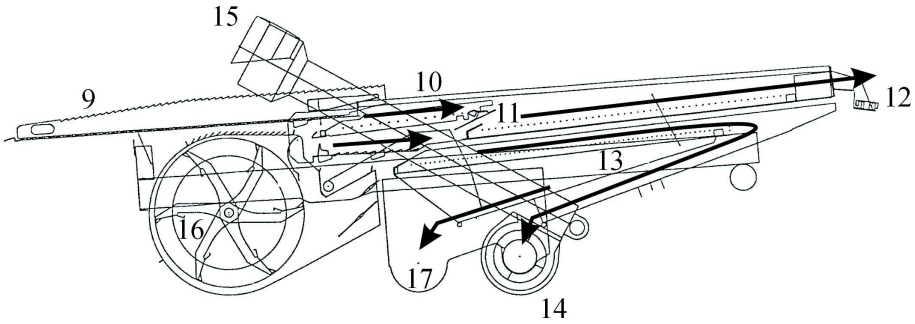

FIGURE 3.3: Overview of the key elements in the cleaning section of a New Holland combine harvester: (9), grain pan; (10), pre-sieve; (11), upper sieve; (12), sieve loss sensor; (13), bottom sieve; (14), return flow cross augers and *Roto-Threshers*®; (15), return auger and return flow impellers; (16), cleaning fan; (17), cross auger collecting the clean grain flow. [89]

A modal analysis on the cabin revealed no flexible modes of the ground plate in the low frequency range (below 20Hz) [4]. The cabin mounts are attached to this ground plate and therefore in this study the cabin is considered to be a rigid body and only the influence of the suspension elements on the six rigid body movements is investigated. This is similar to the approach of other researchers dealing with cabs of tractors [61, 133] and counterbalance trucks [14, 85].

3.2 Properties of the Vibration Load

3.2.1 Measurement Setup

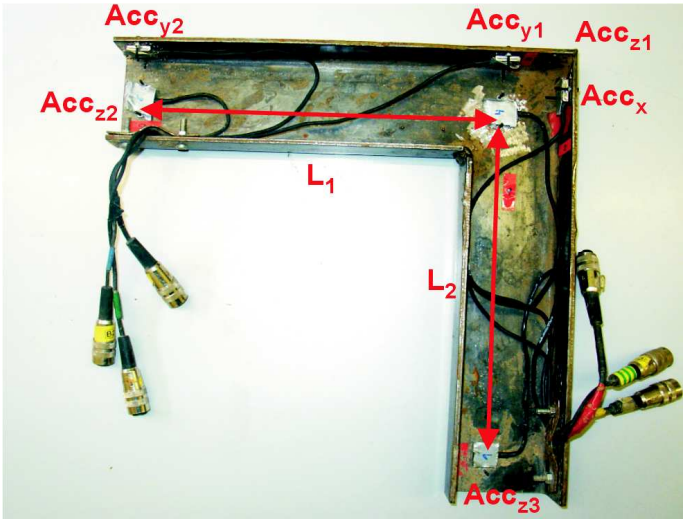

Figure 3.4: L-shape measuring device with six *Kistler* accelerometers

The first step in the evaluation of the current situation, is to measure the properties of the incoming vibrations at the base of the cab suspension. To do this an L-shaped measuring device was constructed on which 6 accelerometers were placed. In this way the 6 rigid body movements, three translations and three rotations, could be recorded by placing that one measuring device on the structure. The fixed distances between the different accelerometers made it straight forward to calculate the rotations.

The following equations give the expression for the angular accelerations in roll, i.e. rotation around the x-axis, in pitch, i.e. rotation around the y-axis, and in yaw, i.e. rotation around the z-axis.

$$\begin{aligned} roll &\cong \frac{Acc_{z3} - Acc_{z1}}{L_2} \\ pitch &\cong \frac{Acc_{z1} - Acc_{z2}}{L_1} \\ yaw &\cong \frac{Acc_{y2} - Acc_{y1}}{L_1} \end{aligned} \tag{3.1}$$

L_1 and L_2 are the distances between the accelerometers as indicated on figure 3.4. Acc_x,Acc_{y1},Acc_{y2},Acc_{z1},Acc_{z2} and Acc_{z3} are the six accelerometer signals obtained by the accelerometers as indicated on the figure.

K-Beam ® *8305A1M2* capacitive accelerometers of *Kistler* were used in order to measure low-level, low-frequency vibrations and even static accelerations. The L-shape is placed on the supporting structure underneath the center of gravity of the cabin, thus recording the vibrations at the base of the suspension (see figure 3.5).

To get an idea of the occurring vibrations, a whole range of measurements was performed under different operational conditions from road transport to fully operational activities in the field. First different stationary conditions were tested. These situations occur when the machine is positioned outside the crop, and fan, drum and header are started up before moving into the crop to harvest. The second group of measurements considered a fully operational machine driving through the crop at different field speeds (2 to $8km/h$). For transport on the road the measurements can be split into two parts: driving on an unpaved road at a moderate speed (5 to $11km/h$) and driving on a paved road at full speed (15 to 28 km/h). All the speeds mentioned are common velocities used by professional drivers.

Table 3.1 labels all the conditions tested. In this table fully operational means that the drum is running at $850rpm$, the fan at $720rpm$ and that the header is engaged. Transport condition on the other hand means that the separation and cleaning section of the harvester is shut down and the header is dismounted.

Every condition was monitored during several minutes to be able to give a clear picture of the average vibration load in every situation. By this the effect of transients was also reduced to a minimum. All measurements were performed using a 200 Hz sample frequency and were filtered using a low pass filter with cutoff frequency of $40Hz$ to prevent aliasing.

Figure 3.5: Placement of the L-shaped measuring device on the supporting structure of the cabin, indicated by the arrow

The signals recorded by the accelerometers were converted into the accelerations for the 6 DOFs. By removing the average of the signal only the variations around the static acceleration were considered. Figure 3.6 gives an example of five seconds of this recalculated data.

Throughout this thesis x will denote the longitudinal direction (the driving direction of the machine), while y will be used for the lateral direction and z for the vertical direction. In that way the meaning of 'pitch', 'yaw' and 'roll' becomes clear.

3.2.2 Frequency Domain Analysis of the Measurements

To analyze the acceleration signals in the frequency domain the power spectral density (PSD) was used. The PSDs were calculated using 4096 points per window, with an overlap of 2048 points. To smooth the effect of leakage, a Hanning window was applied. These parameters were

Number	Description
I	Stationary, drum at $650rmp$, fan at $720rpm$
II	Stationary, drum at $700rmp$, fan at $720rpm$
III	Stationary, drum at $750rmp$, fan at $720rpm$
IV	Stationary, drum at $800rmp$, fan at $720rpm$
V	Stationary, drum at $850rmp$, fan at $720rpm$
VI	Stationary, drum at $900rmp$, fan at $720rpm$
VII	Stationary, fully operational
VIII	Driving on the field at $2km/h$, fully operational
IX	Driving on the field at $4km/h$, fully operational
X	Driving on the field at $6km/h$, fully operational
XI	Driving on the field at $8km/h$, fully operational
XII	Driving on an unpaved road at $5km/h$, transport
XIII	Driving on an unpaved road at $8km/h$, transport
XIV	Driving on an unpaved road at $11km/h$, transport
XV	Driving at on a paved road $15km/h$, transport
XVI	Driving at on a paved road $20km/h$, transport
XVII	Driving at on a paved road $25km/h$, transport
XVIII	Driving at on a paved road $28km/h$, transport

TABLE 3.1: Vibration conditions tested on the combine harvester

identical in every case to avoid to disfigure the results when comparing different measurements in one figure. With a sample frequency of $200Hz$ a frequency resolution of $200/4096 \approx 0.05\ Hz$ was obtained.

Figure 3.7 gives the PSDs for the measurements shown in figure 3.6. Only the low frequencies between 0 and $20Hz$ are shown, since the vibrations in this region are the most harmful for the operators back as discussed in chapter 2. Every other PSD shows this region of frequency. The peaks in the PSD correspond with certain vibrations occurring in the measurements and the height of the peak indicates the severity of that vibration thus pinpointing the specific problems.

Figure 3.8 shows what can be analyzed when comparing PSDs of several measurements. In this so called waterfall diagram the vertical accelerations underneath the cabin for all stationary regimes (I-VI) are shown. The peak at approximately 1 Hz is due to the natural frequency of the tires. The variation of the drum speed is clearly visible. Other peaks can also be detected and their specific frequency makes it possible to link them with certain rotating or translating elements within the machine. Cleaning shoe (a first and second order peak), straw walkers

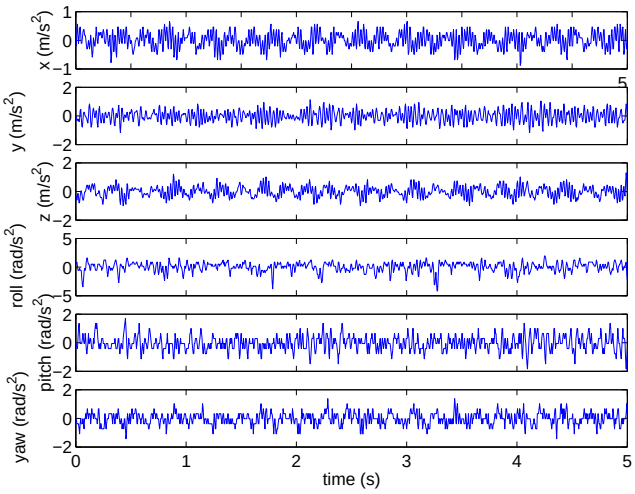

Figure 3.6: A five second frame of accelerations measured at the base of the cabin in condition II

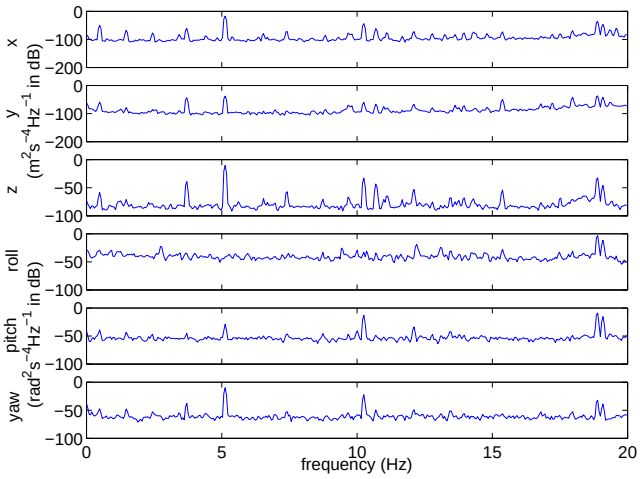

Figure 3.7: Power spectral density of the accelerations at the base of the cabin in condition II

and fan are indicated in figure 3.8. These are, together with the drum, the main vibration sources in the stationary regimes for this combine

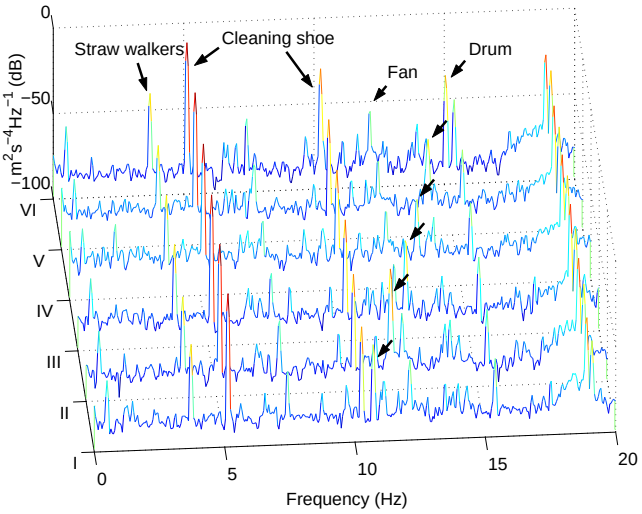

FIGURE 3.8: Waterfall diagram of the vertical accelerations underneath the cabin for different stationary regimes

harvester. The overall level is approximately -85dB but peaks can be seen up till -15dB for the cleaning shoe which means that the cleaning shoe produces a vertical vibration which is 275 times higher than the overall level.

The effect of the engagement of the header and the movement during harvesting can be derived from figure 3.9. The overall level of vertical vibrations increases with some 15dB and a clear peak at 9Hz is introduced by the knife.

With increasing speed two phenomena can be seen clearly. First there is the introduction of an amount of vibrations in the range from 0.5 Hz to 2.5 Hz. The level of vibrations for a harvesting speed of 8 km/h gets to approximately -40 dB which is 30 dB above the vibration level in a stationary condition. These vibrations are introduced by the unevenness of the soil profile [24, 69], that excite the roll, pitch and jump mode of the machine on its tires.

Secondly there is a speed dependent effect visible. At 2 km/h vibrations are introduced slightly above 2 Hz, at 4 km/h vibrations enter at 4 Hz. This gradually shifts to 8 Hz for 8 km/h. Also the level of these vibrations increases with increasing speed. Those vibrations are

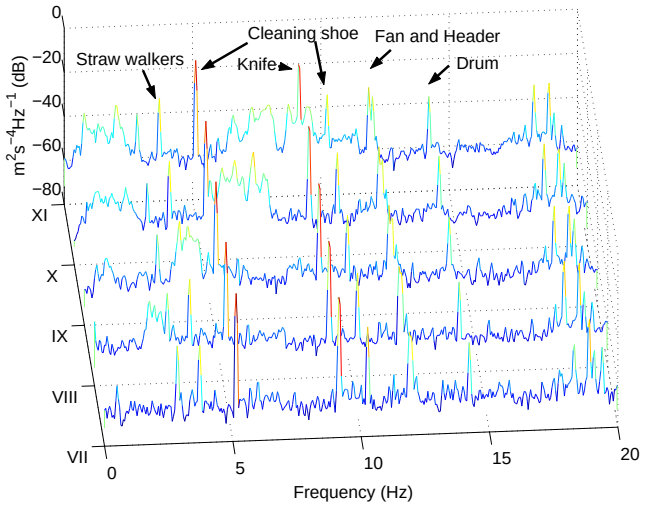

Figure 3.9: Waterfall diagram of the vertical accelerations underneath the cabin for 5 fully operational harvesting regimes (0 to $8km/h$)

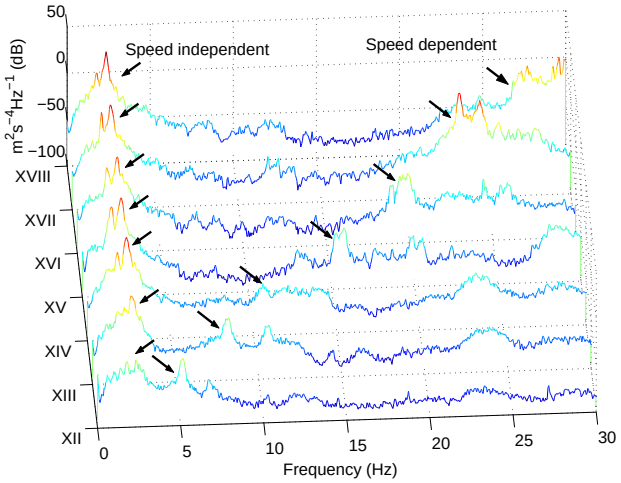

Figure 3.10: Waterfall diagram of the vertical accelerations underneath the cabin for 7 transport conditions (5 to $28km/h$)

caused by the lugs on the front tires of the machine. These lugs have a spacing of approximately 27 cm. For the rear tires with a spacing between the lugs of 20 cm, a similar effect is visible in figure 3.9.

These speed dependent (lugs) and independent effects (level between $0.5Hz$ and 2.5 Hz) can be shown more clearly when comparing the 7 transport conditions as has been done in figure 3.10. Here the vibrations of the header and the threshing and cleaning elements of the machine do not appear and the interaction between tires and road is more pronounced.

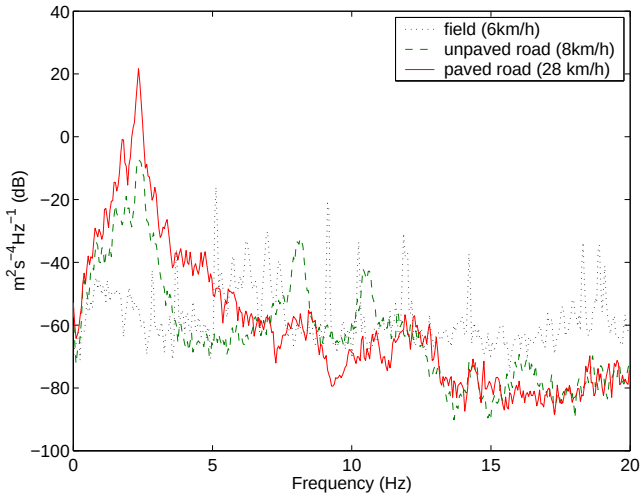

FIGURE 3.11: Comparison between the power spectral densities of the accelerations at the base of the cabin for harvesting at $6km/h$ and driving on a road at 8 and $28km/h$

All figures only expose measured vibrations in the vertical direction. It is clear that certain effects pop up more explicit when looking at the accelerations in an other direction. The effect of the knife for example, which moves in the lateral direction, gives rise to a peak with an amplitude that exceeds the average lateral level with 60 dB.

Figure 3.11 compares the vertical accelerations for three conditions: harvesting on the field at $6km/h$ (condition X), driving at $8km/h$ on an unpaved road (XIII) and at $28km/h$ on a paved road (XVIII). Which of these three conditions is the worst, is difficult to determine. Elements within the machine create several high peaks at specific frequencies

while the effect of riding at higher speeds results in a more broadband aggravation of the vibrational conditions. This band is concentrated in the low frequencies while the peaks of the elements can also occur at higher frequencies.

3.2.3 Time Domain Analysis of the Measurements

To overcome the difficulties of deciding which conditions are the worst for the operator of the machine, the vibrations can be quantified using the single number estimates effRMS and VDV mentioned in chapter 2. Table 3.2 gives these calculated values together with the crest values for the six DOFs of five conditions: two stationary conditions (V and VII), a harvesting condition at 6 km/h (X) and two transport conditions at 11 km/h and 28 km/h (XIV and XVIII).

The VDV is calculated using a time frame of $5min$. For an eight-hour period this value has to be multiplied with 3.13. The values indicated with $\sum$ in the table, are combined VDV and effRMS values. For the combination of effRMS values, equation 2.5 is used. The combined VDV is given by:

$$VDV_{comb} = (VDV_{xs}^4 + VDV_{ys}^4 + VDV_{zs}^4)^{1/4}. \tag{3.2}$$

The values shown in table 3.2 are comparable with those obtained in literature for other agricultural equipment like tractors [56, 116]. Also crest factors above 6 are observed which are typical in agriculture where a lot of shocks occur on mobile machinery during field operations. In these cases the VDV is preferred over the effRMS. Since the crest factor is not consistently above 6, both VDV and effRMS will be used in this thesis to evaluate the vibrations.

VDV and effRMS show clearly that there is a large influence of driving on the translational vibrations. Especially in the vertical direction, levels 3 to 4 times higher can be observed. There is also an increase in rotational vibrations, but here field and even stationary measurements can result in a higher discomfort. Overall, driving on a road at high speed can be considered as the worst condition since the translational levels are the highest and the rotational levels are also relatively high.

Comparing the values in the table with the daily exposure limit and action values described in European legislation (see section 2.1.4), shows that only the stationary conditions stay well below the action values for both the effRMS and the VDV. The action value of 0.5 m/s^2

RMS	V	VII	X	XIV	XVIII
X-axis	0.0662	0.0737	0.1007	0.1661	0.1335
Y-axis	0.0486	0.1135	0.1025	0.4583	0.2800
Z-axis	0.2722	0.3501	1.0078	0.6759	1.2081
$\sum$	0.2955	0.3981	1.0277	0.9605	1.2838
roll	0.2797	0.3558	0.9810	0.2172	0.4270
pitch	0.1105	0.5411	0.3955	0.1893	0.2787
yaw	0.0780	0.5551	0.1150	0.1224	0.1126

VDV	V	VII	X	XIV	XVIII
X-axis	0.3285	0.3789	0.5421	1.0899	0.6952
Y-axis	0.2606	0.5985	0.5670	3.2427	1.5729
Z-axis	1.4321	1.9135	5.1673	3.7664	6.9687
$\sum$	1.4335	1.9187	5.1677	4.2069	6.9734
roll	1.6133	1.9317	5.3093	1.6786	2.3826
pitch	0.6243	3.0438	2.1405	1.1674	1.5695
yaw	0.4414	3.0626	0.6273	0.8092	0.6331

crest	V	VII	X	XIV	XVIII
X-axis	2.5559	2.7340	3.0520	4.5792	3.1751
Y-axis	3.6847	3.0266	4.2816	6.3061	3.5731
Z-axis	3.5370	4.0949	3.1287	5.1655	5.6754
roll	2.5993	3.5316	2.7268	7.5571	4.1719
pitch	4.1516	3.3601	3.8001	6.2235	4.5096
yaw	4.2903	3.6834	3.6703	4.2448	3.6475

TABLE 3.2: Calculated RMS, VDV en Crest values for 5 measured conditions

for effRMS is violated during harvesting and transport at moderated speed, but at high speed even the exposure limit of 1.15 m/s^2 is exceeded for the vertical axis. The VDV action value of 9.1 $m/s^{1.75}$ is violated within 48 minutes of harvesting and 15 minutes of transportation at high speed. The limit value 21 $m/s^{1.75}$ is only exceeded after 6.8 hours of transport and 22 hours of harvesting. Looking at the combined values, the vertical direction is the main factor for discomfort in the machine vibrations.

3.3 Evaluation of Cab Suspension

3.3.1 Vibrational conditions inside the cab

When investigating the vibrations the driver of agricultural machinery is exposed to, not only the vibrations exciting the cabin are important, also the effect of the cabin suspension on the transmission of those vibrations, has to be analyzed.

In order to do so, additional accelerometers were placed on the floor inside the cab during the measurements. These accelerometers made it possible to calculate the accelerations occurring on the floor right beneath the center of gravity of the cab. The following table gives the calculated VDV and effRMS inside the cabin for 3 different conditions: harvesting on the field at 6 km/h (X) and transport condition on the road at 11 (XIV) and 28 km/h (XVIII).

RMS	X	XIV	XVIII
X-axis	0.1073	0.2473	0.2026
Y-axis	0.1002	0.6039	0.4750
Z-axis	1.4186	0.9779	1.8706
$\sum$	1.4262	1.1756	1.9406
roll	0.9499	0.3016	0.7623
pitch	0.3472	0.2247	0.4417
yaw	0.1524	0.1441	0.1358

VDV	X	XIV	XVIII
X-axis	0.5773	1.6023	1.0548
Y-axis	0.5534	4.2823	2.6678
Z-axis	7.1820	5.4481	10.7938
$\sum$	7.1821	5.9147	10.8041
roll	5.1298	2.3301	4.2527
pitch	1.8879	1.3883	2.4878
yaw	0.8313	0.9529	0.7636

Table 3.3: Calculated VDV and effRMS values inside on the cabin floor for 3 measured conditions

Looking at table 3.3 field work for 8 hours with this machine becomes problematic since the VDV and effRMS exceed the limit value given in European regulation. Transport on the road for more than an

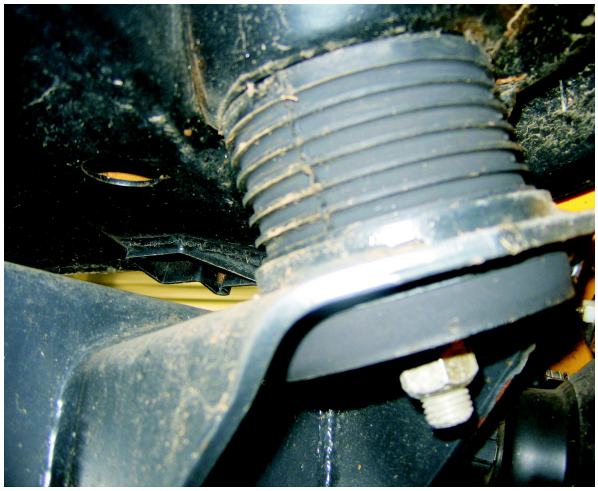

FIGURE 3.12: Photograph of a rubber mount

hour would not be allowed either. A remark has to be made here that the negative or positive effect of the seat suspension is not incorporated in these values

Comparing the values of table 3.3 with those of table 3.2 shows that in almost every condition and for every direction the current suspension system enlarges the discomfort. The amount of degradation of the comfort is speed related, since higher speed leads to a higher increase of the comfort values between base and cabin floor.

3.3.2 Rubber mounts

The only elements responsible for this, are the rubber mounts of the cab suspension. Their behavior in the low frequency range up to 10 Hz, where the comfort filters of BS and ISO put emphasis on, should be investigated closer.

Figure 3.12 shows a rubber mount. Four of those rubber blocks are used at the corners of the cab and are placed such that the intersection point of the centerline of the two mounts in front and that of those at the back is on a vertical line near the center of mass of the cab. These points are situated at approximately 1.5 and $2m$ above the cabin floor.

A method to determine the efficiency of vibration isolation offered by these blocks, is by calculating the transmissibility of the vibrations

between support and cab floor. This is done by determining the frequency response function (FRF) $H(j\omega)$, which is the ratio between response of the system and the input as a function of frequency. The FRF for a time invariant single-input single-output (SISO) system, can be directly calculated by:

$$H(j\omega) = \frac{Y(j\omega)}{X(j\omega)}. \tag{3.3}$$

$X(j\omega)$ and $Y(j\omega)$ denote the Fourier coefficients of respectively the excitations and the steady-state response of the system.

In practice however, input as well as output measurements (subscript m) may be perturbed by stochastic errors and the measured Fourier coefficients differ from the true ones due to e.g. noise in the device under test, ambient noise and measurement noise. Assuming that these perturbations are additive, the following errors-in-variables model can be used:

$$\begin{aligned} X_m(j\omega) &= X(j\omega) + n_x(j\omega), \\ Y_m(j\omega) &= Y(j\omega) + n_y(j\omega), \end{aligned} \tag{3.4}$$

where $n_x(j\omega)$ and $n_y(j\omega)$ stand for the contribution of all the perturbing noise sources at the input and the output.

The measured FRF, also called the empirical transfer function estimate (ETFE [87]) becomes:

$$H_m(j\omega) = \frac{Y_m(j\omega)}{X_m(j\omega)} = H(j\omega)\frac{1 + n_y(j\omega)/Y(j\omega)}{1 + n_x(j\omega)/X(j\omega)}. \tag{3.5}$$

The use of averaging techniques can decrease the effect of the stochastic errors on the FRF estimate. Therefore other alternative ways (H_1, minimizing the error on the response, H_2, minimizing the error on the excitation) of calculating the frequency response function using averaged auto and cross power spectra of input and output signals have been proposed [10].

In this work the FRFs will be estimated using:

$$\hat{H}_{EV}(j\omega) = \frac{\frac{1}{M}\sum_{i=1}^{M} Y_i(j\omega)}{\frac{1}{M}\sum_{i=1}^{M} X_i(j\omega)}, \tag{3.6}$$

with $\hat{}$ denoting the averaging and M the number of periods.

FIGURE 3.13: Setup for evaluation of the rubber mounts by excitement under rear tire of the combine

This estimator has the advantage over the methods with power spectra that it is unbiased when a deterministic excitation is used and generation and acquisition of the signals is synchronized [58, 124]. For more detailed information on this topic, the reader is referred to Pintelon and Schoukens [106].

To be able to establish the transfer functions of the rubber mounts, a method was used where the combine was excited under one of its tires with several excitation signals. This method has been succesfully applied in the work of Clijmans [23, 7], where the behavior of a whole sprayboom could be analyzed using this technique.

To derive clear FRFs, the structure has to be properly excited in the frequency range of interest. For this a vertical electro-hydraulic shaker was used. The shaker consists of a piston pump with electromotor ($22kW$), an oil reservoir, a double rod piston (stroke $180mm$) and a 4-way servo valve with a nominal flow rate of $40\ l/min$. An inductive type displacement sensor, fed back and adjusted to the desired displacements through an analog PID controller, measures the displacements of the piston rod. The top of the piston rod is linked by a spherical joint with a horizontal plate [23]. Due to a lack of force only one of the rear tires of the combine could be positioned on the plate, as can be seen on figure 3.13.

Figure 3.14: Placement of the accelerometers to determine the behavior of the rubber mounts

Accelerometers (*K-Beam* ® *8305A1M2*) were placed (see figure 3.14) at the mounting points of the rubber blocks. The accelerometers measured the vibrations in axial direction, along the centerline of the rubber mounts.

The following excitation signals were used: swept sine, multisine, Schroeder multisine and periodic noise. For a clear discussion on the properties of these excitation signals with respect to the determination of FRFs, the reader is referred to dedicated literature [106, 118]. All signals were 4096 points long, sampled at 200 Hz, had a frequency content between 0.1 and 20 Hz and were repeated 6 times. To deal with transient effects, the first period was discarded.

Figure 3.15 shows the amplitude of the FRF of one of the front rubbers for the four different excitation signals and the average of these four signals. Similar FRFs were found for the other three rubber mounts.

With exception of a few peaks which might be attributed to the lack

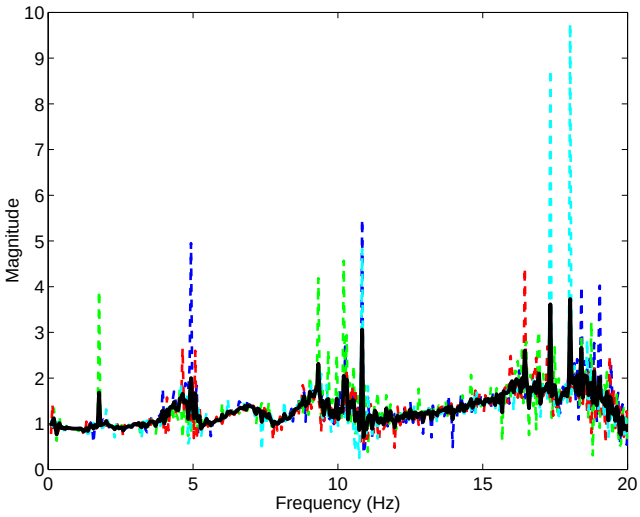

FIGURE 3.15: Magnitude of the frequency response function of the front cabin mount obtained with the average (black) of four different excitation signals: swept sine (dark blue), periodic noise (green), Schroeder multisine (light blue), multisine (red).

of power in the hydraulic shaker, all four signals show similar FRFs. This means that in this frequency range the behavior of the rubber mounts can be considered to be rather linear. Therefore their effect on incoming vibrations under working conditions for this machine can be approximated by the average FRF.

It is clear that below $20Hz$ this suspension system will only amplify the entering vibrations. The shape of the amplitude of the FRF also explains why higher speeds lead to higher amplification of the VDV and effRMS. The main amplification by the rubber mounts starts from $5Hz$ onwards. This is also the region where there is an increase in the level of vibrations with higher speeds.

It is clear that if the level of vibrations in the cabin have to be decreased, the old cabin mounts have to be replaced by new types of isolation devices. For a good attenuation in the low frequency region, devices with a low natural frequency have to be looked for.

3.4 Conclusion

To list the low-frequency vibrational comfort problems occurring on agricultural machines, a closer study was performed on a *New Holland CX820* combine harvester. Since all selfpropelled agricultural machinery behave similar with respect to vibrations, the results of this study give a good description of common comfort problems. The *New Holland CX820* has no primary suspension and only secondary seat and cab suspensions, which is the general standard among agricultural machines.

Modal analysis on the cabin revealed no flexible modes of the ground plate in the low-frequency range. Therefore in this study the cabin is considered to be a rigid body and only the influence of the suspension elements on the six rigid body modes is investigated. This is similar to the approaches of other researchers dealing with tractor cabs and cabins for counterbalance trucks.

Frequency analysis of the various measurements performed under different working conditions for the machine, stationary, harvesting and transport, showed various peaks in the power spectral densities of the accelerations measured underneath the cabin. Many peaks could be related to rotating and translating elements within the machine.

With increasing speed, two phenomena were observed. First there was an increase in vibrations in the range of 0.5 to 2.5 Hz. The level for a harvesting machine at a speed of 8 km/h got approximately 30 dB above the stationary level. These vibrations can be related to the unevenness of the soil profile. Secondly increasingly higher levels of vibrations were observed at frequencies related to the speed of the machine. These speed dependent effect is created by the lugs of the tires used on the machine.

The use of vibration dose value (VDV) and effective root mean square (effRMS), the single number estimates of vibration severity, showed frequent violation of action and limit values prescribed in European regulation. Especially the vibrations in the vertical direction were problematic with violation of the limit value for effRMS during harvesting and transport at 28 km/h. VDV action values were exceeded within an our of harvesting and merely 12 minutes of transport. The effect of the seat suspension was not incorporated.

Measurements inside the cabin showed that the rubber mounts deteriorated in most cases the vibrational conditions for the operator of

the machine. VDV values got above the limit value within 8 hours of harvesting and within the hour of transport. Determination of the frequency response function of one of the rubber supports of the cabin showed clear amplification of the vibrations beneath 20 Hz.

Clear indication of the mediocre low-frequency behavior of the rubber mounts, makes it obvious that to prevent violation of limit and action values, better low-frequency cabin suspensions have to be developed.

Chapter 4

Development of Vibration Reducing Cab Mounts

The previous chapter made clear that additional vibration attenuation is needed and that to attenuate the vibrations with an efficient cabin suspension, new elements have to be developed that show a better transfer function in the low-frequency region than the frequently used rubber mounts . When considering a second order system, attenuation is only possible beyond $\sqrt{2}$ times the natural frequency. Since the first main peak in the spectrum of the input vibrations is around 2 Hz, natural frequencies of a suspension system near $1 - 1.5$ Hz or lower have to be aimed for. This chapter searches for isolator elements that meet this demand.

A first introduction discussing commercially available solutions is followed by two sections where a hydro-pneumatic and a pneumatic system are addressed. In both cases white box models based on physical principles are developed and compared with measurements on experimental setups. The purpose of the white models is to gain insight in the functioning of the systems and to provide a parametric model that can be optimized. In a fourth section the pros and cons of both solutions are compared and a conclusion is drawn to witch cab mount will be used in the final setup.

4.1 Introduction

Commercially available suspension systems with a low natural frequency, frequently incorporate pneumatic devices. Those elements are easy to build in because there is no problem with static deflection as is the case with mechanical springs [131]. In addition by changing the pressure in the pneumatic element, spring characteristics can be simply adapted or the system can become self levelling independently of the payload [60]. The low natural frequency of such systems however can provoke motion sickness [56]. Therefore these systems are often combined with a damper, in most cases a hydraulic one. The Cabin Air Levelling Module of SF Sachs and Wabco is a good example of such a system [138].

An alternative way of providing a low natural frequency is the use of hydro-pneumatic elements. They consist of a hydraulic cylinder and an accumulator, containing gas under pressure within a diaphragm. This 'balloon' compresses like a normal spring in case pressurized fluid is forced into the accumulator. When the pressure drops the gas pushes the fluid back out of the accumulator. Damping in this system is created by a constriction between accumulator and cylinder. Such elements can be found as axle suspension on sprayers (Delvano, Knight and Toselli). Giliomee and Els [53] discussed the use of a semi-active variant on armed fighting vehicles and heavy off-road vehicles. Citroën had already introduced a car suspension based on hydro-pneumatic devices in the forties.

4.2 Hydro-pneumatic suspension system

The hydro-pneumatic system studied here consists of a hydraulic cylinder with a rod diameter of $18mm$, a cylinder diameter of $32mm$ and a stroke of 190 mm. The two ports of the cylinder are connected with two nitrogen bulbs of $2.5l$, called accumulators, containing approximately 1.5 l nitrogen. Between the cylinder and one of the bulbs, a valve is placed to provide the damping. The idea is to put four of these elements underneath a cabin. The system has to support a weight of $185kg$, which is near to one fourth of the 705 kg of a normal cabin. Figure 4.1 shows the physical system and indicates all elements of the hydro-pneumatic suspension.

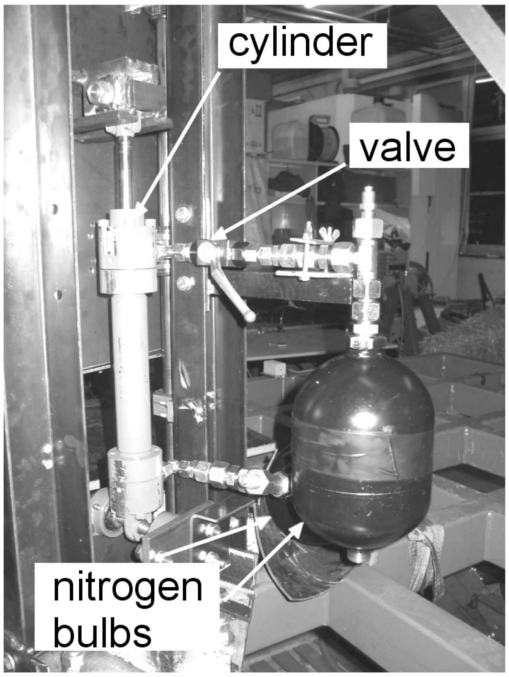

FIGURE 4.1: Photograph of the hydro-pneumatic setup

4.2.1 Modelling

The model of the suspension is derived starting from a more schematic representation of the system (see figure 4.2). The idea is to find a relation between the movement of the mass y and the input x. This leads to a so called 'base motion' model of a quarter cabin. Applying Newton's law to the mass m results in the following equation:

$$m\ddot{y} = p_2 S_{cyl} - mg - p_3(S_{cyl} - S_{rod}) - F_W, \tag{4.1}$$

with $\ddot{y}$ the acceleration of the mass, p_2 and p_3 the pressures in the system (see Fig 4.2), S_{cyl} the surface of the piston, S_{rod} the surface of the rod, g the gravitational acceleration and F_W the friction force acting between piston and cylinder.

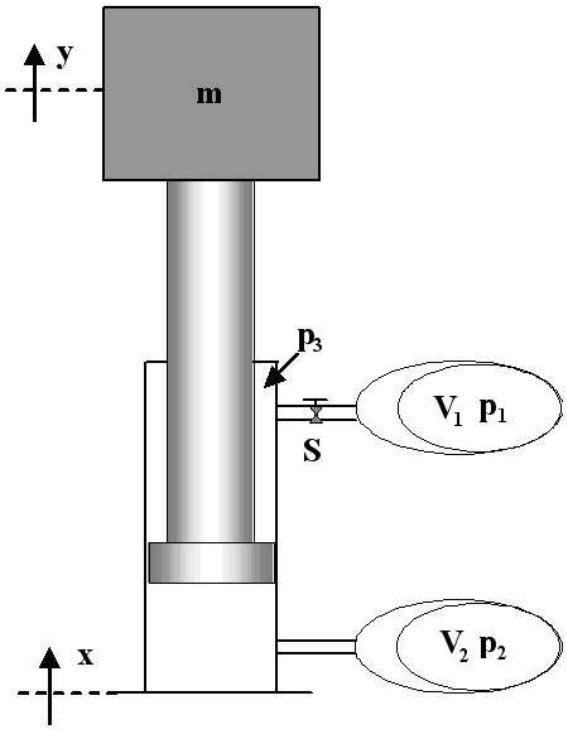

Figure 4.2: Scheme of the hydro-pneumatic setup (p_i pressures, V_i volumes of the nitrogen, x and y positions of respectively ground and mass m)

Since the vibrations result in fast compression and expansion of the nitrogen in the bulbs, transformations of the nitrogen are considered to be adiabatic [18]. The adiabatic law:

$$pV^{\kappa} = constant, \tag{4.2}$$

in which V stands for the volume and κ for the ratio of specific heats of nitrogen, is applied to the two nitrogen bulbs. Owing to the incompressibility of the oil in the cylinder, the volume of nitrogen in the bulbs is determined using the initial volumes V_{i0} together with the positions x and y. This leads to the following two equations:

$$\begin{aligned} p_{10}V_{10}^{\kappa} &= p_1\left(V_{10} + (y-x)\left(S_{cyl} - S_{rod}\right)\right)^{\kappa}, \\ p_{20}V_{20}^{\kappa} &= p_2\left(V_{20} + (x-y)\, S_{cyl}\right)^{\kappa}, \end{aligned} \tag{4.3}$$

with index $_0$ indicating the initial conditions. These two equations generate the pressures p_1 and p_2.

Pressure p_1 can be related to pressure p_3 and the velocities $\dot{x}$ and $\dot{y}$ using equation 4.4 which describes the rate of oil flow through the valve [11]:

$$(S_{cyl} - S_{rod})(\dot{y} - \dot{x}) \cong S\sqrt{p_1 - p_3}, \tag{4.4}$$

with S the surface of the opening of the valve.

The only unknown in equation 4.1 is the friction force F_W. The friction between the cylinder and the rod causes stick-slip behavior and is therefore described by the following function [9]:

$$F_W = F_C + (F_s - F_C)e^{-((\dot{y}-\dot{x})/\dot{x}_s)^2} + F_v(\dot{y} - \dot{x}), \tag{4.5}$$

in which F_C is the minimum Coulomb friction, F_s the level of static friction and F_v the viscous friction term. The parameter $\dot{x}_s$ is empirically determined and is set to $0.003m/s$. It regulates the transition between the static friction and the Coulomb friction, called the Stribeck effect, and is not a critical parameter in this model, since variations up to 100 % change VDV of signals with less than one percent only.

The combination of equations 4.1 to 4.5 results in a non-linear model of the hydro-pneumatic suspension.

4.2.2 Measurements

To verify the correctness of this model, a comparison has been made between the model and the real physical system (see figure 4.1). Therefore the physical system was placed on a hydraulic shaker that applied several vertical vibration signals to it. The accelerations of the input ($\ddot{x}$) and the output ($\ddot{y}$), were recorded using accelerometers. The input accelerometer was placed on the shaker at the base of the suspension, while the accelerometer recording the output was positioned on the vibrating platform that was supported by the suspension. The model was implemented in Matlab [92] and the measured input accelerations were used as excitations to the model.

Figure 4.3 compares the FRFs of the Matlab model and the physical system when excited by a swept sine displacement signal with a frequency content between 0.8 and 5 Hz, a constant rate of sweep, a duration of 41 s and an amplitude of 1.5 cm.

When using the following values for the coefficients: $F_s = 220\ N$, $F_C = 100\ N$, $F_v = 2\ Ns/m$, $p_3 = 3.5\ MPa$, $S = 9.6\ mm^2$ and nitrogen volumes of 1.5 l, it can be seen that there is good agreement between the model and the experimental results. Some simple experiments give an indication of the coefficients values. Determining the maximum static load the suspension can carry without any movement for example, provides F_s. The minimum load needed to keep the suspension vibrating at a certain frequencies makes it possible to determine F_C and F_v. FRF of the model and the measurement show two peaks, one at 1.1 and a second at 1.7 Hz. These come from the non-linear behavior of the enclosed nitrogen. The disagreement between both FRFs near 3 Hz is due to a structural problem with the setup.

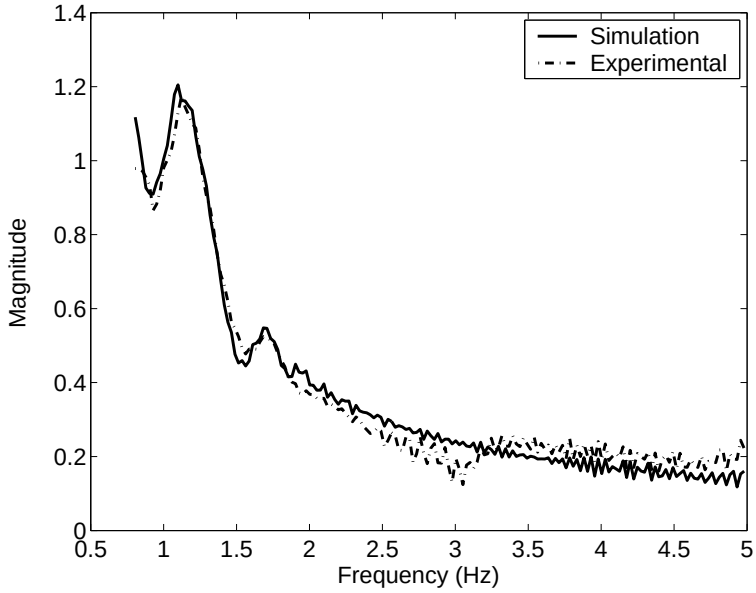

Figure 4.3: Comparison between the magnitude of the Frequency Response Function of the model (solid line) and the physical system (dashed line) for a swept sine excitation signal

Figure 4.4 compares the output of the model with the measured output when the system is excited by a multisine having the same frequency content and duration as the swept sine and a maximum amplitude of $1.5cm$.

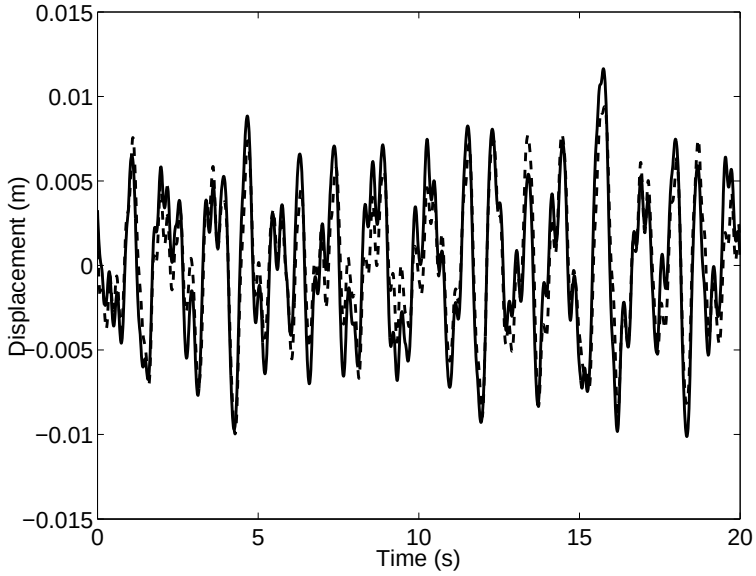

FIGURE 4.4: Comparison in time domain between the output of the model (solid line) and that of the physical system (dashed line) for a multisine excitation signal

Since the objective is to look for improvements concerning comfort behavior, it is of great importance that the VDV of the output of the model is closely related to the VDV of the measured signal. For the multi sine as input, shown in figure 4.4, following equation describes the error in the prediction of the VDV:

$$\frac{|VDV_{real} - VDV_{model}|}{VDV_{real}} = \frac{|1.794 - 1.673|}{1.794} = 0.068. \qquad (4.6)$$

The error is approximately 7 % for the multisine and with 3 % even less for the swept sine. The model is considered to be a useful simulation of the real suspension system.

4.2.3 Discussion

The advantage of this system is that with some knowledge of simple physics like the law of adiabatic compression of a fluid, the flow of a fluid through a nozzle and friction, a model can be built that represents the real setup quite accurately. This makes it possible to use this model in the design phase of the cab suspension system and give a realistic idea of the behavior of the cab suspension without actually having to build the system.

The total height of the setup (figure 4.1) is approximately 300 mm when the cylinder is in its mid position. This makes the device unsuitable as a replacement for the actual suspension system (rubber mounts of approx 80 mm) since a whole new support system should be constructed. A full cab suspension would require six of these devices, to deal with all six DOFs. Due to the relatively low mass of the cabin, low friction hydraulic cylinders are required with an approximated cost of € 800 a piece.

The hydro-pneumatic suspension system is a good system with respect to attenuation of vibrations. The magnitude of the FRF of the model (see figure 4.3) shows a natural frequency around 1.2 Hz with a reasonable low amplification at this frequency and a good attenuation of the frequencies beyond 1.5 Hz, as put forward at the start of this chapter. Despite the good behavior of the element a cheaper and smaller device is preferred.

4.3 Pneumatic suspension system

To overcome the shortcomings of the previous system an alternative system based on a pneumatic spring is considered. A large variety of springs exist as can be seen in catalogues like the Firestone Airstroke and Airmount Engineering Manual & Design Guide [50]. The type used here is the *Firestone Airmount 1M1A-1*. Looking at its datasheet of figure 4.5 it can be seen that the design height of this spring is 75mm which means that there are no built in problems with this spring.

The natural frequency of this air spring remains almost constant, independent of the pressure inside the air spring. This can be explained by looking at the expression for the spring stiffness k of this air spring. The spring stiffness determines the relation between the force F acting on the air spring and the height h of the spring.

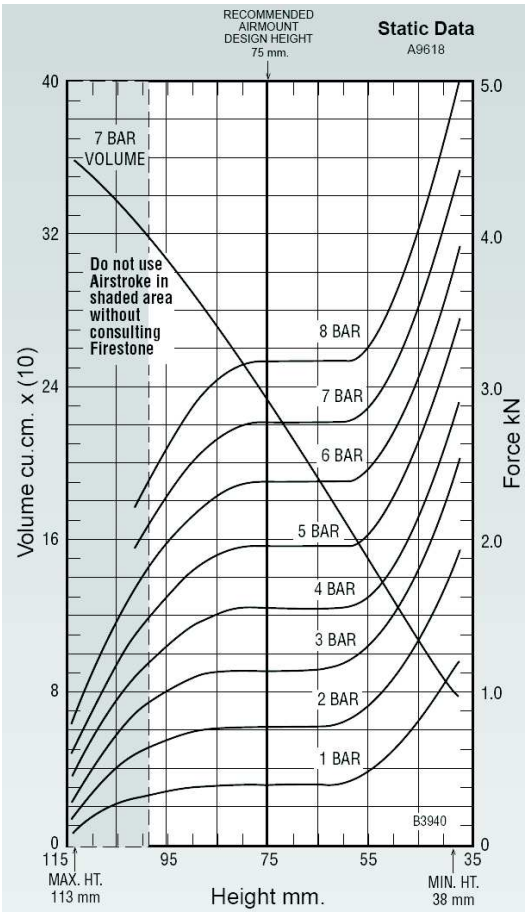

FIGURE 4.5: Datasheet of 1M1A-1 air spring [50]

$$k = \frac{dF}{dh} \tag{4.7}$$

When considering an air spring as a cylindrical column of air with a surface A and making abstraction of **the stiffness of the rubber**, the behavior of the spring is fully determined by the column of air. The adiabatic law given in equation 4.8 determines its behavior.

$$pV^{\kappa} = constant, \tag{4.8}$$

in which V stands for the volume of the air column and κ for the ratio of specific heats of air. Differentiation of this equation gives:

$$dpV^{\kappa} + p\kappa V^{\kappa-1}dV = 0. \tag{4.9}$$

Since $F = pA$ and $V = hA$, dp can be replaced with $\frac{dF}{A}$ and dV with Adh resulting in:

$$\frac{dF}{A}V^{\kappa} + p\kappa V^{\kappa-1}Adh = 0, \tag{4.10}$$

which leads to the expression for the air spring stiffness:

$$k = \frac{-p\kappa V^{\kappa-1}A^2}{V^{\kappa}} = \frac{-p\kappa A^2}{V} = \frac{-p\kappa A}{h}. \tag{4.11}$$

The negative sign of this expression is due to the fact that an increase of height of the pneumatic spring corresponds to a reduction of the exerted force by the spring. The pressure p inside an air spring is set according to the mass m the spring has to support and thus the natural frequency when using the air spring will not vary provided that the height of the air spring is constant as can be seen in the following expression:

$$f_S = \sqrt{\frac{k}{m}} = \sqrt{\frac{p\kappa A}{hm}} = \sqrt{\frac{g\kappa}{h}}. \tag{4.12}$$

The *Firestone Airmount 1M1A-1* will provide a natural frequency of 2.8 Hz when used at its design height of 75 mm. The only way of softening the system without changing the design height of the spring, is to enlarge the volume (see 4.11). This can be realized by connecting the spring to an auxiliary reservoir as can be seen on figure 4.6. The damping properties of an air spring are rather poor but here this can be solved by introducing a throttle valve in the connection between air spring and auxiliary reservoir. The behavior of the system is modelled in the following section.

4.3.1 Modelling of an air spring with auxiliary reservoir

The aim of the suspension shown in figure 4.6 is to isolate the mass m from the vibrations entering at the base of the system. The behavior

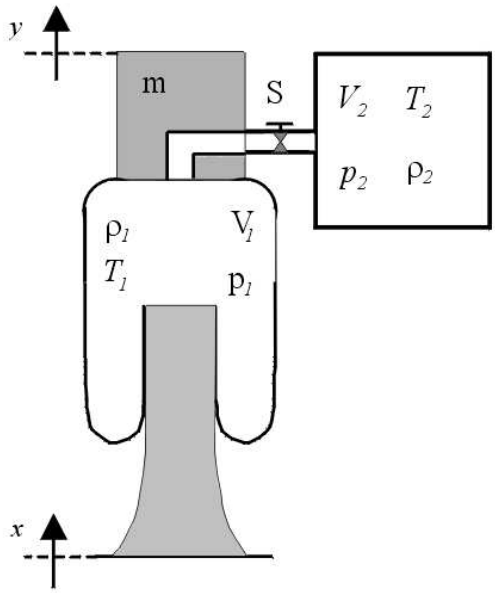

FIGURE 4.6: Scheme of the air system (p_i pressures, V_i volumes, T_i temperatures, ρ_i densities, S surface of the valve opening, x and y positions of respectively ground and mass m)

of this suspension can be fully understood by deriving the transfer function between vibration input x and output y.

In order to do so the movement of the mass m is described by Newton's second law:

$$m\ddot{y} = (p_1 - p_0)A - mg \tag{4.13}$$

with
- m mass
- $\ddot{y}$ acceleration of mass m
- p_1 pressure in air spring
- p_0 ambient pressure
- A effective area of air spring
- g gravitational acceleration

Generally the effective area A of an air spring is not a constant, it is function of the height and the internal pressure of the spring.

The manual [50] states that the influence of the internal pressure on the effective area is quite small and that of the height depends on the type of spring used. For the rolling diaphragm spring in this setup the influence of the height is also small and the effective area can be considered as a constant.

In that way the spring volume V_1 can be described through the following equation:

$$V_1 = V_{10} + (y - x)A, \tag{4.14}$$

in which V_{10} is the volume of the spring when the system is at rest. The volume of the auxiliary reservoir V_2 is constant. The only unknown parameter in 4.13 is p_1. To solve this pressure the energy state of both the air spring and the auxiliary reservoir are formulated.

The conservation of energy of open systems states that the energy inflow minus the energy outflow equals the rate at which energy is stored inside a certain control volume. This can be expressed by equation [93]:

$$\sum \dot{m}_{in} \acute{h}_{in} - \sum \dot{m}_{out} \acute{h}_{out} + \frac{dQ_h}{dt} - \frac{d\Phi}{dt} = \frac{dE}{dt} \tag{4.15}$$

with
- Q_h heat flow to the control volume
- Φ work done by the system
- $\dot{m}$ mass flow rate
- $\frac{d}{dt}$ time derivative
- E total internal energy inside the control volume
- $\acute{h}$ total energy per unit mass of fluid
  $$\acute{h} = u + \frac{p}{\rho} + \frac{v^2}{2} + gz = h + \frac{v^2}{2} + gz$$
- h enthalpy of the fluid
- u internal energy
- z elevation
- v fluid velocity
- ρ fluid density

This general equation can be simplified in this case. The two enclosures, the spring and the auxiliary reservoir, are considered both as

control volumes. All mass flowing from one control volume enters the other and vice versa and is represented by $\dot{m}$. Since there are no substantial height differences and changes in fluid speed, energy flow can be describes by the enthalpy h. Assuming further that changes to the system happen instantly, eliminates the heat flow Q_h to the system. This leads to equation 4.16 where the first term indicates the energy flow to the control volume, the second the work done by the system and the third term the total internal energy in the system.

$$C_p \dot{m} T - p \frac{dV}{dt} = \frac{d}{dt} \left(C_v \rho V T \right) \tag{4.16}$$

with
- C_p specific heat at constant pressure
- T temperature (K)
- V volume
- C_v specific heat at constant volume

An expression for the mass flow in the system is found by relating the mass flow through the throttle valve to the pressure over it and that for a compressible fluid [11]. The mass flow is considered to be positive going to the auxiliary reservoir.

$$\begin{aligned} \dot{m} &= \frac{d}{dt} \left(\rho_2 V_2 \right) \\ &= S \sqrt{2 \rho_2 p_2 \left(\frac{\kappa}{\kappa - 1} \right) \left[\left(\frac{p_1}{p_2} \right)^{\frac{2}{\kappa}} - \left(\frac{p_1}{p_2} \right)^{\frac{\kappa+1}{\kappa}} \right]} \end{aligned} \tag{4.17}$$

with
- κ ratio of specific heats
- S surface of valve opening

Applying equation 4.16 to both control volumes results in:

$$-C_p \dot{m} T_1 - p_1 \frac{dV_1}{dt} = \frac{d}{dt} \left(C_v \rho_1 V_1 T_1 \right), \tag{4.18}$$

$$C_p \dot{m} T_2 = \frac{d}{dt} \left(C_v \rho_2 V_2 T_2 \right), \tag{4.19}$$

with index 1 indicating the spring properties and index 2 the properties of the auxiliary reservoir. Combining equations 4.13, 4.14, 4.17, 4.18 and 4.19 with the law for an ideal gas ($pV = mRT$) results in the model of the air spring with auxiliary reservoir. This model was implemented in Matlab [92].

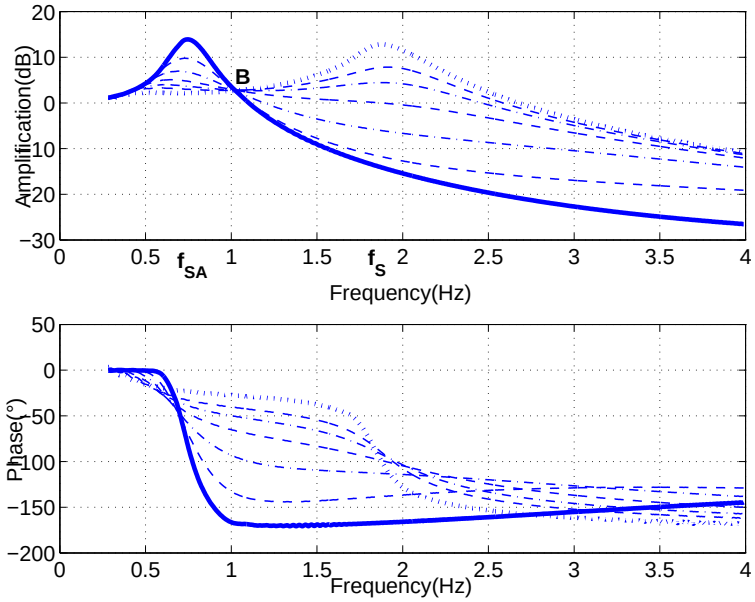

Figure 4.7: Simulated Frequency Response Function for different valve openings: open valve (dotted line), closed valve (solid line), intermediate valve openings (dashed lines)

Figure 4.7 shows the FRF of the model using an air spring *Firestone Airmount 1T14C-1* of $5.3l$, an auxiliary volume of $26l$ and various valve openings. The FRFs are obtained by exciting the system with a swept sine signal between 0.2 and $5Hz$ with an amplitude of $1.5cm$. The FRFs show a resonance frequency that shifts, depending on the valve opening, between the natural frequency of the air spring f_S given by equation 4.12 and the natural frequency of an air spring with the same surface of the original one but with a volume equal to both air volumes in the system, f_{SA}. Here these frequencies are respectively $0.74Hz$ and $1.88Hz$.

The resistance created by the throttle valve determines the behavior

of the system. At a high resistance or almost closed valve the system behaves as the air spring itself. With nearly no volume flow through the valve, the auxiliary volume is cut off from the system and no energy is dissipated at the orifice which leads to the high amplification. At low resistance or fully open valve the energy dissipation is low again. The volume flow is higher but with no pressure drop, damping in the system is low again and the amplification is high but now at a lower frequency. Intermediate resistances show the damping effect of the system and result in systems with better attenuation capabilities.

Non-linear effects can be seen when applying vibrations with different amplitudes. Small amplitudes make the system behave more stiff since the auxiliary volume of air is not used, while larger amplitudes result in more flow through the throttle valve and a more flexible system.

Quaglia and Sorli investigated the same system and formulated a similar model, but used a somewhat different approach. In [111] the air spring and the auxiliary volume are described starting from energy laws of closed volumes and the flow through the valve depends on the conditions of both closed volumes. The results of both models are equal.

This non-linear model is used as the basis for a linearized model. Linearization point is the system at rest, where $x = y = 0$, the air spring at it's design height and the pressure in the system $p_1 = p_2 = m/A$. Taylor series development cut off at the first term in the neighborhood of the linearization point yields the linear equations 4.20 and 4.21 for equations 4.18 and 4.19. Temperatures T_1 and T_2 are eliminated using the law for an ideal gas, an index $_0$ indicates the conditions for the parameters at rest and $\dot{}$ is used for a time derivative of a parameter.

$$-\frac{C_p}{R}\dot{m}\frac{p_{10}}{\rho_{10}} - p_{10}\dot{V_1} = \frac{C_v}{R}p_{10}\dot{V_1} + \frac{C_v}{R}V_{10}\dot{p_1}, \tag{4.20}$$

$$-\frac{C_p}{R}\dot{m}\frac{p_{20}}{\rho_{20}} = \frac{C_v}{R}V_2\dot{p_2}. \tag{4.21}$$

Linearization of equation 4.17 poses the problem that the mass flow has a vertical tangent at the linearization point. In this case a secant linearization is used resulting in:

$$\dot{m}R_F = p_1 - p_2, \tag{4.22}$$

where R_F represents the linear flow resistance.

Combining the linear equations results in the following transfer function between suspension height $(y - x)$ and the exerted force F on the spring:

$$\frac{F}{(y-x)} = -k_{SA}\frac{sD+1}{sD\frac{k_{SA}}{k_S}+1}, \tag{4.23}$$

with $D = R_F\dfrac{V_{20}}{\kappa R T_0}$ and s the Laplace variable. This equation shows the transition of the spring stiffness from k_{SA} at low frequencies $(s \longrightarrow 0)$ to k_S at high frequencies $(s \longrightarrow \infty)$. The transition of the stiffness is controlled by parameter D.

Knowing this the linearized 'base motion' model of a quarter cabin becomes the following third order model:

$$\frac{y}{x} = \frac{sD+1}{s^3 D\frac{m}{k_S} + s^2\frac{m}{k_{SA}} + sD + 1}. \tag{4.24}$$

Figure 4.8 shows the bode plot of the linearized model. Investigations of this and figure 4.7 shows that all curves pass though a common point B. It is possible to choose the valve opening in such a way that point B is the natural frequency of the system. In this configuration the suspension will have the lowest amplification at the natural frequency and overall a very good attenuation level.

Quaglia and Sorli determined the coordinates of this point and found out that it only depends on the ratio of natural frequencies Ω being:

$$\Omega = \frac{f_S}{f_{SA}} = \sqrt{\frac{k_S}{k_{SA}}}, \tag{4.25}$$

with k_S the stiffness of the air spring and k_{SA} the stiffness of the air spring with auxiliary volume.

The abscissa and ordinate of point B are given by:

$$f_B = f_S\sqrt{\frac{2}{1+\Omega^2}} \qquad A_B = \frac{\Omega^2+1}{\Omega^2-1}, \tag{4.26}$$

which means that the higher the value of Ω, the lower the amplification of point B will be and the better the suspension will perform on condition that the resistance in the connection of both air volumes is well chosen.

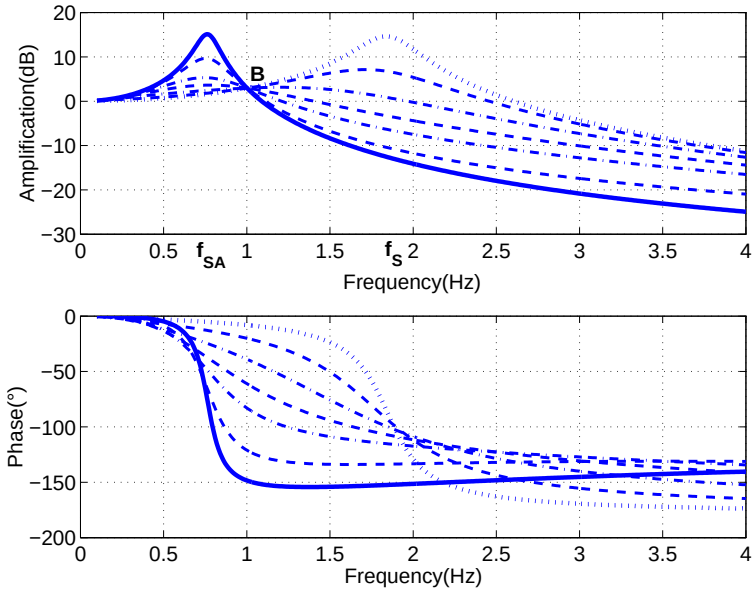

FIGURE 4.8: Bode plot for different valve openings: open valve (dotted line), closed valve (solid line), intermediate valve openings (dashed lines)

4.3.2 Measurement

To verify this model several tests are performed using different air springs and auxiliary air tanks with different volumes. In the connecting tube between both volumes, a valve is fitted to change the resistance and thus the airflow between both air volumes. A sliding platform is used to be able to load the suspension system and the suspension is excited by the hydraulic platform it is put on. One of these setups is shown on figure 4.9 where a *Firestone Airmount 1M1A-1* with an approximated air volume of 0.2 liter is used in combination with an auxiliary air tank of 0.6 liter.

Two accelerometers, one on the hydraulic shaker at the base of the suspension system and one on the sliding platform supported by the suspension system, record the input and output vibrations when the hydraulic shaker excites the setup. Figure 4.10 shows the FRF of the *Firestone Airmount 1T14C-1* with an auxiliary volume of 26 l,

Figure 4.9: Photograph of the pneumatic system

obtained using a swept sine excitation signal with a frequency content between 0.2 and 5 Hz, a constant rate of sweep, a duration of 41 s and an amplitude of 1.5 cm. Some non-linear effects are visible for the system with closed valve.

To get a notion of the non-linear behavior of the pneumatic system, figure 4.11 shows the amplitude of the FRFs of the pneumatic system combining a *Firestone Airmount 1M1A-1* with an auxiliary air tank of 0.6 liter. The two FRFs are obtained exciting the above mentioned system using a swept sine and a multisine signal. The swept sine has a frequency content between 0.7 and 7 Hz, a constant rate of sweep, a duration of 41s and an amplitude of 1.5 cm. The multi sine has the same frequency content, duration and a maximum amplitude of 1.5 cm.

As can be seen on figure 4.11, only small differences are observed

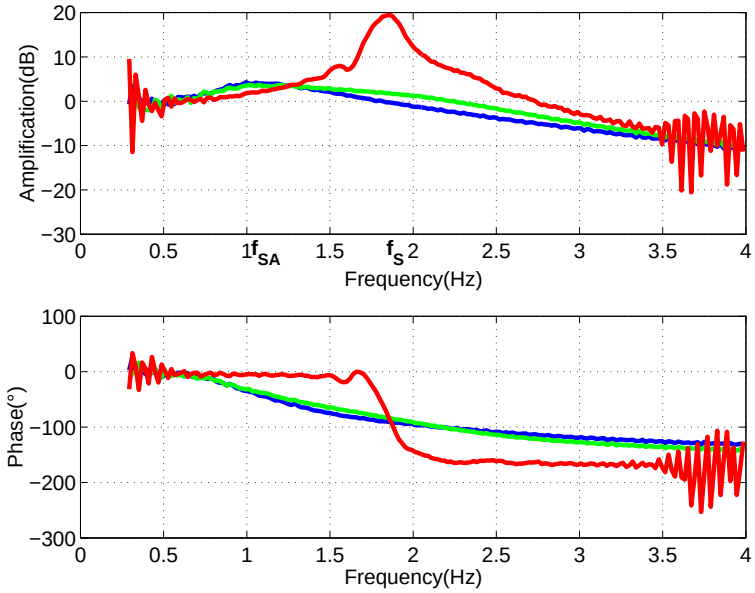

FIGURE 4.10: Experimental frequency response function for different valve openings: closed valve (red line), open valve (blue line), intermediate valve opening (green line)

between the magnitude of the FRFs. This would indicate that the system behaves rather linear. Since the RMS of both signals differs with approximately 20 %, this can not be concluded with certainty. A more precise quantification of the non-linearity is necessary and this could be performed using odd-odd multisine excitation signals [106].

As can be seen on the figure, the system behaves rather linear. Only at resonance small differences are observed. This phenomenon has been mentioned in the previous section and has to do with the constant amplitude of the swept sine in comparison with the random amplitude of the multi sine.

4.3.3 Discussion

Looking at figures 4.7 and 4.10, it is clear that the model simulates the behavior of the real physical system accurately. Both gain and phase show a good resemblance. The model has only problems predicting the

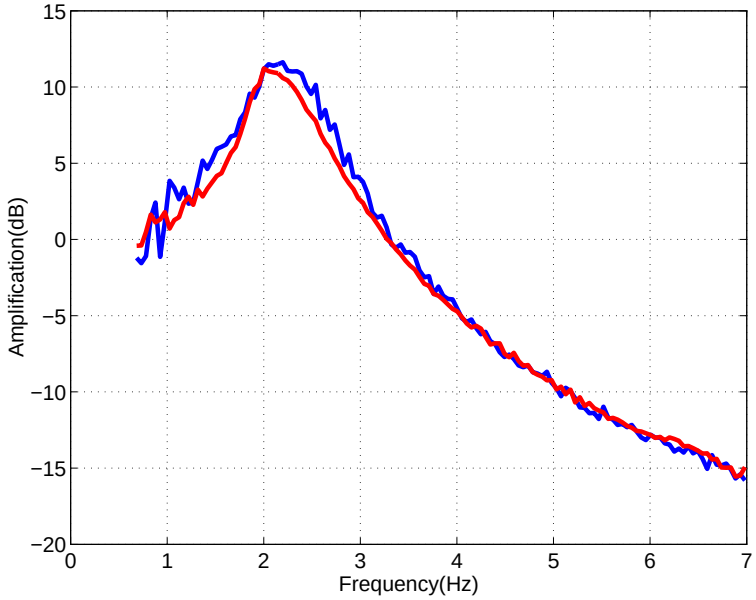

Figure 4.11: Magnitude of the experimental frequency response functions of a pneumatic cab mount using different excitation signals (blue line: swept sine; red line: multi sine)

natural frequency of the system with auxiliary volume, f_{SA}. The real physical setup shows a f_{SA} of $1Hz$ while the model predicts $0.74Hz$.

The reason for this fault is that the model makes abstraction of the rubber of the air spring as described in the beginning of this section. When the stiffness of the air column is significantly higher than the stiffness of the rubber of the air spring, this is a good assumption. Adding an auxiliary volume decreases the stiffness of the air column and makes the influence of the rubber more significant. This results in a higher f_{SA} for the physical system. To determine the correct stiffness, the Firestone Airstroke and Airmount Engineering Manual & Design Guide [50] uses experimental measured stiffness curves (an example is shown in figure 4.5) and the following formula:

$$K = [(P_g + 1.01)100]\left[\left(\frac{A_c}{10000}\right)\left(\frac{V_d}{V_c}\right)^{1.38} - \left(\frac{A_e}{10000}\right)\left(\frac{V_d}{V_e}\right)^{1.38}\right] - \left[101\left(\frac{A_c - A_e}{10000}\right)\right] \quad (4.27)$$

with
- K Vertical Spring Rate in kN/m
- P_g Pressure at design height (bar)
- A_c Effective Area at 10 mm below design height (cm^2)
- A_e Effective Area at 10 mm above design height (cm^2)
- V_d Internal Volume at design height (cm^3)
- V_c Internal Volume at 10 mm above design height (cm^3)
- V_e Internal Volume at 10 mm above design height (cm^3)

Calculating f_{SA} using this formula, results in a frequency of 1 Hz, which is exactly the natural frequency of the physical system.

The total height of this system depends entirely on the air spring used. A *Firestone Airmount 1M1A-1* with a design height of 75 mm, has ample space to replace the rubber blocks. Combined with an auxiliary air volume of 1l, the f_{SA} gets down to 1,71Hz which is below the demanded 2 Hz. Compared to the hydro-pneumatic suspension, this air spring is also cheaper, € 300 for an air spring. The only negative feature of the air spring is its limited travel, for this type only 40mm.

This system has already successfully been implemented in a new design of passive suspension for agricultural machinery seats as described in the paper of Hostens *et. al* [68]. This system will also be used for the cab suspension system in this study.

4.4 Conclusion

For the attenuation of low-frequency vibrations commercial systems frequently incorporate pneumatic elements in combination with hydraulic dampers. The pneumatic elements provide low natural frequencies and the dampers prevent high amplification at those frequencies. This chapter addressed a hydro-pneumatic and a pneumatic system that can serve as vibration reducing cab mount.

The hydro-pneumatic consists out of a hydraulic cylinder combined with two nitrogen accumulators, supplying a low natural frequency, and a valve, controlling the flow of the hydraulic fluid and thus the damping. A non-linear white box model based on physical principles incorporating the friction behavior of the hydraulic piston in the cylinder was derived. The model proved to be accurate with close resemblance between the frequency response function of the model and obtained through measurement on a real setup. Also less than 7 % difference between vibration dose values of model versus measurement were found. Despite the good behavior of the system with a natural frequency of 1.2 Hz and a low maximum amplification, this system was not selected as the most promising due to a high price, a high volume and difficulties with implementation as a cab mount.

The pneumatic alternative was built using an air spring in combination with an auxiliary air volume. Damping was introduced in the system through a throttle valve in the interconnection between spring and auxiliary volume. White box modelling of the system using thermodynamics laws resulted in a non-linear model, but also a linear equivalent was deduced. Experimental verification showed the accuracy of the models. Both the models and the experiments showed that a good selection of the resistance in the interconnection between spring and auxiliary volume results in low amplification at the natural frequency and an overall very good attenuation level.

With its reasonable price, good overall behavior and the easy way the system can replace the current rubber cab mounts, the pneumatic system is the better choice.

Chapter 5

Design of a Multi Dimensional Cab Suspension

Chapter 3 showed that the vibrations are multidirectional and attenuation in several directions is desirable to fulfill the action and limit values prescribed by the European legislation. Here the pneumatic elements modelled in the previous chapter will be used in a three dimensional setup, thus giving a tool to predict the behavior of the new suspension concept. The linear model techniques used are based on Harris' Shock and Vibration Handbook [64].

In the model of the cabin suspension the cab has a mass of $706kg$. It is considered to be rigid. A good assumption since no flexible modes were shown in the low frequency band of interest (below 20Hz) [4]. It is also assumed to be symmetrical with respect to the suspension points, which is almost the case, as can be seen in figure 5.1. Due to the symmetry, the inertia products are considered to be zero and only the moments of inertia remain. I_{xx}, I_{yy} and I_{zz} are respectively $380kgm^2$, $305kgm^2$ and $350kgm^2$ where x is the driving or longitudinal direction of the machine, z the vertical direction and y the lateral direction. The cab's center of gravity is located $78cm$ above the cab floor containing the connection points for the suspension.

The chapter first develops a general theoretical model for a cabin suspension that is validated in a second section using a suspension setup with four air springs. In the third section the linear model of the

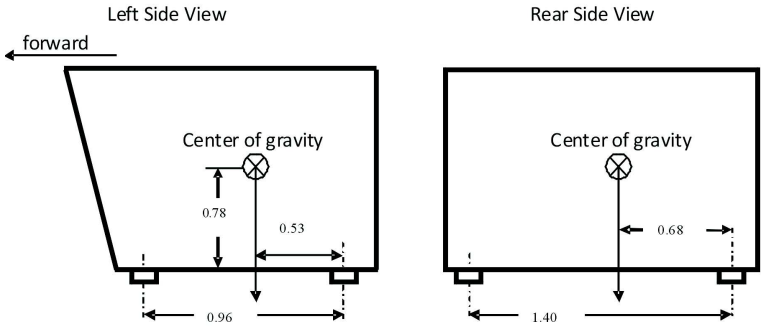

Figure 5.1: Scheme of a cabin with relative positions of cabin mounts to the center of gravity

pneumatic cab mount is introduced into the multidimensional model. This model is used to predict the possible improvement of the comfort values.

5.1 Theoretical model

5.1.1 System of coordinates

Two coordinate systems are used. The fixed "inertial"frame of reference with cartesian coordinates X_0, Y_0 and Z_0 and a similar system of coordinates X, Y and Z fixed to the cabin. Both systems have their origin at the center of mass of the cabin and coincide when the cab is in equilibrium.

The motions of the cab are described by giving the displacement of the cab axes relatively to the inertial axes. The translational displacements of the center of mass of the cab are x_{out}, y_{out} and z_{out} in the X_0, Y_0 and Z_0 directions, respectively.

The rotational displacements of the body are characterized by the angles of rotation α_{out}, β_{out} and γ_{out} of the cabin axes about the X_0, Y_0 and Z_0 axes respectively (see figure 5.2). Only small translations and rotations are considered. Hence, the rotations are commutative and the angles of rotations about the cab axes are equal to those about the inertial axes.

The general equations of motion for the translation of the cabin are:

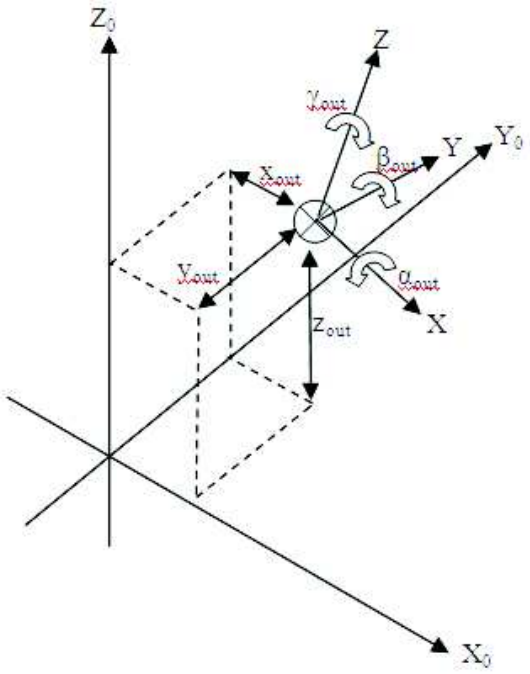

FIGURE 5.2: System of coordinates used to build up the model

$$\begin{cases} m\ddot{x}_{out} &= F_x, \\ m\ddot{y}_{out} &= F_y, \\ m\ddot{z}_{out} &= F_z, \end{cases} \tag{5.1}$$

where m is the mass of the cab, F_x, F_y and F_z the summations of the forces acting on the cab and $\ddot{x}_{out}$, $\ddot{y}_{out}$ and $\ddot{z}_{out}$ the accelerations of the center of mass of the cab in the X_0, Y_0 and Z_0 axis respectively.

The equations of motion for the rotations of the cabin are:

$$\begin{cases} I_{xx}\ddot{\alpha}_{out} - I_{xy}\ddot{\beta}_{out} - I_{xz}\ddot{\gamma}_{out} &= M_x, \\ -I_{xy}\ddot{\alpha}_{out} + I_{yy}\ddot{\beta}_{out} - I_{yz}\ddot{\gamma}_{out} &= M_y, \\ -I_{zx}\ddot{\alpha}_{out} - I_{zy}\ddot{\beta}_{out} + I_{zz}\ddot{\gamma}_{out} &= M_z, \end{cases} \tag{5.2}$$

where $\ddot{\alpha}_{out}$, $\ddot{\beta}_{out}$ and $\ddot{\gamma}_{out}$ are the rotational accelerations about the X, Y, Z axes as shown in figure 5.2, M_x,M_y,M_z the summations of the torques acting on the cab about the axes X,Y and Z, and I_{ij} the moments of inertia if $i = j \in \{x, y, z\}$ and the products of inertia if $i \neq j \in \{x, y, z\}$.

5.1.2 Resilient supports

Every passive cab suspension is built using a number of resilient supports. These three dimensional elements connect the cab with the supporting structure and resist the relative movement between those two. These supports are considered to be massless and are a combination of a spring and damper. For the linear model spring and damper force are proportional to the relative displacement and velocity respectively.

The spring constant k_{xx} of the resilient element in a single degree of freedom system where constraints restrict the path of motion of the element, determines the relation of the motion in the X direction to the force opposing it. In a three dimensional system the behavior is more complex. Force applied on a resilient element in a certain direction does not necessary mean motion in that same direction. Spring constant k_{xy} exists which expresses the relationship between force in the X direction and a displacement in the Y direction.

The behavior can be described with respect to the principal axes, the axes for which the element, when unconstrained, experiences a deflection co-linear with the direction of the applied force. In this study these axes are given by the cartesian coordinates P, Q and R. Spring and damping constants for these given directions are then k_p, k_q and k_r, and c_p, c_q and c_r. Using an air spring as cabin support, those principal axes are the axis of symmetry and two axes perpendicular to it (see figure 5.4 for an example).

In the model the spring stiffness and damping coefficients have to be known with respect to the inertial coordinate system (X_0,Y_0,Z_0). The following equations give the relationship between the stiffness coefficients along the principal axes and those along the inertial axes.

$$\begin{aligned} k_{xx} &= k_p\lambda_{xp}^2 + k_q\lambda_{xq}^2 + k_r\lambda_{xr}^2, \\ k_{yy} &= k_p\lambda_{yp}^2 + k_q\lambda_{yq}^2 + k_r\lambda_{yr}^2, \\ k_{zz} &= k_p\lambda_{zp}^2 + k_q\lambda_{zq}^2 + k_r\lambda_{zr}^2, \\ k_{xy} &= k_p\lambda_{xp}\lambda_{yp} + k_q\lambda_{xq}\lambda_{yq} + k_r\lambda_{xr}\lambda_{yr}, \\ k_{xz} &= k_p\lambda_{xp}\lambda_{zp} + k_q\lambda_{xq}\lambda_{zq} + k_r\lambda_{xr}\lambda_{zr}, \\ k_{yz} &= k_p\lambda_{yp}\lambda_{zp} + k_q\lambda_{yq}\lambda_{zq} + k_r\lambda_{yr}\lambda_{zr}. \end{aligned} \tag{5.3}$$

In these equations the λ's are the cosines of the angles between the principal elastic axes of the resilient elements and the coordinate axes. Similar equations give this same relationship for the damping coefficients.

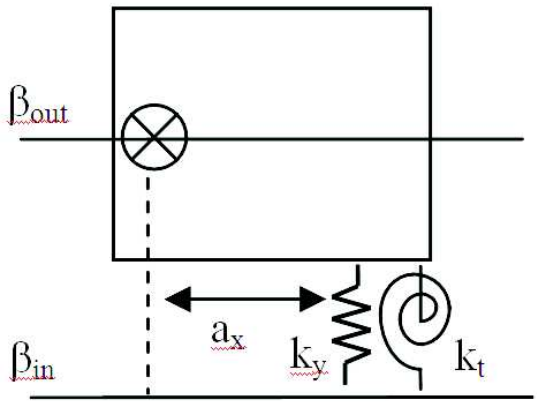

FIGURE 5.3: Effect of torsion

Usually it is assumed that resilient elements are connected to the rigid bodies by means of ball joints. In such cases the spring and damping coefficients above are sufficient to describe the forces acting on the cab and the support. If this assumption is not made additional torsional springs and dampers resisting rotation about the principle axes are introduced. Figure 5.3 shows the effect of a combination of a linear and a torsional spring. The torque which acts on the cab due to a rotation β_{out} of the cab and β_{in} of the support is given here by

$$torque = (k_t + a_x^2 k_y)(\beta_{in} - \beta_{out}), \tag{5.4}$$

where k_t is the torsional stiffness and a_x the distance between the resilient element to the center of gravity of the cab.

In many cases the effect of the torsional stiffness is small in comparison with $a_x^2 k_y$, and therefore neglected. Here the suspension elements are designed to have a low stiffness k_y and the effect of the torsional stiffness is larger in comparison.

Comparable with the spring stiffness, the effect of the torsional stiffness for a resilient element is given with respect to the principal axes of the element. Similar equations give the relationship between those and the torsional stiffness along the inertial axes. To distinguish between linear spring coefficients and torsional coefficients a superscript ^{t} is used. Again similar equations can be deduced for the torsional damping coefficients.

$$\begin{aligned}
k^t_{xx} &= k^t_p\lambda^2_{xp} + k^t_q\lambda^2_{xq} + k^t_r\lambda^2_{xr},\\
k^t_{yy} &= k^t_p\lambda^2_{yp} + k^t_q\lambda^2_{yq} + k^t_r\lambda^2_{yr},\\
k^t_{zz} &= k^t_p\lambda^2_{zp} + k^t_q\lambda^2_{zq} + k^t_r\lambda^2_{zr},\\
k^t_{xy} &= k^t_p\lambda_{xp}\lambda_{yp} + k^t_q\lambda_{xq}\lambda_{yq} + k^t_r\lambda_{xr}\lambda_{yr},\\
k^t_{xz} &= k^t_p\lambda_{xp}\lambda_{zp} + k^t_q\lambda_{xq}\lambda_{zq} + k^t_r\lambda_{xr}\lambda_{zr},\\
k^t_{yz} &= k^t_p\lambda_{yp}\lambda_{zp} + k^t_q\lambda_{yq}\lambda_{zq} + k^t_r\lambda_{yr}\lambda_{zr}.
\end{aligned} \tag{5.5}$$

5.1.3 Full model

The full linear model consists out of the six equations given by 5.1 and 5.2. The forces and the moments in these equations are the result of the motion of the support and the effect this motion has on the displacement and rotation of the cab. The following equations explicit the forces and moments. The index i in the equations denotes that the sums are taken over the different resilient supports of the cabin.

$$\begin{aligned}
m\ddot{x}_{out} &= \Sigma k^i_{xx}(x_{in} - x_{out}) + \Sigma k^i_{xy}(y_{in} - y_{out}) + \Sigma k^i_{xz}(z_{in} - z_{out})\\
&\quad +\Sigma(k^i_{xz}a^i_y - k^i_{xy}a^i_z)(\alpha_{in} - \alpha_{out})\\
&\quad +\Sigma(k^i_{xx}a^i_z - k^i_{xz}a^i_x)(\beta_{in} - \beta_{out})\\
&\quad +\Sigma(k^i_{xy}a^i_x - k^i_{xx}a^i_y)(\gamma_{in} - \gamma_{out})\\
&\quad +\Sigma c^i_{xx}(\dot{x}_{in} - \dot{x}_{out}) + \Sigma c^i_{xy}(\dot{y}_{in} - \dot{y}_{out}) + \Sigma c^i_{xz}(\dot{z}_{in} - \dot{z}_{out})\\
&\quad +\Sigma(c^i_{xz}a^i_y - c^i_{xy}a^i_z)(\dot{\alpha}_{in} - \dot{\alpha}_{out})\\
&\quad +\Sigma(c^i_{xx}a^i_z - c^i_{xz}a^i_x)(\dot{\beta}_{in} - \dot{\beta}_{out})\\
&\quad +\Sigma(c^i_{xy}a^i_x - c^i_{xx}a^i_y)(\dot{\gamma}_{in} - \dot{\gamma}_{out})
\end{aligned} \tag{5.6}$$

$$
\begin{aligned}
m\ddot{y}_{out} &= \Sigma k^i_{xy}(x_{in} - x_{out}) + \Sigma k^i_{yy}(y_{in} - y_{out}) + \Sigma k^i_{yz}(z_{in} - z_{out}) \\
&+\Sigma(k^i_{yz}a^i_y - k^i_{yy}a^i_z)(\alpha_{in} - \alpha_{out}) \\
&+\Sigma(k^i_{xy}a^i_z - k^i_{yz}a^i_x)(\beta_{in} - \beta_{out}) \\
&+\Sigma(k^i_{yy}a^i_x - k^i_{xy}a^i_y)(\gamma_{in} - \gamma_{out}) \\
&+\Sigma c^i_{xy}(\dot{x}_{in} - \dot{x}_{out}) + \Sigma c^i_{yy}(\dot{y}_{in} - \dot{y}_{out}) + \Sigma c^i_{yz}(\dot{z}_{in} - \dot{z}_{out}) \\
&+\Sigma(c^i_{yz}a^i_y - c^i_{yy}a^i_z)(\dot{\alpha}_{in} - \dot{\alpha}_{out}) \\
&+\Sigma(c^i_{xy}a^i_z - c^i_{yz}a^i_x)(\dot{\beta}_{in} - \dot{\beta}_{out}) \\
&+\Sigma(c^i_{yy}a^i_x - c^i_{xy}a^i_y)(\dot{\gamma}_{in} - \dot{\gamma}_{out})
\end{aligned}
\tag{5.7}
$$

$$
\begin{aligned}
m\ddot{z}_{out} &= \Sigma k^i_{xz}(x_{in} - x_{out}) + \Sigma k^i_{yz}(y_{in} - y_{out}) + \Sigma k^i_{zz}(z_{in} - z_{out}) \\
&+\Sigma(k^i_{zz}a^i_y - k^i_{yz}a^i_z)(\alpha_{in} - \alpha_{out}) \\
&+\Sigma(k^i_{xz}a^i_z - k^i_{zz}a^i_x)(\beta_{in} - \beta_{out}) \\
&+\Sigma(k^i_{yz}a^i_x - k^i_{xz}a^i_y)(\gamma_{in} - \gamma_{out}) \\
&+\Sigma c^i_{xz}(\dot{x}_{in} - \dot{x}_{out}) + \Sigma c^i_{yz}(\dot{y}_{in} - \dot{y}_{out}) + \Sigma c^i_{zz}(\dot{z}_{in} - \dot{z}_{out}) \\
&+\Sigma(c^i_{zz}a^i_y - c^i_{yz}a^i_z)(\dot{\alpha}_{in} - \dot{\alpha}_{out}) \\
&+\Sigma(c^i_{xz}a^i_z - c^i_{zz}a^i_x)(\dot{\beta}_{in} - \dot{\beta}_{out}) \\
&+\Sigma(c^i_{yz}a^i_x - c^i_{xz}a^i_y)(\dot{\gamma}_{in} - \dot{\gamma}_{out})
\end{aligned}
\tag{5.8}
$$

$$
\begin{aligned}
I_{xx}\ddot{\alpha}_{out} \quad & \Sigma(k^i_{xz}a^i_y - k^i_{xy}a^i_z)(x_{in} - x_{out}) \\
-I_{xy}\ddot{\beta}_{out} \;=\; & +\Sigma(k^i_{yz}a^i_y - k^i_{yy}a^i_z)(y_{in} - y_{out}) \\
-I_{xz}\ddot{\gamma}_{out} \quad & +\Sigma(k^i_{zz}a^i_y - k^i_{yz}a^i_z)(z_{in} - z_{out}) \\
& +\Sigma(k^i_{yy}{a^i_z}^2 + k^i_{zz}{a^i_y}^2 - 2k^i_{yz}a^i_y a^i_z)(\alpha_{in} - \alpha_{out}) \\
& +\Sigma(k^i_{xz}a^i_y a^i_z + k^i_{yz}a^i_x a^i_z - k^i_{zz}a^i_x a^i_y - k^i_{xy}{a^i_z}^2)(\beta_{in} - \beta_{out}) \\
& +\Sigma(k^i_{xy}a^i_y a^i_z + k^i_{yz}a^i_x a^i_y - k^i_{yy}a^i_x a^i_z - k^i_{xz}{a^i_y}^2)(\gamma_{in} - \gamma_{out}) \\
& +\Sigma(c^i_{xz}a^i_y - c^i_{xy}a^i_z)(\dot{x}_{in} - \dot{x}_{out}) \\
& +\Sigma(c^i_{yz}a^i_y - c_{yy}a^i_z)(\dot{y}_{in} - \dot{y}_{out}) \\
& +\Sigma(c^i_{zz}a^i_y - c_{yz}a^i_z)(\dot{z}_{in} - \dot{z}_{out}) \\
& +\Sigma(c^i_{yy}{a^i_z}^2 + c^i_{zz}{a^i_y}^2 - 2c^i_{yz}a^i_y a^i_z)(\dot{\alpha}_{in} - \dot{\alpha}_{out}) \\
& +\Sigma(c^i_{xz}a^i_y a^i_z + c^i_{yz}a^i_x a^i_z - c^i_{zz}a^i_x a^i_y - c^i_{xy}{a^i_z}^2)(\dot{\beta}_{in} - \dot{\beta}_{out}) \\
& +\Sigma(c^i_{xy}a^i_y a^i_z + c^i_{yz}a^i_x a^i_y - c^i_{yy}a^i_x a^i_z - c^i_{xz}{a^i_y}^2)(\dot{\gamma}_{in} - \dot{\gamma}_{out}) \\
& +\Sigma k^{ti}_{xx}(\alpha_{in} - \alpha_{out}) + \Sigma k^{ti}_{xy}(\beta_{in} - \beta_{out}) \\
& +\Sigma k^{ti}_{xz}(\gamma_{in} - \gamma_{out}) + \Sigma c^{ti}_{xx}(\dot{\alpha}_{in} - \dot{\alpha}_{out}) \\
& +\Sigma c^{ti}_{xy}(\dot{\beta}_{in} - \dot{\beta}_{out}) + \Sigma c^{ti}_{xz}(\dot{\gamma}_{in} - \dot{\gamma}_{out})
\end{aligned}
\tag{5.9}
$$

$$
\begin{aligned}
-I_{xy}\ddot{\alpha}_{out} \quad & \Sigma(k^i_{xx}a^i_z - k^i_{xz}a^i_x)(x_{in} - x_{out}) \\
+I_{yy}\ddot{\beta}_{out} \;=\; & +\Sigma(k^i_{xy}a^i_z - k^i_{yz}a^i_x)(y_{in} - y_{out}) \\
-I_{yz}\ddot{\gamma}_{out} \quad & +\Sigma(k^i_{xz}a^i_z - k^i_{zz}a^i_x)(z_{in} - z_{out}) \\
& +\Sigma(k^i_{xz}a^i_y a^i_z + k^i_{yz}a^i_x a^i_z - k^i_{zz}a^i_x a^i_y - k^i_{xy}{a^i_z}^2)(\alpha_{in} - \alpha_{out}) \\
& +\Sigma(k^i_{xx}{a^i_z}^2 + k^i_{zz}{a^i_x}^2 - 2k^i_{xz}a^i_x a^i_z)(\beta_{in} - \beta_{out}) \\
& +\Sigma(k^i_{xy}a^i_x a^i_z + k^i_{xz}a^i_x a^i_y - k^i_{xx}a^i_y a^i_z - k^i_{yz}{a^i_x}^2)(\gamma_{in} - \gamma_{out}) \\
& +\Sigma(c^i_{xx}a^i_z - c^i_{xz}a^i_x)(\dot{x}_{in} - \dot{x}_{out}) \\
& +\Sigma(c^i_{xy}a^i_z - c^i_{yz}a^i_x)(\dot{y}_{in} - \dot{y}_{out}) \\
& +\Sigma(c^i_{xz}a^i_z - c^i_{zz}a^i_x)(\dot{z}_{in} - \dot{z}_{out}) \\
& +\Sigma(c^i_{xz}a^i_y a^i_z + c^i_{yz}a^i_x a^i_z - c^i_{zz}a^i_x a^i_y - c^i_{xy}{a^i_z}^2)(\dot{\alpha}_{in} - \dot{\alpha}_{out}) \\
& +\Sigma(c^i_{xx}{a^i_z}^2 + c^i_{zz}{a^i_x}^2 - 2c^i_{xz}a^i_x a^i_z)(\dot{\beta}_{in} - \dot{\beta}_{out}) \\
& +\Sigma(c^i_{xy}a^i_x a^i_z + c^i_{xz}a^i_x a^i_y - c^i_{xx}a^i_y a^i_z - c^i_{yz}{a^i_x}^2)(\dot{\gamma}_{in} - \dot{\gamma}_{out}) \\
& +\Sigma k^{ti}_{xy}(\alpha_{in} - \alpha_{out}) + \Sigma k^{ti}_{yy}(\beta_{in} - \beta_{out}) \\
& +\Sigma k^{ti}_{yz}(\gamma_{in} - \gamma_{out}) + \Sigma c^{ti}_{xy}(\dot{\alpha}_{in} - \dot{\alpha}_{out}) \\
& +\Sigma c^{ti}_{yy}(\dot{\beta}_{in} - \dot{\beta}_{out}) + \Sigma c^{ti}_{yz}(\dot{\gamma}_{in} - \dot{\gamma}_{out})
\end{aligned}
\tag{5.10}
$$

$$
\begin{array}{lcl}
-I_{zx}\ddot{\alpha}_{out} & & \Sigma(k^i_{xy}a^i_x - k^i_{xx}a^i_y)(x_{in} - x_{out}) \\
-I_{zy}\ddot{\beta}_{out} & = & +\Sigma(k^i_{yy}a^i_x - k^i_{xy}a^i_y)(y_{in} - y_{out}) \\
+I_{zz}\ddot{\gamma}_{out} & & +\Sigma(k^i_{yz}a^i_x - k^i_{xz}a^i_y)(z_{in} - z_{out}) \\
 & & +\Sigma(k^i_{xy}a^i_y a^i_z + k^i_{yz}a^i_x a^i_y - k^i_{yy}a^i_x a^i_z - k^i_{xz}{a^i_y}^2)(\alpha_{in} - \alpha_{out}) \\
 & & +\Sigma(k^i_{xy}a^i_y a^i_z + k^i_{xz}a^i_x a^i_y - k^i_{xx}a^i_y a^i_z - k^i_{yz}{a^i_x}^2)(\beta_{in} - \beta_{out}) \\
 & & +\Sigma(k^i_{xx}{a^i_y}^2 + k^i_{yy}{a^i_x}^2 - 2k^i_{xy}a^i_x a^i_y)(\gamma_{in} - \gamma_{out}) \\
 & & +\Sigma(c^i_{xy}a^i_x - c^i_{xx}a^i_y)(\dot{x}_{in} - \dot{x}_{out}) \\
 & & +\Sigma(c^i_{yy}a^i_x - c^i_{xy}a^i_y)(\dot{y}_{in} - \dot{y}_{out}) \\
 & & +\Sigma(c^i_{yz}a^i_x - c^i_{xz}a^i_y)(\dot{z}_{in} - \dot{z}_{out}) \\
 & & +\Sigma(c^i_{xy}a^i_y a^i_z + c^i_{yz}a^i_x a^i_y - c^i_{yy}a^i_x a^i_z - c^i_{xz}{a^i_y}^2)(\dot{\alpha}_{in} - \dot{\alpha}_{out}) \\
 & & +\Sigma(c^i_{xy}a^i_y a^i_z + c^i_{xz}a^i_x a^i_y - c^i_{xx}a^i_y a^i_z - c^i_{yz}{a^i_x}^2)(\dot{\beta}_{in} - \dot{\beta}_{out}) \\
 & & +\Sigma(c_{xx}{a^i_y}^2 + c^i_{yy}{a^i_x}^2 - 2c^i_{xy}a^i_x a^i_y)(\dot{\gamma}_{in} - \dot{\gamma}_{out}) \\
 & & +\Sigma k^{ti}_{xz}(\alpha_{in} - \alpha_{out}) + \Sigma k^{ti}_{yz}(\beta_{in} - \beta_{out}) \\
 & & +\Sigma k^{ti}_{zz}(\gamma_{in} - \gamma_{out}) + \Sigma c^{ti}_{xz}(\dot{\alpha}_{in} - \dot{\alpha}_{out}) \\
 & & +\Sigma c^{ti}_{yz}(\dot{\beta}_{in} - \dot{\beta}_{out}) + \Sigma c^{ti}_{zz}(\dot{\gamma}_{in} - \dot{\gamma}_{out})
\end{array}
\tag{5.11}
$$

These six equations of the 6 DOF linear model written in a more convenient way result in following matrix equation:

$$M_q\ddot{q} + C_q\dot{q} + K_q q = C_w\dot{w} + K_w w, \tag{5.12}$$

with $q = [\ x_{out} \quad y_{out} \quad z_{out} \quad \alpha_{out} \quad \beta_{out} \quad \gamma_{out}\ ]^T$, $\dot{q}$ the time derivative, and $\ddot{q}$ the second time derivative of q. Vector w stands for $[\ x_{in} \quad y_{in} \quad z_{in} \quad \alpha_{in} \quad \beta_{in} \quad \gamma_{in}\ ]^T$ and $\dot{w}$ is its time derivative. The M_q matrix is built up out of mass properties of the cabin combined with moments and products of inertia. All damper forces create elements in the C matrices while the forces related to the spring properties show up in the K matrices. In this case both C matrices, C_q and C_w, are equal, as are both K matrices.

5.2 Validation of the model

5.2.1 Description of the setup

Figure 5.4 shows the experimental setup used to validate the linear model of the previous section. The system is built using four air springs

Figure 5.4: Spring suspension system with four *Firestone Airmount 7012* springs put at a 45 degree angle with respect to the vertical direction [33] (P,Q and R indicate the principle axes for one spring)

of the type *Firestone Airmount 7012*. These airsprings are put at a 45 degree angle with respect to the vertical direction but also with respect to the longitudinal and transversal directions as can be seen in the figure. The four air springs support a main structure containing two square plates measuring $0.8m$ on $0.8m$ and weighing $111.88kg$. The moments of inertia of the system are $I_{xx} = 7.16kgm^2$, $I_{yy} = 4.78kgm^2$ and $I_{zz} = 11.92kgm^2$. Due to the symmetrical setup no inertia products are needed to build up the model.

The spring and damping constants of the air springs can be directly taken out of the catalogue since no expansion volumes are used. The spring stiffness along the axis of symmetry k_p is set to $2.64kN/m$. The spring stiffnesses perpendicular to this axis, k_q and k_r are set to one third of k_p according to the guidelines in the air spring catalogue [50] and the Harris' Shock and Vibration Handbook [64]. The Firestone catalogue mentions that the damping ratio for these elements is approximately 0.03. This means that c_p, c_q and c_r are respectively $65Ns/m$, $38Ns/m$ and $38Ns/m$.

Figure 5.5 shows the experiment to determine k_p^t of an air spring. Torque is applied to the spring by placing a weight at a certain distance

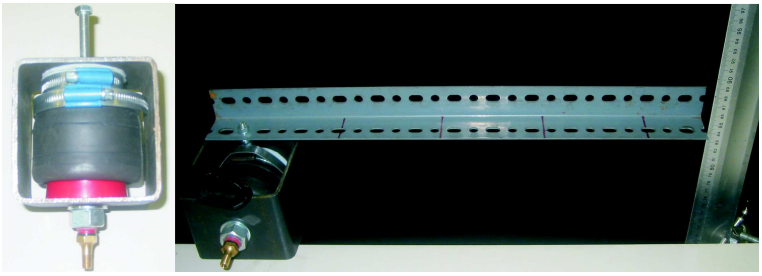

FIGURE 5.5: Experimental setup to determine k_p^t of an air spring

on a lever connected to one side of the spring while the other is fixed. The air spring is boxed in to make it possible to perform experiments at different internal pressures. Friction is reduced by using teflon elements in the setup. For the *Firestone Airmount 7012* a k_p^t of $700 Nm/rad$ is measured. The value is pressure independent and thus merely a characteristic of the rubber of the spring.

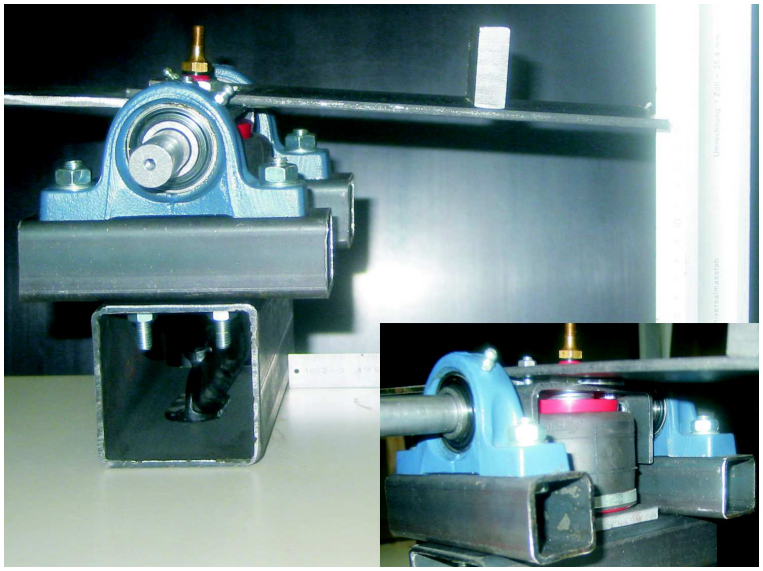

FIGURE 5.6: Experimental setup to determine k_q^t and k_r^t of an air spring

Figure 5.6 shows the setup to determine k_q^t and k_r^t. Almost an

identical method as for k_p^t is used, but here a "bending" property of the air spring is evaluated. The bottom of the air spring is fixed, while the top is connected to a plate that can rotate around an axis perpendicular to the symmetry axis. This setup allows again to conduct experiments at different internal pressures. k_q^t and k_r^t are $70Nm/rad$ with a minimal influence of the pressure.

For the torsional damping the same assumption is made as for the linear damping coefficients. A damping ratio of 0.03 is proposed.

5.2.2 Measurements and evaluation

To compare the behavior of the real setup with that of the model, the system is put on a hydraulic shaker. Swept sine and random signals with a frequency content between 0.7 and $7Hz$ are used to determine the natural frequencies of the six rigid body modes of the setup. Two L shaped measuring devices (see chapter 3) record input and output accelerations.

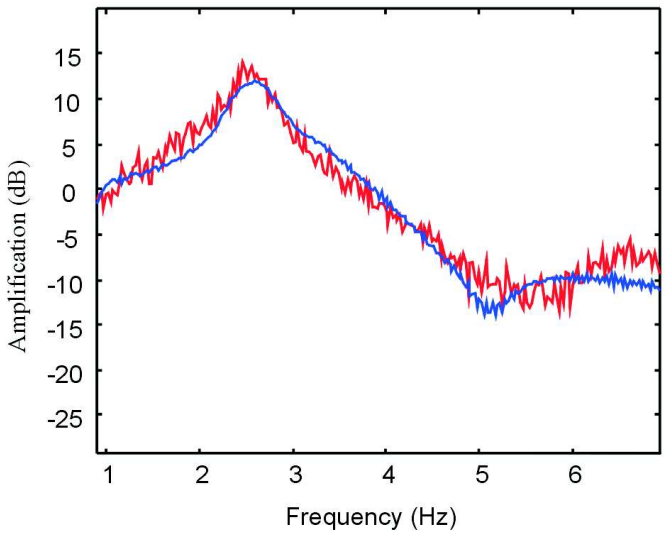

Figure 5.7: Frequency response function of the swept sine (blue) and the random (red) signals for the vertical degree of freedom of the experimental setup [33]

Figure 5.7 compares the magnitude of the FRF of two measurements evaluating the vertical DOF of the setup. The similarity of both FRFs shows that using a linear model to determine the behavior of the setup below 5Hz is justified. Above 5Hz the setup is considered to be non-linear. This is also visible in the figure where the FRF becomes more dependent on the input signal [33].

Table 5.1 compares the natural frequencies of the six rigid body modes of the setup with the calculated natural frequencies of the model.

DOF	setup	model
X-axis	2.3	2.3
Y-axis	2.2	2.3
Z-axis	2.5	2.6
roll	3.3	3.4
pitch	5.2	5.3
yaw	3.1	3.2

TABLE 5.1: Natural frequencies of the rigid body modes of the setup compared with the calculated natural frequencies from the linear model

The model shows good resemblance with the experimental setup and only slight differences in the natural frequencies are observed.

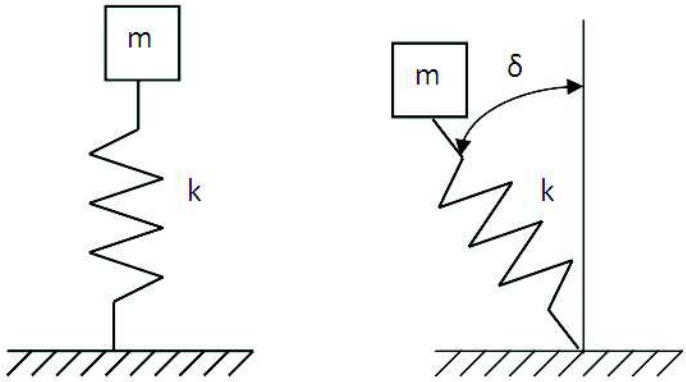

FIGURE 5.8: Effect of putting a spring under an angle δ

The catalogue indicates that using the *Firestone Airmount 7012* in

a vertical setup would result in a system with a natural frequency of $1.3Hz$. To calculate the effect of inclination of a spring on the natural frequency, figure 5.8 shows two suspensions, one with a vertical spring k supporting the mass m and another with the same spring making an angle δ with the vertical axis.

$$\begin{aligned} & m\ddot{y} && = && k(-y+x), \\ \Rightarrow \quad & m\ddot{y}+ky && = && kx. \end{aligned} \tag{5.13}$$

$$\begin{aligned} & m\ddot{y} && = && k(-y+x)\cos^2\delta, \\ \Rightarrow \quad & m\ddot{y}+ky\cos^2\delta && = && kx\cos^2\delta. \end{aligned} \tag{5.14}$$

The equation of motion of both systems is given by formulas 5.13 and 5.14. The natural frequency for the system with the vertical spring is $\sqrt{k/m}$ while that of the other system is $\sqrt{kcos^2\delta/m}$. Since $-1 \leq \cos\delta \leq 1$, putting the spring at an angle to the vertical axis will result in a weaker system with a lower natural frequency. Looking at the natural frequency of the vertical rigid body mode of the experimental setup the opposite is observed.

This phenomenon can be explained by two facts. First, to support the mass with an air spring at an angle δ, the pressure in the spring has to be augmented. It is augmented with a factor $1/\cos\delta$. A second effect here is the fact that the air springs are not fully inflated. Due to the low weight of the plates the internal pressure of the air springs is barely $0.5bar$ while the catalogue mentions a minimum of $0.7bar$ to have good behavior of the air springs. At these low pressures the influence of the rubber of the spring is bigger, resulting in a higher stiffness.

An additional remark has to be made that the stiffness responsible for the natural frequency of the vertical rigid body mode is k_{zz}. This stiffness is, looking at equations 5.3, a combination of different stiffnesses and λ's. If k_q and k_r are larger than k_p then the spring stiffness in the vertical direction could increase by putting the air spring under an angle with the vertical axis. This is not the reason here since k_q and k_r are one third of k_p. When altering the spring stiffness by adding a volume of air, this can occur because the volume of air changes k_p of the air spring and k_q and k_r keep their original value since these are for the main part characteristics of the rubber.

While using the setup with air springs at an angle with the vertical axis, problems occurred with the stability of the whole setup. Due to the angle a part of the force of the air spring is in the horizontal

plane which makes that the pressures in all four air springs have to be equal to center the plates. Exposing the suspension to vibrations made the suspension sometimes collapse when one or more of the air springs overextended itself. To prevent this, metal wires were used as can be seen on figure 5.4.

It can be concluded that using air springs at an angle with the vertical axis can cause several problems. This is the reason why for the final design this line of thought is abandoned. The air springs will be used in a vertical position. In that way the spring stiffness along the axis of symmetry k_p, which can be altered by using an expansion volume, is orientated in the direction where highest vibrations occur and where the attenuation of the vibrations is the most important.

5.3 Practical implementation of the linear model

Now that a model for the cab suspension system is established, it can be used to predict the behavior of new designs. Using the knowledge of previous section, the final cab suspension design will make use of four vertically orientated *Firestone Airmount 1M1A-1* air springs. As derived in chapter 4 auxiliary volumes of $0.6liter$ will be used to lower the spring stiffness of the air springs and to make it possible to increase the damping of the suspension.

The characteristics of the cabin are set to the values mentioned at the beginning of this chapter. For the characteristics of the *1M1A-1* air spring several elements are important. The behavior of the spring in the P direction, k_p, is here replaced by the linear model (equation 4.23) of the previous chapter. Three parameters are important in this equation: k_S, the spring stiffness of the air spring, k_{SA}, the spring stiffness of the air spring when the auxiliary volume is attached to it and D, a parameter depending on the damping in the system. For the *1M1A-1* air spring k_S is $86kN/m$ when supporting a cabin of $706kg$ and k_{SA} is $27kN/m$. When D is put to a value of 0.11 the maximal amplification can be set to 1.8 at a natural frequency of $2.33Hz$. This is a relative low amplification and natural frequency but this can still be improved to respectively 1.4 and $1.93Hz$ if the auxiliary volume is expanded to $2liter$.

k_r and k_q are set to a constant $29kN/m$, one third of k_S according to the guidelines in the air spring catalogue [50] and the Harris' Shock and

Vibration Handbook [64]. The values for k_p^t, k_q^t and k_r^t are measured using the setups explained in previous section. For k_p^t $230Nm/rad$ is measured, while for k_q^t and k_r^t $5Nm/rad$ is found. For all damping parameters a damping ratio of 0.03 is used.

When incorporating the linear model of the new pneumatic cab mount (see equation 4.23), the k_p spring stiffness gets replaced by a first order function resulting in:

$$k_p = -k_{SA}\frac{sD+1}{sD\frac{k_{SA}}{k_S}+1}. \tag{5.15}$$

Equation 5.12 is then converted to:

$$\begin{aligned} M_q\ddot{q} + C_q\dot{q} + K_{SA}\frac{sD+1}{sD\frac{K_{SA}}{K_S}+1}q \\ = C_w\dot{w} + K_{SA}\frac{sD+1}{sD\frac{K_{SA}}{K_S}+1}w, \end{aligned} \tag{5.16}$$

where K_{SA} represents the K_q and the K_w matrix where k_p is set to k_{SA} while K_S represents the same matrices where k_p now is set to k_S. Working equation 5.16 out results in:

$$\begin{aligned} M_q q s^2(sD\frac{K_{SA}}{K_S}+1) + C_q q s(sD\frac{K_{SA}}{K_S}+1) + K_{SA}q(sD+1) \\ = C_w w s(sD\frac{K_{SA}}{K_S}+1) + K_{SA}(sD+1)w, \end{aligned} \tag{5.17}$$

and is simplified to:

$$\begin{aligned} M_q D\frac{K_{SA}}{K_S}qs^3 + \left(M_q + C_q D\frac{K_{SA}}{K_S}\right)qs^2 + (C_q + K_{SA}D)\,qs + K_{SA}q \\ = (C_w + K_{SA}D)\,ws + K_{SA}w. \end{aligned} \tag{5.18}$$

The order of the six DOF model of the suspension system augments from two to three due to the replacement of the constant k_p by a first order system.

It is clear that only the elements in mass, damping and stiffness matrices alter if k_p is involved in their formulation. Due to the vertical

positioning of the air springs only the z, α and β degrees of freedom are affected by the air spring model.

The most important issue in this thesis is the effectiveness of the cab suspension to suppress vibrations. This is evaluated in the time domain using VDV and effRMS. The purpose of the above derived linear model, is to predict as accurate as possible the comfort values. This accurate computation can only be done properly if the assumption that the set-up behaves linear in the for the comfort values import frequency band, is correct.

Since no multiple input multiple output identification of the cabin suspension is performed, only an approximate evaluation of the linearity of the suspension is possible. This was performed by applying in-situ measured acceleration signals to the cab suspension system. For this conditions IX, XIV and XVIII, respectively harvesting at $4km/h$, transport on an unpaved road at $11km/h$ and transport on a paved road at $28km/h$ of chapter 3 were used. To prevent the occurrence of end stop impacts that have a big non linear influence on the behavior a the system [65], the amplitude of the signals was reduced to 5 and 10 % of the real value resulting in six excitation signals. The frequency content of these signals was limited to the band between 0.7 and 15 Hz.

Figure 5.9 shows the amplitude of the measured FRFs obtained (in blue) together with the average signal (in black) for the vertical DOF of the suspension system (see figure 7.6). Comparing the average signal with figure 4.11 of section 4.3.2 shows a similar behavior up to 7 Hz. Noise on the measurement is present, but whether this is due to the presence of non-linearities or due to the use of improper excitation signals is not clear. Claiming that the system behaves linear is not possible but can be assumed in the low frequencies, up to 8 Hz. Since comfort values focus mainly on this low frequency region, calculating the comfort values based on the linear model of the suspension is valid. Looking at figure 5.9 it is assumed that the comfort values calculated based on the linear model will be lower than the actual values.

The model of the suspension was evaluated by computing the VDV and effRMS values inside the cab if the suspension is excited using the vibrations recorded during harvesting on the field at $6km/h$ and transport conditions on the road at 11 and $28km/h$. Table 5.2 gives these computed values. The VDV is calculated again using a time frame of $5min$.

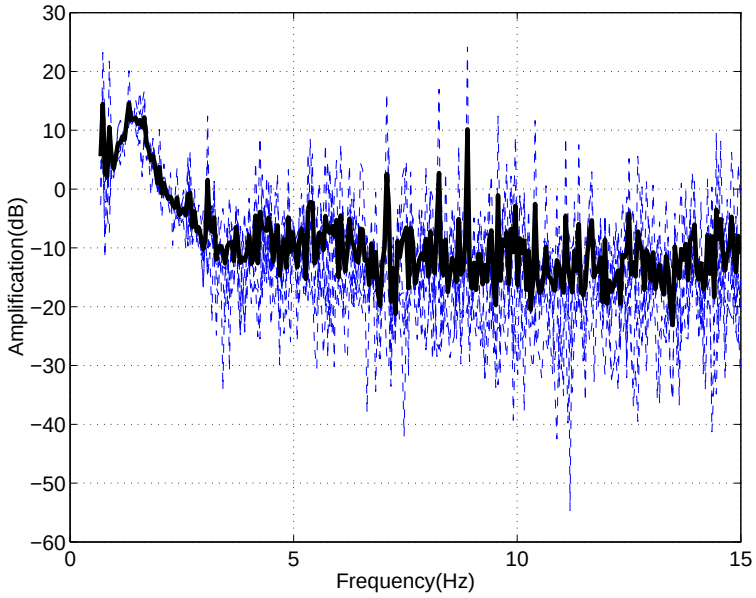

Figure 5.9: Experimentally obtained frequency response functions for the vertical degree of freedom of the cab suspension using six in-situ measured excitation signals (signals: blue; average signal: black)

The model predicts very good comfort values for the new pneumatic cab suspension. As can be seen on table 5.2 with exception of the rolling behavior of the cab during harvesting, no action values for the effRMS and VDV are violated using this new suspension. If this suspension system works in practice needs to be seen during evaluation of a real setup.

5.4 Conclusion

A general linear model of a cabin suspension was derived, in which all cab mounts were considered to be a combination of linear springs and dampers. Additional torsional stiffness and damping was introduced to deal with the torsion and bending properties of the air springs.

The resulting six degree of freedom linear model was validated with an experimental setup using four *Firestone Airmount 7012* air springs.

	RMS		VDV	
	in	out	in	out
harvesting				
X-axis	0.1007	0.0743	0.5421	0.3890
Y-axis	0.1025	0.0703	0.5670	0.3695
Z-axis	1.0078	0.1074	5.1673	0.5206
$\sum$	1.0277	0.1790	5.1677	0.5823
roll	0.9810	0.7346	5.3093	3.9850
pitch	0.3955	0.1927	2.4105	1.0146
yaw	0.1150	0.0367	0.6373	0.1892
transport unpaved road				
X-axis	0.1661	0.0563	1.0899	0.3801
Y-axis	0.4583	0.1734	3.2427	1.2200
Z-axis	0.6759	0.0916	3.7664	0.5113
$\sum$	0.9605	0.2712	4.2069	1.2321
roll	0.2172	0.1469	1.6786	1.1416
pitch	0.1893	0.1837	1.1674	1.0189
yaw	0.1224	0.0573	0.8092	0.3922
transport paved road				
X-axis	0.1335	0.0446	0.6952	0.2173
Y-axis	0.2800	0.1054	1.5729	0.5651
Z-axis	1.2081	0.2121	6.9687	1.8227
$\sum$	1.2838	0.2658	6.9734	1.8270
roll	0.4270	0.2735	2.3826	1.5499
pitch	0.2787	0.1863	1.5695	1.0185
yaw	0.1126	0.0422	0.6331	0.2203

TABLE 5.2: Calculated VDV and effRMS values using the model of the pneumatic cab suspension

The orientation of the springs was at a 45 degree angle with respect to the vertical direction. The model clearly predicted the natural fre-

quencies of the rigid body modes. Experimental tests showed stability problems due to the orientation of the springs. Therefore the final cab suspension concept uses vertically oriented springs.

The linear model of the pneumatic cab mount was introduced in the linear cabin model. This model was used to predict the improvement in comfort values the new cab suspension will result in. The validity of the linear model was checked. In the low-frequency region of interest (below 8 Hz) no real nonlinear behavior was observed. At higher frequencies experimental data showed a higher magnitude than the linear model due to possible nonlinearities.

The predicted comfort values showed no violation of action values. Only the rolling behavior of the cabin is somewhat too high.

Chapter 6

Optimization of Non-Linear Suspension Models

To obtain optimal comfort improvement from a suspension system, a good optimization is indispensable. Now that the parametric models of the new cabin mounts have been derived in chapter 4 the parameters in these models are optimized in this chapter with respect to comfort using in-situ measurements.

To evaluate the behavior of off-road machinery, a large number of test drives are performed under different conditions e.g. road profile, motor load, use of implements, ... (see chapter 3). During these tests, a lot of data is collected varying from the vibration levels at different positions on the machine over the noise levels produced in- and outside the cabin to the efficiency of the harvesting process in relation to the slope of the field [89]. During such tests also the behavior of the suspension is monitored by measuring the vibrations levels before and after the suspension elements. The outcome of all these tests not only results in diagnostic information on the behavior of the machine, but also in a large amount of additional data.

This chapter sets up an optimization procedure to make use of in-situ measured vibrational data to optimize non-linear suspension models. The collected vibrational data, displacements, velocities, accelerations are used to preliminary investigate if the new elements would perform adequately under real conditions. The procedure can be seen

as an additional test to prevent setting up prototypes with would result in mediocre results.

The procedure is explained in the first section. The second section optimizes the hydro-pneumatic cab mount as a test case.

6.1 Optimization Procedure

The proposed optimization procedure incorporates in-situ measurements in the optimization of non-linear suspensions. The following four steps can be detected in the procedure:

1. Data Collection
2. Modelling
3. Selection of the Objective Function
4. Optimization

The whole procedure is developed using Matlab [92] and Simulink [121]. This gives the main advantage that all steps are performed in the same environment and problems like conversion of data can be avoided.

6.1.1 Data Collection

The data of interest here are the vibration levels, accelerations, velocities or displacements, measured during several field tests with the machine, at the base of a suspension device that has to be replaced by a new one or at places where a suspension will be introduced. Examples of these are the vibrations at the support of the cabin and vibrations of the cabin floor at the place where the seat is situated.

6.1.2 Modelling

In order to be able to optimize a suspension, all of it or at least a part of it, has to be modelled using physical principles resulting in a white box or hybrid model. (Models like those developed in chapter 4). Since the method uses in-situ input measurements, it is not necessary to limit the modelling to the linear case. The use of real measurements makes it possible to give a correct interpretation to the behavior of a non-linear model in both time and frequency domain.

6.1.3 Selection of the Objective Function

The aim of this thesis is to look for suspension devices that give an added value with respect to improvement of comfort, therefore the goal functions are drawn up with respect to this comfort issue.

In the time domain it is possible to optimize the suspension with respect to comfort improvement by using the objective comfort parameters VDV and effRMS stated in the standards ISO 2631 and BS 6841 [2, 3]. Both of these parameters use a single value to determine the comfort and are therefore adequate to serve as goal to be minimized.

Despite the fact that the time domain approach is straightforward, an optimization using a goal function determined in the frequency domain is also possible. In the ideal case the Frequency Response Function (FRF) of the suspension must show a gain of 1 for low frequencies (lower than $1Hz$) and must be null for high frequencies (higher than around $1Hz$) [114]. Postulating a desired magnitude of the FRF resembling this ideal case and using the deviation between this desired magnitude and the magnitude of the measured FRF in a certain frequency band, renders the function to be minimized. The formula for this deviation, DIFF, is given by:

$$DIFF = \left[\frac{1}{K} \sum_{k=1}^{k=K} W_k (A_k - B_k)^2 \right]^{\frac{1}{2}}, \tag{6.1}$$

in which K stands for the number of frequency lines used, W_k for the weighing factor at frequency line k, A_k for the desired magnitude and B_k for the measured magnitude at frequency line k, all expressed in a linear scale.

Figure 6.1 gives an example on how optimization using DIFF can be applied. The desired FRF for a one degree of freedom suspension system is labelled as "aim" in figure 6.1. Applying different weighing functions in the formulation of DIFF will lead to different solutions. Putting emphasis on suppressing the resonance peak leads to solution 1 while stressing the behavior above resonance results in solution 3. The weighing function should be chosen in such a way that it reflects the designers purpose for the suspension.

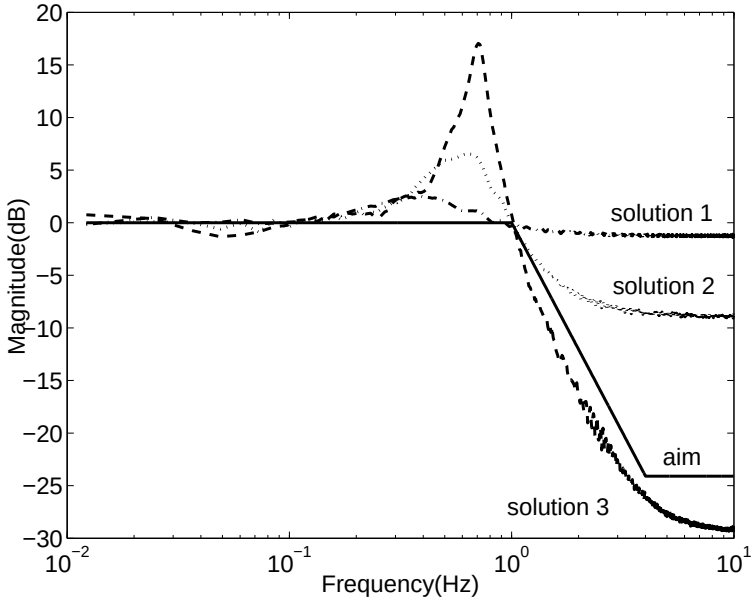

Figure 6.1: Magnitude plot of three solutions obtained by optimization in the frequency domain using different weighting functions together with the desired magnitude plot

6.1.4 Optimization

Once the objective function is established, the problem can be described in the following way:

$$\min f(x), \tag{6.2}$$

subject to $x \in [l, u]$,
with $[l, u] := \{x \in \mathbf{R}^n \mid l_i \leq x_i \leq u_i, i = 1, \cdots, n\}$.

In this equation $f(x)$ is the objective function, x represents the n parameters and l and u the parameter bounds. Derivative based optimization techniques have no problem optimizing smooth functions [98] but this is not the case for a goal function obtained during optimization of the hydro-pneumatic suspension of chapter 4 as illustrated by figure

6.2. Due to the use of in-situ measured signals, the objective function becomes very non smooth. This function could not be optimized using the standard techniques in Matlab [92], which are all derivative based and got stuck in the various local minima. To overcome such a problem a global optimization technique was used.

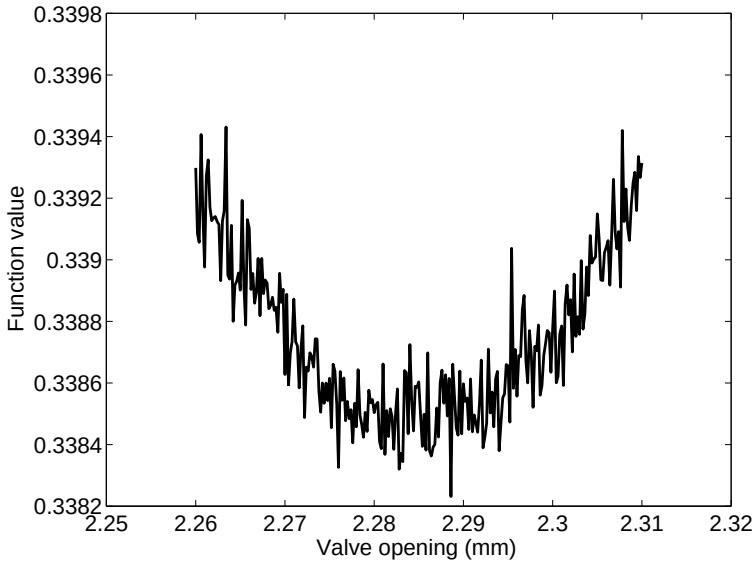

FIGURE 6.2: Objective function near global minimum when changing one parameter of the hydropneumatic passive suspension system

There exists a variety of global methods to solve this problem but the algorithms can be classified into two main groups: heuristic methods, like evolutionary algorithms and simulated annealing, that find the global minimum with a high probability and deterministic methods that guarantee to find the global minimum with a required accuracy [73]. The method used here is called DIRECT. It's a deterministic, 'branch and bound' technique implemented in the Matlab routine glbSolve [12].

DIRECT is an algorithm, presented by Jones et al. in [78], for finding the global minimum of a multivariate function subject to simple bounds. The algorithm is a modification of the standard Lipschitzian approach that eliminates the need to specify a Lipschitz constant. This is done by carrying out simultaneous searches using all possible Lips-

chitz constants from zero to infinity. In [78], Jones et al. introduces a different way of looking at the Lipschitz constant. In particular , the Lipschitz constant is viewed as a weighing parameter that indicates how much emphasis to place on global versus local search. In standard Lipschitzian methods, this constant is usually large because it must equal or exceed the maximum rate of change of the objective function. As a result, these methods place a high emphasis on global search which leads to slow convergence. In contrast, the DIRECT algorithm carries out simultaneous searches using all possible constants, and therefore operates on both the global and local level. Once the global part of the algorithm finds the basin of convergence of the optimum, the local part quickly and automatically exploits it. This accounts for the fast convergence of the DIRECT algorithm.

For a clear overview of global optimization techniques and more details concerning the DIRECT algorithm, consult appendix A.

6.2 Test Case: Hydro-pneumatic Suspension

6.2.1 Optimization parameters

To test the procedure of section 6.1, parameters in the nonlinear model of the hydro-pneumatic suspension element of figure 4.5 were optimized. The next paragraphs follow the steps of the procedure and point out specific details in this optimization.

Data Collection

The in-situ measurements were a selection of signals provided in chapter 3. The vertical accelerations at the base of the cabin suspension during field harvesting at $4km/h$ (condition IX), transport on an unpaved road at $11km/h$ (condition XIV) and on a paved road at $28km/h$ (condition XVIII) were used. The input signals were all 122.88 seconds long, sampled at 200Hz which resulted in VDVs for the paved road of $5.606m/s^{1.75}$, for the unpaved road of $3.049m/s^{1.75}$ and for the field track of $4.108m/s^{1.75}$.

Modelling

The non-linear model of the hydro-pneumatic suspension was taken from chapter 4. In the model the parameters of the hydraulic cylinder,

the rod diameter of $18mm$, the cylinder diameter of $32mm$ and the stroke of $190mm$, together with the mass of $185kg$ that had to be supported, were kept constant. The four other parameters in the model were allowed to vary. The volume of the nitrogen in the accumulators V_1 and V_2, the pressure p_2 and the opening area S of the valve. Pressures p_1 and p_3 could be determined using the pressure p_2, the mass and the areas of the rod and the cylinder. The schematic figure 4.2 indicates all these parameters.

Selection of the Objective Function

Two different objective functions were compared with each other during the optimization of the hydro-pneumatic suspension. In the time domain the VDV of the output acceleration was used as a goal to be minimized. In the frequency domain the desired FRF resembled the aim of figure 6.1. The magnitude up till 1 Hz was 1 and between 1 and 4 Hz it dropped down at a ratio of -40 dB/decade to an attenuation level of approximately -17 dB above 4 Hz. The objective function in the frequency domain was given by equation 6.1. A uniform weighing has been applied in the DIFF formulation.

Optimization

Before the optimization could be performed, realistic bounds were set for the four variables. The volume of the nitrogen in the accumulators V_1 and V_2 was allowed to change between 0.5 and $2l$, the pressure p_2 was bound between 2.5 and $5MPa$ and the opening area S of the valve was limited to $75mm^2$.

The optimization was performed combining the three different input signals called "field", "paved road" and "unpaved road" with the objective function in the time and frequency domain. This resulted in 6 possible optimal solutions for the problem. Tables 6.1 and 6.2 show for each optimal solution the retrieved parameters and indicate the minimum value of the objective function with a bold figure. Using the obtained parameters, the value of the objective function in the other five cases, is also included in the tables.

input profile	VDV $[m/s^{1.75}]$	DIFF	parameters
paved road	**1.132**	3.256	$p_2 = 2.51MPa$
unpaved road	1.105	2.979	$S = 19.4mm^2$
field	1.056	8.169	$V_1 = 1.21l, V_2 = 1.12l$
paved road	1.165	2.513	$p_2 = 2.51MPa$
unpaved road	**1.073**	2.629	$S = 19.1mm^2$
field	1.327	9.178	$V_1 = 1.35l, V_2 = 0.88l$
paved road	1.717	1.174	$p_2 = 2.55MPa$
unpaved road	1.186	1.426	$S = 14.7mm^2$
field	**1.022**	9.104	$V_1 = 1.73l, V_2 = 1.58l$

Table 6.1: Calculated objective function value for suspensions developed using time domain optimization

input profile	VDV $[m/s^{1.75}]$	DIFF	parameters
paved road	2.442	**0.424**	$p_2 = 4.12MPa$
unpaved road	1.646	1.251	$S = 9.3mm^2$
field	1.357	11.007	$V_1 = 1.31l, V_2 = 0.97l$
paved road	2.867	0.660	$p_2 = 2.58MPa$
unpaved road	1.562	**0.598**	$S = 7.1mm^2$
field	1.064	8.972	$V_1 = 1.31l, V_2 = 0.75l$
paved road	1.170	3.498	$p_2 = 2.55MPa$
unpaved road	1.139	2.846	$S = 17.9mm^2$
field	1.359	**7.274**	$V_1 = 1.36l, V_2 = 1.02l$

Table 6.2: Calculated objective function value for suspensions developed using frequency domain optimization

6.2.2 Discussion

The optimization procedure was able to determine the best solution for each of the six optimizations since the bold figures are always the lowest in their category. This also means that 6 distinct suspension systems are retrieved. The origin of that lies in the use of a nonlinear model and the fact that although both objective functions aimed at the improvement of the comfort behavior, the expression for it is different.

This raises the question if this method serves a purpose since every measurement of the machine under distinct operating conditions will result in a different input signal and could lead to a different optimal suspension system. Therefore it is crucial to select those input signals

that give a good representation for the general behavior of the machine under normal working conditions. Table 6.1 shows also that the optimal suspension for one input signal does not mean bad behavior for the other input signals. In this case one passive suspension system can be used. If on the other hand higher performance is required, the optimal solutions can be used in a semi-active approach of the suspension system [53].

Table 6.1 shows that the optimization based on the VDV resulted in three almost equal suspensions with a low natural frequency (low pressure and large volumes of nitrogen) and a small amount of damping (large S). The natural frequencies of the three systems are 0.6 Hz, 0.65 Hz and 0.4 Hz. This was not the case when the optimization was done based on DIFF which resulted in three distinct suspension systems (see table 6.2). The natural frequencies are here 0.85 Hz, 0.7 Hz and 0.6 Hz. The explanation for this lies in the fact that the VDV focuses on low acceleration levels and these can be provided for all input signals with a suspension with a low natural frequency. DIFF on the other hand shapes the transmissibility of the suspension and thus restricts high displacements at low frequency which will not show up in the VDV since the acceleration level of low frequency displacements is low. This leads to the conclusion that for the design of suspension systems the choice of objective function is a crucial factor. In this specific case the suspension systems of table 6.2 will be preferred above those of table 6.1 despite the fact that their VDV is higher. Slow movements generated by the low natural frequency of the latter could lead to the seasickness phenomenon for the driver which has to be prevented [56].

Both tables also show that whatever optimization method is used, a reduction of the VDV in comparison with the input signals between 30% and 75% could be established. Based on this information only, even in light of the 7% error in predicting the VDV as mentioned in equation 4.6 of chapter 4, it can be said that using this type of hydropneumatic element in the design of a cabin suspension gives satisfactory results. In that way the method presents a means for deciding if a suspension system can be optimized to perform adequately under real conditions.

During the optimization, the advantages of the used optimization method DIRECT became clear. The combination of local and global search resulted in fast convergence to the global minimum of the goal function. That fast convergence compensated to a great extent the

disadvantage of not having a stopping criterium, which is the case for deterministic optimization methods [29].

6.3 Conclusion

This chapter showed how vibration measurements collected during field tests could be used in the optimization of non-linear suspension systems. Optimization was performed with respect to the objective comfort parameters vibration dose value and effective root mean square in time domain. Alternatively an optimization was proposed where the deviation of the frequency response function was used as cost function. Due to various local minima in the cost function, global optimization was necessary.

The procedure was applied to the non-linear model of a hydropneumatic suspension element. It predicted the effect the implementation of the suspension element would have on the comfort values without actually having to build a real set-up. The procedure could be seen as a design approach incorporating a feasibility assessment.

Chapter 7

Evaluation of the Cab Suspension

This chapter describes the final stage in the development of the cab suspension. Models derived in previous chapters predicted significant comfort improvement applying the pneumatic cab mounts in a full cabin suspension. For the evaluation in-situ measured signals are reproduced on a six degree of freedom electro-hydraulic shaker. The evaluation of the suspension not only shows the effectiveness of the cabin suspension but also validates the modelling approach.

The first section describes the evaluation platform that is utilized in a second section to evaluate the pneumatic cabin suspension.

7.1 Evaluation platform for suspension systems

7.1.1 A 6 DOF vibration simulator

Vibration simulators are an indispensable tool for gaining insight into vehicle dynamics and for model validation by producing repeatable signals under controlled laboratory conditions. In this thesis the final evaluation of the suspension system is performed on a six degree of freedom (6 DOF) electro-hydraulic shaker originally designed to evaluate the behavior of spray booms (see figure 7.1). The $2.25m$ square platform of this test rig is able to reproduce the vibrations (three translations and three rotations) at the hitchpoint of the spray boom. There-

Figure 7.1: Electro-hydraulic shaker; top left: cylinders in Stewart configuration; top right: hydraulic group and numerical controllers; bottom: platform

fore the basic features for the simulator are that it is able to produce vibration signals in a frequency range from $1Hz$ with an amplitude of $0.1m$ till $10Hz$ with an amplitude of $0.001m$ when carrying a load of $500kg$ [66, 67].

To fulfill these specifications the rig is equipped with six differential cylinders with a stroke of $0.3m$ and a piston and rod diameter of respectively 0.05 and $0.032m$, put in a Stewart configuration [123]. This means that the cylinders are placed under the platform in such way that the connection points of the cylinders with the platform and the ground form a perfect hexagon in top view. This configuration makes it possible to get, in this case, amplitudes of $0.15m$ for each translational degree of freedom and to perform rotations with amplitudes up to $0.2rad$.

Each cylinder is equipped with a two-stage, four-way servo valve with electrical and mechanical feedback and integral control electronics. The valves have a bandwidth of $120Hz$ and a nominal flow of

$90l/min$ ($1.5 \times 10^{-3} m^3/s$) which is necessary to reach the $0.1m$ amplitude at $1Hz$. The system is powered with a hydraulic group containing a variable displacement axial piston pump with a maximum flow of $285l/min$ ($4.75 \times 10^{-3} m^3/s$). The pump is driven by an electric motor of 90kW and operates at a nominal pressure of $16MPa$. The central programmable logic controller system makes it possible to manually operate all six actuators or can make them follow externally imposed movements generated by e.g. a personal computer.

Finite element analysis on the platform shows that the first eigenfrequency of the platform loaded with the mass of $500kg$, is situated near $40Hz$, more specific $38.52Hz$. The maximum acceleration needed to fulfill the specifications of $0.1m$ at $1Hz$ to $0.001m$ at $10Hz$ is about $4m/s^2$. The force needed to impose this on the platform with load is only approximately $3kN$. This means that the cylinders, which can each give at the nominal operating pressure of $16MPa$ a force of 31 and $15kN$ respectively at the piston and the rod side, deliver ample force. The option could be to use smaller actuators but the chosen piston/rod diameter of $50/36mm$ is necessary to reach a lowest eigenfrequency of $40Hz$ for the actuators. All other elements in the construction of the simulator guarantee that same lowest eigenfrequency. This makes the construction fit to excite test objects up to $20Hz$.

The specifications of the vibration simulator make it very suitable to mimic the vibrations encountered on mobile agricultural machines. This shaker was therefore used to reproduce the vibrations at the base of the cab suspension system.

7.1.2 Time Waveform Replication Monitor

When designing a new vehicle, car manufacturers and also designers of modern mobile agricultural machinery, make extensively use of test drives on public roads and test tracks. During these test drives, so called service loads at some specific points of the vehicle are measured. These service loads can be accelerations, forces or displacements, and are referred to as *target signals* in the rest of the chapter. On one hand the test drives measurements are indispensable to optimize and sign-off the design of the car for aspects such as durability and comfort. On the other hand, test drives on the road or in the field are expensive, time consuming and uncomfortable for the driver who has to drive for hours and hours in often severe conditions [32].

An alternative to this is simulating the measured service loads in

a laboratory environment. The target signals measured during a test drive are reproduced using a multi axial shaker. This typically involves reproducing high amplitude loading conditions causing non-linear test object and test rig behavior. This makes it difficult to derive the input signals, or *drives*, that have to be applied to the test rig to produce responses that approximate the target signals as close as possible.

LMS International developed CADA-X Time Waveform Replication Monitor (TWR), software to perform fast and accurate service load simulations. The software develops the drive files using two phases. In a first step an accurate description of the non-linear dynamics of the test rig is derived, using system identification techniques in time and frequency domain. For that TWR uses a modelling technique based on the calculation of the Frequency Response Function (FRF) matrix, to obtain a mathematical multiple input, multiple output (MIMO) model between the voltages sent to the test rig and the responses measured on the test subject. The excitation levels are made comparable to the operational excitation level of the target signals. In that way the best linear approximation for the non-linear system characteristics is obtained.

The second phase, the target simulation, is due to the non-linear behavior of the test rig and object, performed using an iterative procedure. The initial drives are calculated using the FRF matrix model:

$$Drives = FRF^{-1} \times Targets \times Gains, \tag{7.1}$$

where $Drives$ and $Targets$ denote the FFT of the drive and target signals and the $Gains$ are factors between 0 and 1 to prevent overexcitation of the test rig as well as divergence in the iteration process. The inverse of the FRF is calculated using a Singular Value Decomposition. In the following iteration steps the errors between the targets and the responses are used to update the drives (see equation 7.2).

$$\begin{aligned} Correction &= FRF^{-1} \times Errors \times Gains \\ NewDrive &= OldDrive + Correction \end{aligned} \tag{7.2}$$

In TWR several error indicators, both in the time and the frequency domain, are available to evaluate the process of service load calculation. The following formulas give two of these quantitative measures:

FIGURE 7.2: Interface of the Time Waveform Replication Monitor

$$\frac{RMS_{error}}{RMS_{target}} = \frac{\sum_{i=1}^{i=N} e_i^2}{\sum_{i=1}^{i=N} t_i^2}, \tag{7.3}$$

$$\frac{RMS_{response}}{RMS_{target}} = \frac{\sum_{i=1}^{i=N} r_i^2}{\sum_{i=1}^{i=N} t_i^2}. \tag{7.4}$$

Here N denotes the number of measurement points used, t is the target acceleration, r is the acceleration of the response of the test rig and e represents the error between the target and the response. The values of these two give an indication of the convergence between the target signal and the measured signal. These values are used to determine when to stop the updating of the drives.

Besides these quantitative measures, a qualitative evaluation is also possible. Figure 7.2 gives a typical TWR interface, here during the identification of the test rig. The three top graphs compare the power spectral density (PSD) of the target signals with that of measured accelerations. During the identification of the rig, these graphs compare the amount of power put in the various degrees of freedom, to the power of the targets. During the process of target simulation these graphs will

give a good indication of how closely the drives are able to reproduce the targets.

The four middle graphs show four of the elements of the FRF matrix. The relative changes of the FRFs between different identification steps will indicate if the model converges. The graph in the right bottom, which shows the coherence of the FRFs, also helps to determine that.

Several other numeric and graphical aids are available in TWR. For a description of them, the reader is referred to the CADA-X Time Waveform Replication user manual [88]. For a more elaborated description on the working of TWR the reader is referred to De Cuyper et al.[32].

Recent papers of Vaes et al. [129] and Anthonis et al. [8] describe improvements to the sometimes time consuming TWR procedure to obtain accurate service load signals. Extending the off-line iterative feedforward procedure of TWR with a feedback controller reduces the number of iterations and improves the accuracy. This new approach was not yet available when the tests for this thesis were performed.

7.1.3 Reproduced signals

For the evaluation of the suspension three conditions are reproduced on the hydraulic shaker. The signals represent the in-situ acceleration measurements at the base of the cab suspension for the conditions IX, XIV and XVIII, respectively harvesting at $4km/h$, transport on an unpaved road at $11km/h$ and transport on a paved road at $28km/h$ of chapter 3. These three conditions give a good overall idea of the conditions the cab suspension is going to be exposed to during the work of the machine.

The L-shape measuring device containing the 6 accelerometers (see 3.4), used for the in-situ measurements at the base of the cab suspension, is placed here on the platform of the hydraulic shaker. The 6 accelerometers are connected to the response channels on the CADAX input/output box. The 6 signals for the hydraulic cylinders are connected to the output channels. The box is connected to the PC running the TWR software.

The target signals selected are all $81.92s$ long at a sample rate of $800Hz$. The high sample rate is necessary to overcome some numerical problems with the central programmable logic controllers. The identification of the test rig takes approximately 7 iterations, while the target

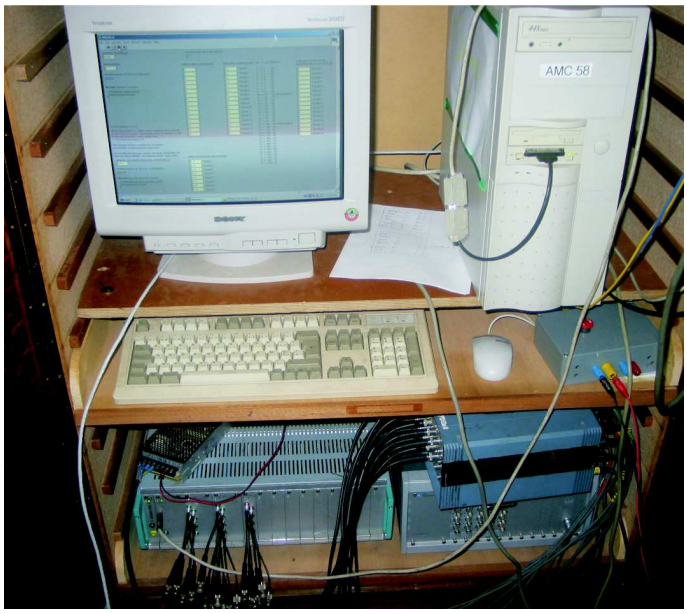

FIGURE 7.3: Personal computer with Time Waveform Replication software together with an ADwin-pro and a SCADASIII data acquisition and control system

simulation converges around 12 iterations.

The results for the signal recorded on an unpaved road are shown on figures 7.4 and 7.5. In the figures the following three lines are visible: the target signal, the reproduced signal with TWR and a third signal that shows an actual measurement when the created drive files are sent directly by a personal computer to the shaker, without interference of TWR. The comparison is done both in time and frequency domain. The figures show only the result for three accelerometers, representing the three translational DOFs, vertical, lateral and longitudinal. The other three accelerometers give similar results.

To quantify the preciseness of the reproduction, table 7.1 uses the error indicators of equations 7.3 and 7.4 to compare the signals.

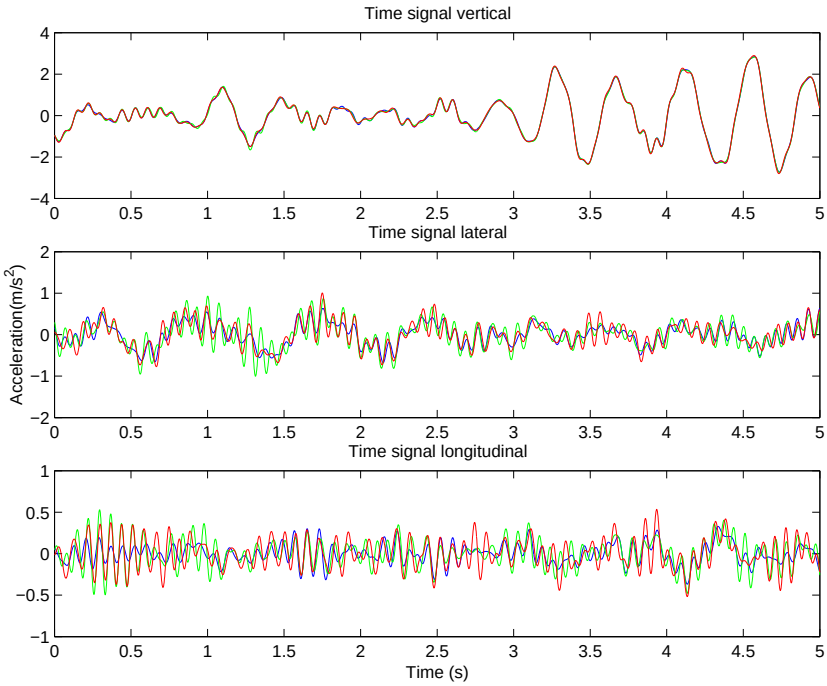

Figure 7.4: Comparison in the time domain between the targets (blue line), the created signals by TWR (red line) and actual measurements (green line) for the vertical, transversal and longitudinal translations

7.1.4 Discussion

Looking at figures 7.4 and 7.5 and table 7.1 it is clear that the performance of the system in vertical direction is quite satisfactory. Differences in the PSD of the target, the TWR produced signal and the measurement are minor and this results in a time signal that is almost spot on. The error indicators show that signal and target differ a few percents.

Looking at the PSD, the performance in the lateral and longitudinal direction also show relatively good results. Above $5Hz$ the differences between the target and the TWR produced signal become clear. This effect clearly appears in the time signals where oscillations at higher frequencies show up. This has its influence on the error indicators that give differences for the transport on the unpaved road of approximately

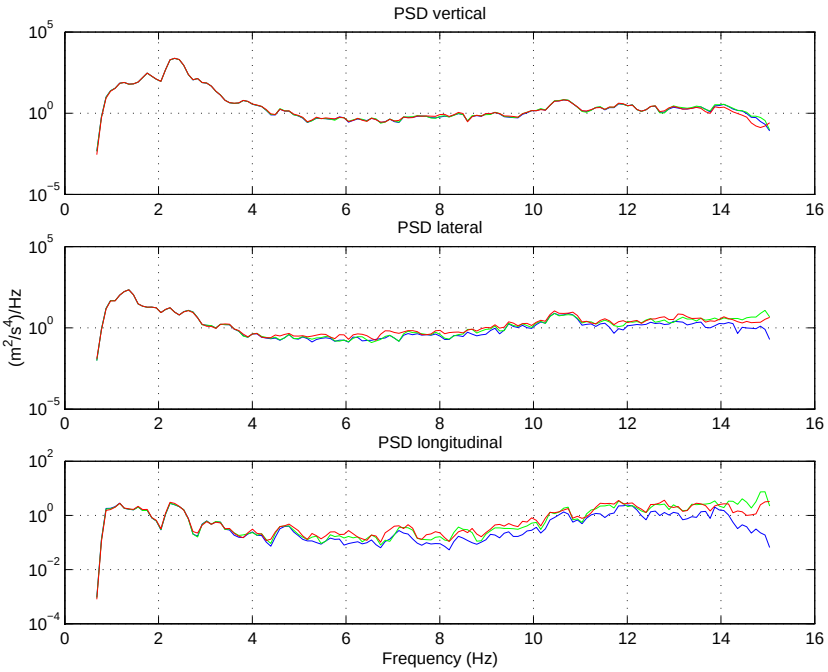

FIGURE 7.5: Comparison in the frequency domain between the targets (blue line), the created signals by TWR (red line) and actual measurements (green line) for the vertical, transversal and longitudinal translations

5% for the lateral movement and 30% for the longitudinal movement.

This phenomenon also shows up with the other two signals. The error indicators for the field signal are slightly worse than those of the unpaved road signal, but those for the paved road vibration sequence are not in proportion. The explanation for this can be found by combining two issues. First there is the difference in acceleration levels between the vertical and the other directions. When the vertical vibrations are of a higher magnitude than the lateral and longitudinal vibrations, then small errors in the vertical direction will result in errors that are relatively big in the other directions, making it difficult to get a good accuracy in those directions. This is especially the case for the reproduction of the paved road signal. Secondly there is a difference in available power in every direction due to the configuration

		$\frac{RMS_{error}}{RMS_{target}}$	$\frac{RMS_{signal}}{RMS_{target}}$
harvesting			
vertical	TWR	0.1630	1.0100
	measurement	0.2765	1.1135
lateral	TWR	0.5043	1.1033
	measurement	0.6731	1.1931
longitudinal	TWR	0.8642	1.3186
	measurement	0.9849	1.3954
transport unpaved road			
vertical	TWR	0.0242	1.0001
	measurement	0.0374	1.0054
lateral	TWR	0.3160	1.0424
	measurement	0.3704	1.0601
longitudinal	TWR	0.8246	1.3278
	measurement	0.9106	1.3478
transport paved road			
vertical	TWR	0.0672	1.0225
	measurement	0.2430	1.0722
lateral	TWR	1.7869	2.0135
	measurement	3.4173	3.6064
longitudinal	TWR	5.1728	5.2399
	measurement	6.1385	6.3476

Table 7.1: Calculated error indicators

of the hydraulic cylinders of the test rig (ratio: vertical=10, lateral =5, longitudinal=4). This can also affect the results shown in every direction.

Due to the numerical controllers of the shaker, differences occur between the reproduced signal with TWR (indicated in green in the figures) and the measured signals when the created drive files are send directly by a personal computer to the shaker (in blue in the figures). This again has the most influence on the vibration pattern with the greatest difference between the individual signals.

All in all it can be concluded that this shaker can produce relatively good signals when the ratio of the amplitude in the different directions is not too big. Accuracy problems in the controls make it otherwise too difficult to obtain satisfactory results in the directions with the lowest

amplitude.

7.2 Cab suspension evaluation

For the evaluation of the suspension, a prototype suspension system is built on the hydraulic shaker and put to the test. It consists of four suspension elements as discussed in chapter 4, positioned vertically at the same place as the rubbers of the conventional suspension used on a harvester.

To make sure the results of the prototype suspension are a prediction of results that would occur when implemented on a harvester, real conditions have to be reproduced as closely as possible. The reproduced signals using TWR, described in the previous section, provide the adequate excitation, but the prototype suspension has to be loaded with a mass and moments of inertia that resemble those of the cab of a harvester. The obvious way to do this is to use a real cab on top of the suspension system. This was not possible due to unavailable space and mounting tools. Therefore the setup shown in figure 7.6 was realized.

A cabin weighs $706kg$, driver included and has moments of inertia along the longitudinal, lateral and vertical axis of respectively $380kgm^2$, $305kgm^2$ and $350kgm^2$. These moments of inertia are given around the center of mass of the cabin situated $78cm$ above the cab floor and approximately in the middle of the square formed by the four suspension elements. All these specifications were met within a margin of 10% by arranging iron plates, weights and a pallox with sand bags in the appropriate way.

For the evaluation two L-shape measuring devices are used to record both the input acceleration to and the output accelerations from the suspension. Using these accelerations RMS and VDV values are calculated for all six degrees of freedom. To make the VDV values comparable with those of table 3.2, the values are adjusted to give the equivalent value for a five minutes drive, which was also the case in tables 3.3 and 5.2.

Comparing the input values of table 7.2 with those of table 3.2 shows the effectiveness of TWR in reproducing the in-situ signals. The simulated harvesting conditions are very representative for the real conditions. The translational degrees of freedom for both transport conditions are resembling the in-situ signals, but the rotational degrees of freedom show over-excitation. The reasons for that were discussed

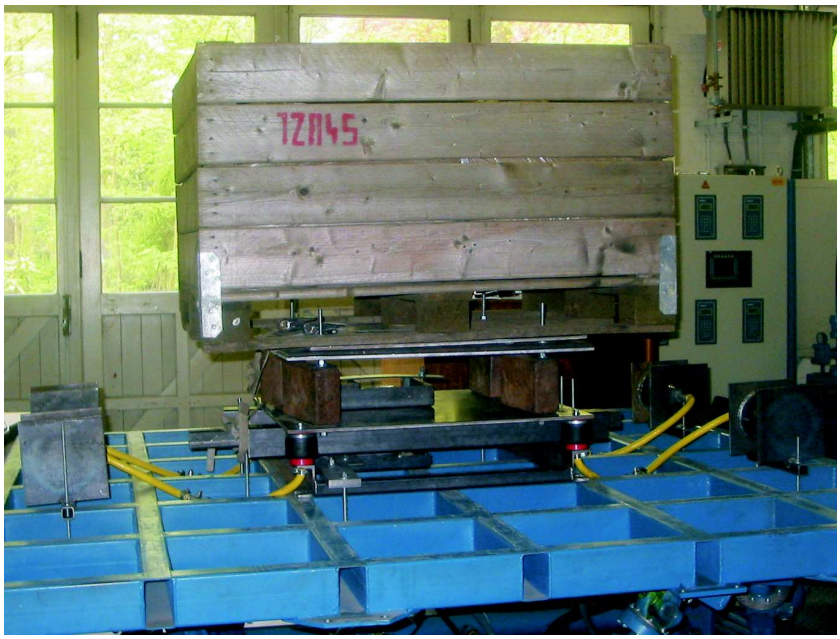

Figure 7.6: Evaluation setup containing suspension system loaded with a mass resembling a real cabin

earlier in this chapter.

The behavior of the suspension is very good in almost every case. Only for the driving and lateral direction during harvesting, the suspension system shows mediocre results. For all other degrees of freedom in all three conditions, the suspension shows high attenuation levels even above 50% in VDV.

A good performance in the vertical direction, and the roll and pitch, was to be expected due to the orientation of the suspension elements. Nevertheless the performances in X, Y and yaw are also satisfactory. Here the rubber of the air springs accounts for the attenuation of the vibrations.

Keeping the research objective in mind, limit values are avoided in all directions and for all conditions. During harvesting action values are not violated within 24 hours. Due to the over excitation of certain degrees of freedom during evaluation it is difficult to claim that the suspension will not violate the action values under transport conditions.

	RMS		VDV	
	in	out	in	out
harvesting				
X-axis	0.0869	0.1040	0.4228	0.4540
Y-axis	0.0930	0.0895	0.4490	0.4395
Z-axis	0.9106	0.2172	4.6173	1.0685
$\sum$	0.9279	0.2900	4.6175	1.0845
roll	0.5277	0.1818	2.6314	0.8880
pitch	0.2630	0.1674	1.3457	0.7911
yaw	0.2931	0.2073	1.4170	1.0089
transport unpaved road				
X-axis	0.3339	0.1939	1.6629	0.9816
Y-axis	0.4872	0.2786	2.4888	1.3968
Z-axis	0.9502	0.7647	4.7810	3.9029
$\sum$	1.2596	0.9003	4.8830	3.9227
roll	2.5269	1.4455	13.4873	7.5711
pitch	1.2244	1.0540	6.1086	5.2943
yaw	1.3330	0.7155	6.5541	3.9043
transport paved road				
X-axis	0.3467	0.1899	1.7203	0.9107
Y-axis	0.3819	0.1488	1.8740	0.7169
Z-axis	1.0781	0.8813	5.1445	3.5859
$\sum$	1.2956	0.9438	5.1828	3.5921
roll	2.5854	1.5342	12.3426	7.0928
pitch	1.4642	1.2063	6.8184	5.5655
yaw	1.2317	0.6273	6.0794	3.0504

TABLE 7.2: Final evaluation results of cabin with new suspension system

If assumed that similar attenuation levels will be obtained under real conditions, only the vertical degree of freedom during transport on the

road at high speed will result in a comfort value above the action value. Due to the limited travel of the cab suspension it is questionable if this suspension is able to deal with these vibrations.

Comparing the results obtained here with the predicted results of the multi dimensional linear model given in table 5.2, it is clear that the model predicts more favorable results. The main reason for this is that the air springs have a rather small operating region of $40mm$. The real conditions the suspension is exposed to during the evaluation makes that the end zones of the operating region are frequently used. Apparently the behavior of the air springs there can not be covered by the linear model used, resulting in erroneous results. This explains also the fact that the model is good at predicting the natural frequencies of the rigid body modes of the cab. Those frequencies were measured using excitation signal with rather low amplitudes.

7.3 Conclusion

The final evaluation of the suspension system was not performed on the combine harvester but instead on an electro-hydraulic shaker. The shaker, that had the ability to reproduce vibrations in six degree of freedom up to 20 Hz, was equipped with Time Waveform Replication Monitor to perform service load simulations. In-situ measured acceleration levels at the base of the cabin suspension could be reproduced relatively good when the ratio of the amplitude in the different directions was not to large. The signals recorded during transport on the road was difficult to reproduce and showed over-excitation at high frequencies.

For the final evaluation no real cabin was used but the suspension was loaded with the mass and the moments of inertia resembling those of the real cabin closely. The behavior of the suspension is very good in almost every case with high attenuation levels up to 50 % and higher in vibration dose value. High performance in vertical direction and in roll and pitch was expected, due to the orientation of the pneumatic cab mounts, but also the lateral and drive direction and yaw show satisfactory results.

With respect to the research objective, avoiding limit values in all directions and for all signals was observed. The action value was only violated at high speeds but this was caused by the limited travel of the air springs. The linear six degree of freedom model predicted more

favorable results. This difference could be linked to the frequent use of the end zones of the springs.

Chapter 8

Conclusions and Future Perspectives

8.1 General conclusions

This thesis has developed a commercially viable cab suspension system to improve the low frequency vibrational comfort of the operators on mobile agricultural machines. A combine harvester was used as a case study and since this machine can be considered to be a mobile agricultural machine of average size, most of the conclusions found here are transferable to other mobile agricultural machines.

Low back pain is common among operators of agricultural machines. The mechanism that lies at the origin of this problem is not clear yet but it is generally accepted that reduction of whole body vibrations could definitely improve the situation. The European legislation on the matter makes that manufacturers of agricultural machinery have to look at introducing and fine tuning existing suspension systems. Chapter 2 has shown that agricultural machines, with exception of tractors, do not use primary suspension systems. Vibration attenuation has to come from seat and cab suspension systems. Good seat suspensions are already available but this is not the case for low frequency cab suspensions, hence some work needs to be done.

The combine harvester used in this research has been investigated more closely in chapter 3. Vibration measurements were performed underneath the cabin for stationary, harvesting and transport conditions. Many peaks in the power spectra of the accelerations measured dur-

ing stationary and harvesting conditions originate from rotating and translating elements in the machine. Higher driving speed resulted in a severe increase of the vibrations around 0.5 to $2.5Hz$ and gave rise to speed dependent excitations due to the lugs of the tires hitting the road.

The vibrations measurements showed also that the vibration dose value and effective root mean square of the accelerations exceed for several conditions the action and even the limit values of the European legislation. Measurements inside the cabin show that the rubber mounts deteriorate in most cases the vibrational conditions for the operator and that better cab suspension elements have to be developed. To make such elements commercially viable, the elements should be relatively cheap and it would be favorable if they would fit in the same space that is provided for the rubber mounts. In that way the changes to the cabin and the supporting structure are minor which makes a new suspension interchangeable with the current one.

Chapter 4 developed a pneumatic and a hydro-pneumatic alternative for the rubber cab mounts. White box models based on physical principals were derived successfully. Both elements have the ability to create systems with low natural frequencies and reasonably low amplification. The hydro-pneumatic element is however more expensive and needs more changes to cab and supporting structure to implement. The pneumatic element on the other hand can simply be fitted in the space of the rubber mounts without changing too much to the connections points with the cab and the supporting structure. A negative feature of the pneumatic element is its limited travel space of $40mm$ but on the other hand it is a cheaper system and therefore the preferred choice.

To be able to predict the behavior of the new cab suspension system using the pneumatic elements, chapter 5 developed a three dimensional model. Linear model techniques are used and a validation of the model shows that it is good at predicting the natural frequencies of the rigid body modes of the suspension. The model is used to predict the comfort values for the pneumatic cab suspension system and shows that the chosen pneumatic cab suspension has the ability to improve the comfort values drastically. With exception of the rolling behavior of the cabin action values are not violated.

Once models, linear and nonlinear, are developed chapter 6 showed how vibration measurements collected during field tests could be used in the optimization of the suspension systems. The procedure proposed

made it possible to optimize a suspension system and predict the effect it would have on the vibrations at the base of the cabin, without having to build an actual prototype. The procedure could be seen as a design approach incorporating a feasibility assessment.

The final evaluation of the pneumatic suspension was performed on an elector-hydraulic shaker. In-situ measured vibrations were successfully reproduced on the shaker by means of time waveform replication monitor. The evaluation of the cab suspension showed improvements in vibration dose value and effective root mean square of 50 % and above. The research objective, not violating limit values and avoiding action values, is met for every direction with exception of the vertical degree of freedom during high speed road transport. Due to the limited travel of the cab suspension it is questionable if this suspension is able to deal with these vibrations.

8.2 Perspectives and future work

This thesis developed a new cab suspension and evaluated it under simulated real conditions. The final step in its development is to introduce this suspension on a combine harvester and evaluate the system under different conditions. Minor changes to the comfort values found in this thesis are expected because the evaluation platform, the hydraulic shaker, had a margin of error when reproducing the measured in-situ vibrations. Also the effect of not being able to evaluate the suspension by using a real cabin, will come into play.

With increasing working speeds increasingly higher vibration levels are observed. The secondary seat and cab suspension systems with their limited travel space are not able to deal with those and in future the use of primary suspension systems will become inevitable. Also tuning cabin, seat and primary suspension to each other will become more and more important to deal with the high levels of vibrations.

In appendix B the use of semi-active control laws in the design of a cab suspension was discussed. On a model of a hydro-pneumatic suspension, reduction of vibration dose value up to 90% was observed. This substantial reduction shows that a semi-active cab suspension could improve the vibrational comfort conditions of the operator of this and other agricultural machines. A real proof that these concepts work can only be found when implementing the concepts on a real setup.

Further investigation can also be performed in the optimization of the semi-active control law parameters. The technique proposed in chapter 6 could be used for that.

Bibliography

[1] *ISO 2631, Guide for the evaluation of human exposure to whole-body vibration.* International Organization for Standardization, Geneva, 1974.

[2] *BS 6841, Measurement and evaluation of human exposure to whole-body mechanical vibration and repeated shock.* British Standards Institution, London, 1987.

[3] *ISO 2631-1, Mechanical vibration and shock - evaluation of human exposure to whole-body vibration - part 1: general requirements.* International Organization for Standardization, Geneva, 1997.

[4] Vibro-aucoustic study on a protoype, phase 1. Technical report, LMS Engineering Services, 1998.

[5] Council of the european communties, directive 2002/44/ec, on the minimum healt and safety requirements regarding the exposure of workers to the risks arising from physical agents (vibration) (sixteenth individual directive within the meaning of article 16(1) of directive 98/391/eec). *Official Journal of the EUropean Communities*, pages L 177/13–19, 6 July 2002.

[6] *ISO 5008, Agricultural wheeled tractors and field machinery - Measurement of whole-body vibration of the operator.* International Organization for Standardization, Geneva, 2002.

[7] J. Anthonis, K. Deprez, and H. Ramon. Design and evaluation of a low power portable test rig for vibration tests an mobile agricultural machinery. *Transactions of the ASAE*, 45(1):5–12, 2002.

[8] J. Anthonis, D. Vaes, K. Engelen, H. Ramon, and J. Swevers. Reedback approach for reproduction of field maesurements on a hydraulic four poster. *Biosystems Engineering*, 96(4):435–445, 2007.

[9] B. Armstrong-Hélouvry, P. Dupont, and C. Cadunas de Wit. A survey of models, analysis tools and compensation methods for the control of machines with friction. *Automatica*, 30(7):1083–1138, 1994.

[10] J. Bendat and A. Piersol. *Engineering applications of correlation and spectral analysis*. Wiley, New York, USA, 1980.

[11] R. B. Bird, W. E. Stewart, and E. N. Lightfoot. *Transport Phenomena*. John Wiley & Sons Inc., New York, 1960.

[12] M. Bjőrkman and K. Holmstrőm. Global optimization with the direct algorithm in matlab. *Journal of Advanced Modeling and Optimization*, 1(2):17–27, 1999.

[13] H. C. Boshuizen, P. M. Bongers, and C. T. J. Hulshof. Self-reported back pain in tractor drivers exposed to whole-body vibration. *International Archives of Occupational and Environmental Health*, 62(2):109–115, 1990.

[14] P. Boulanger, G. Lovat, and P. Donati. Development of a low frequency suspension cab for fork lift truck. In *Proceedings of United Kingdom Group Meeting on Human Response to Vibration, MIRA, UK*, 18-20 September 1996.

[15] M. Bovenzi and C. T. J. Hulshof. An updated review of epidemiologic studies on the relationship between exposure to whole-body vibration and low back pain (1986-1997). *International Archives of Occupational and Environmental Health*, 72:351–365, 1999.

[16] M. Bovenzi and A. Zadini. Self-reported low back symptoms in urban bus drivers exposed to whole-body vibration. *Spine*, 17(9):1048–1059, 1992.

[17] D. A. Bowman and T. Woods. John deere quad wheel suspension ^{TM}. In *Proceedings of AgEng2002, Budapest, Hungary*, 30 June - 5 July 2002.

[18] Y. A. Çengel and M. A. Boles. *Thermodynamics: an engineering approach*. Mc Graw Hill, New York, 4th edition, 2002.

[19] J. S. Cho, K. U. Kim, and H. J. Park. Determination of dynamic parameters of agricultrual tractor cab mount system by a modified dsim. *Transactions of the ASAE*, 43(6):1365–1369, 2000.

[20] S. B. Choi and Y. M. Han. Vibration control of electrorheological seat suspension with human-body model using slinding mode control. *Journal of Sound and Vibration*, 303:391–404, 2007.

[21] S. B. Choi, H. K. Lee, and E. G. Chang. Field test results of a semi-active er suspension system associated with skyhook controller. *Mechatronics*, 11:345–353, 2001.

[22] S. B. Choi, M. S. Suh, D. W. Park, and M. J. Shin. Neuro-fuzzy control of a tracked vehicle featuring semi-active electro-rheological suspension units. *Vehicle System Dynamics*, 35(3):141–162, 2001.

[23] L. Clijmans. *A model-based approach to assess sprayer's quality*. Dissertation, Katholieke Universiteit Leuven, Departement of Agro-Machinery and -Economics, Kasteelpark Arenberg 30, B-3001 Leuven, Belgium, 1999.

[24] L. Clijmans, H. Ramon, and J. De Baerdemaeker. Structural modification effects on the dynamic behavior of an agricultural tractor. *Transactions of the ASAE*, 41(1):5–10, 1998.

[25] L. Clijmans, H. Ramon, J. Langenakens, and J. De Baerdemaeker. The influence of tyres on the dynamic behaviour of a lawn mower. *Journal of Terramechanics*, 33(4):195–208, 1997.

[26] D. J. Cole. Fundamental issues in suspension design for heavy road vehicles. *Vehicle System Dynamics*, 35(4-5):319–360, 2001.

[27] R. Deng, P. Davies, and A. K. Bajaj. Flexible polyurethane foam modelling and identification of viscoelastic parameters for automotive seating applications. *Journal of Sound and Vibration*, 262:391–417, 2003.

[28] K. Deprez, K. Maertens, and H. Ramon. Comfort improvement by passive and semi-active hydropneumatic suspension using global optimization technique. In *American Control Conference, Anchorage, United States*, 8-10 May 2002.

[29] K. Deprez, D. Moshou, and H. Ramon. Comfort improvement of nonlinear suspension using global optimization and in-situ measurements. *Journal of Sound and Vibration*, 284(3-5):1003–1014, 2005.

[30] K. Deprez, D. Moshou, H. Ramon, and J. De Baerdemaeker. Comfort improvement of agricultural vehicles by passive and semi-active suspensions. In *Proc. of 15th IFAC World Congress, Barcelona, Spain*, 21-26 July 2002.

[31] W. De Craecker, H. Druyts, I. Hostens, and H. Ramon. Whole-body vibration comfort analysis bases upon spine modelling. In *AGENG 2004, Leuven, Belgium*, 12-16 September 2004.

[32] J. De Cuyper, D. Coppens, C. Liefooghe, and J. Debille. Advanced system identification methods for improved service load simulation on multi axial test rigs. *European Journal of Mechanical and Environmental Engineers*, 44(1):27–39, 1999.

[33] J. De Temmerman, K. Deprez, J. Anthonis, and H. Ramon. Conceptual cab suspension system for a self-propelled agricultural machine, part 1: Development of a linear mathematical model. *Biosystems Engineering*, 89(4):409–416, 2004.

[34] P. Donati. Survey of technical preventative measures to reduce whole-body vibration effects when designing mobile machinery. *Journal of Sound and Vibration*, 253(1):169–183, 2002.

[35] H. Druyts, W. De Craecker, I. Hostens, B. Haex, R. Van Audekercke, P. Coorevits, G. Vanderstraeten, and H. Ramon. Measurement and analysis of whole-body vibration comfort parameters for advanced human modelling. In *AGENG2004, Leuven, Belgium*, 12-16 September 2004.

[36] D. L. Dufner and T. E. Schick. John deere active seat ^{TM}: A new level of seat performance. In *Proceedings of AgEng2002, Budapest, Hungary*, 30 June - 5 July 2002.

[37] M. Duke and G. Goss. Investigation of tractor driver seat performance with non-linear stiffness and on-off damper. *Biosystems Engineering*, 96(4):477–486, 2007.

[38] S. Duym. Simulation tools, modelling and identification, for an automotive shock absorber in the context of vehicle dynamics. *Vehicle System Dynamics*, 33:261–285, 2000.

[39] S. Duym and K. Reybrouck. Physical characterization of nonlinear shock absorber dynamics. *European Journal of Mechanical Engineering*, 43(4):181–188, 1998.

[40] G. A. B. Edwards. Innovation in the farm tractor world - 1970-2010 who leads? who follows? In *Proceeding of the 2002 ASAE Annual International Meeting, Chicago, Illinois, USA*, 28-31 July 2002.

[41] E. M. ElBeheiry and D. C. Karnopp. Optimal control of vehicle random vibration with constrained suspension deflection. *Journal of Sound and Vibration*, 189(5):547–564, 1996.

[42] M. M. ElMadany and A. El-Tamimi. On a subclass of nonlinear passive and semi-active damping for vibration isolation. *Computers & Structures*, 36(5):921–931, 1990.

[43] P. S. Els and T. J. Holman. Semi-active rotary damper for a heavy off-road wheeled vehicle. *Journal of Terramechanics*, 36:51–60, 1999.

[44] P. S. Els, N. J. Theron, P. E. Uys, and M. J. Thoresson. The ride comfort vs. handling compromise for off-road vehicles. *Journal of Terramechanics*, 44:303–317, 2007.

[45] L. F. P. Etman, R. C. N. Vermeulen, J. G. A. M. Heck, A. J. G. Schoofs, and D. H. V. Campen. Design of a stroke dependent damper for the front axle suspension of a truck using multibody systems dynamics and numerical optimization. *Vehicle System Dynamics*, 38(2):85–101, 2002.

[46] T. E. Fairley. Predicting the discomfort caused by tractor vibration. *Ergonomics*, 38(10):2091–2106, 1995.

[47] T. E. Fairley and M. J. Griffin. The apparent mass of the seated human body: vertical vibration. *Journal of Biomechanics*, 22(2):81–94, 1989.

[48] C. Ferraresi, G. Quaglia, and M. Sorli. Force control laws for semi-active vehicular suspensions. *European journal of mechanical engineering*, 42(3):145–151, 1997.

[49] J. B. Ferris. Factors affecting perceptions of ride quality in automobiles. In *ASME International Congress and Exposition, Nashville, United States*. ASME, ASME, New York, 7-11 November 1999.

[50] Firestone Industrial Products, Inc., Middlesex, England. *Airstroke Actuators Airmount Isolators: Engineering Manual & Design Guide*, metric edition edition, 1997.

[51] D. Fischer and R. Isermann. Mechatronic semi-active and active vehicle suspensions. *Control Engineering Practice*, 12:1353–1367, 2004.

[52] G. F. Franklin, J. D. Powell, and A. Emami-Naeini. *Feedback control of dynamic systems*. Addison-Wesley Publishing Company, New York, 3th edition, 1994.

[53] C. L. Giliomee and P. S. Els. Semi-active hydropneumatic spring and damper system. *Journal of Terramechanics*, 35:109–117, 1998.

[54] T. A. Gillespie. *Fundamentals of Vehicle Dynamics*. Society of Automotive Engineers, Inc. Warrendale (PA), 1992.

[55] D. E. Goldberg. *Genetic Algorithms in Search, Optimization & Machine Learning*. Addison-Wesley, Reading, 1989.

[56] M. J. Griffin. *Handbook of Human Vibrations*. Academic Press, Harcourt Brace & Company, Publishers, London, 1990.

[57] M. J. Griffin. A comparison of standardized methods for predicting the hazards of whole-body vibration and repeated shocks. *Journal of sound and vibration*, 215(4):883–914, 1998.

[58] P. Guillaume, R. Pintelon, and J. Schoukens. Nonparametric frequency response function estimators based on nonlinear averaging techniques. *IEEE Transactions on Instrumentation and Measurement*, 41(6):739–746, 1992.

[59] T. Gunston. An investigation of suspension seat damping using a theoretical model. In *Proceedings of United Kingdom Group Meeting on Human Response to Vibration, Southampton, UK*, 13-15 September 2000.

[60] B. B. Hall and J. S. Tang. Analysis of active and semi-active vehicle suspension fitted with a pneumatic self-energizing levelling device. *Proceedings of the I MECH E Part D Journal of Automobile Engineering*, 204:161–171, 1990.

[61] P. Hansson. *Modelling and Optimization of Passive adn Adptively controlled Active Cab Suspensions on Terrain Vehicles especially Agricultural Tractors.* Dissertation, Swedish University of Agricultrual Sciences, Department of Agricultural Engineering, Swedish University of Agricultural Sciences, P.O. Box 7033, S-750 07 Uppsala, Sweden, 1993.

[62] P. A. Hansson. Optimization of agricultural tractor cab suspension using the evolution method. *Computers and Electronics in Agriculture*, 12:34–49, 1995.

[63] P. A. Hansson. Gain scheduling based controller for active cab suspension on agricultural tractors. In *Proceedings of ISHS Acta Horticulturae 406: II IFAC/ISHS Workshop :Mathematical & Control Applications in Agriculture & Horticulture*, volume 406 of *ISHS Acta Horticulturae*, pages 249–256, 1996.

[64] C. M. Harris. *Shock an Vibration Handbook.* McGraw-Hill Book Company, 3 edition, 1961.

[65] I. Hostens. *Analysis of seating during low frequency vibration exposure.* Dissertation, Katholieke Universiteit Leuven, Departement of Agro-Machinery and -Economics, Kasteelpark Arenberg 30, B-3001 Leuven, Belgium, 2004.

[66] I. Hostens, J. Anthonis, P. Kennes, and H. Ramon. Six-degree-of-freedom test rig design for simulation of mobile agricultural

machinery vibrations. *Journal of Agricultural Engeneering Research*, 77(2):155–169, 2000.

[67] I. Hostens, J. Anthonis, P. Kennes, and H. Ramon. New design for a 6dof vibration simulator with improved reliability and performance. *Journal of Mechanical Systems and Signal Processing*, 19(1):105–122, 2005.

[68] I. Hostens, K. Deprez, and H. Ramon. An improved design of air suspension for seats of mobile agricultural machines. *Journal of Sound and Vibration*, 276:141–156, 2004.

[69] I. Hostens and H. Ramon. Descriptive analysis of agricultural machinery cabin vibrations and their effect on the human body. *Journal of Sound and Vibration*, 266(3):453–464, 2003.

[70] C. R. Houck, J. A. Joines, and M. G. Kay. A genetic algorithm for function optimization: a matlab implementation. *NCSU-IE Technical Report 95-09, North Carolina State University*, 1995.

[71] D. Hrovat, D. L. Margolis, and M. Hubbard. An approach toward the optimal semi-active suspension. *Journal of Dynamic Systems, Measurement, and Control, Transactions of the ASME*, 110:288–296, 1988.

[72] C. T. J. Hulshof, G. van der Laan, I. T. J. Braam, and J. H. A. M. Verbeek. The fate of mrs robinson: Criteria for recognition of whole-body vibration injury as an accupational disease. *Journal of Sound and Vibration*, 253(1):185–194, 2002.

[73] W. Huyer and A. Neumaier. Global optimization by multilevel coordinate search. *Journal of Global Optimization*, 14:331–355, 1999.

[74] V. B. Issurin, D. G. Liebermann, and G. Tenenbaum. Effect of vibratory stimulation training on maximal force and flexibility. *Journal of Sports Sciences*, 12:561–566, 1994.

[75] H. M. Jacklin. Human reactions to vibration. *SAE Transactions*, 39(4):401–407, 1936.

[76] H. K. Jang and M. J. Griffin. Effect of phase, frequency, magnitude and posture on discomfort associated with differential vertical vibration at the seat and feet. *Journal of sound and vibration*, 229(2):273–286, 2000.

[77] J. R. Jang, C. Sun, and E. Mizutani. *Neuro-Fuzzy and Soft Computing*. Prentice Hall, 1997.

[78] D. R. Jones, C. D. Perttunen, and B. E. Stuckman. Lipschitzian optimization without the lipschitz constant. *Journal of Optimization Theory and Applications*, 79(1):157–181, 1993.

[79] D. Karnopp. Design principles for vibration control systems using semi-active dampers. *Journal of Dynamic Systems, Measurement, and Control, Transactions of the ASME*, 112:448–455, 1990.

[80] D. Karnopp, M. J. Crosby, and R. A. Harwood. Vibration control using semi-active force generators. *Journal of Engineering for Industrie, Transactions of the ASME*, 96(2):619–626, 1974.

[81] T. Keller and J. Arvidsson. Technical solutions to reduce the risk of subsoil compaction: effects of dual wheels, tandem wheels and tyre inflation pressure on tress propagation in soil. *Soil & Tillage Research*, 79:191—205, 2004.

[82] S. K. Kim, S. W. White, A. K. Bajaj, and P. Davies. Simplified models of the vibration of mannequins in car seats. *Journal of Sound and Vibration*, 264:49–90, 2003.

[83] S. Kitazaki and M. J. Griffin. Resonance behavour of the seated human body and effects of posture. *Journal of Biomechanics*, 31(2):143–149, 1998.

[84] A. Kumar, P. Mahajan, D. Mohan, and M. Varghese. Tractor vibration severity and driver health: a study from rural india. *Journal of Agricultural Engineering Research*, 80(4):313–328, 2001.

[85] P. Lemerle, P. Boulanger, and R. Poirot. A simplified method to design suspended cabs for counterbalace trucks. *Journal of Sound and Vibration*, 253(1):283–293, 2002.

[86] J. Lines, M. Stiles, and R. Whyte. Whole body vibration during tractor driving. *Journal of Low Frequency Noise and Vibration*, 14:87–95, 1995.

[87] L. Ljung. On the estimation of transfer functions. In *Proceedings of 7th IFAC Symposium on System Identification adn Parameter Estimation, York, United Kingdom*, volume 2, pages 1653–1657, 1985.

[88] LMS International. *CADA-X Time Waveform Replication, User Manual*, revision 3.5.c edition.

[89] K. Maertens. *Data-driven techniques for the on-the-go evaluation of separation processes in combine harvesters*. Dissertation, Katholieke Universiteit Leuven, Departement of Agro-Machinery and -Economics, Kasteelpark Arenberg 30, B-3001 Leuven, Belgium, 2004.

[90] D. L. Margolis, J. L. Tylee, and D. Hrovat. Heave mode dynamics of a tracked air cushion vehicle with semiactive airbag secondary suspension. *Journal of Dynamic Systems, Measurement, and Control, Transactions of the ASME*, 97(4):399–407, 1975.

[91] A. Marsili, L. Ragni, G. Santoro, P. Servadio, and G. Vassalini. Innovative systems to reduce vibrations on garicultural tractors: comparative analysis of acceleration transmitted through the driving seat. *Biosystems Engineering*, 81(1):35–47, 2002.

[92] MATLAB. *The Language of Technical Computing*. Copyright © by The MathWorks Inc., Version 6.1, 2001.

[93] D. McCloy and H. R. Martin. *Control of Fluid Power: Analysis and Design*. John Wiley & Sons Inc., New York, 2nd edition, 1980.

[94] S. J. McManus, K. A. St. Clair, P. E. Boileau, J. Boutin, and S. Rakheja. Evaluation of vibration and shock attenuation performance of a suspension seat with a semi-active magnetorheological fluid damper. *Journal of Sound and Vibration*, 253(1):313–327, 2002.

[95] T. A. G. McMullan, C. W. Plackett, R. O. Peachey, and V. Nguyen. The behaviour of tractor drive tyres at low inflation pressures when reacting high side forces. *Journal of Agricultural Engineering Research*, 39(3):221–229, 1988.

[96] N. Nawayseh and M. J. Griffin. Non-linear dual-axis biodynmic response to vertical whole-body vibration. *Journal of Sound and Vibration*, 268(3):503–523, 2002.

[97] N. Nawayseh and M. J. Griffin. Tri-axial forces at the seat and backrest during whole-body vertical vibration. *Journal of Sound and Vibration*, 277(1-2):309–326, 2004.

[98] J. Nocedal and S. J. Wright. *Numerical Optimization*. Springer Series in Operations Research and Financial Engineering. Springer, New York, 2nd edition, 1999.

[99] G. S. Paddan and M. J. Griffin. The transmission of translational seat vibration to the head - i. vertical seat vibration. *Journal of Biomechanics*, 21(3):191–197, 1988.

[100] G. S. Paddan and M. J. Griffin. The transmission of translational seat vibration to the head - ii. horizontal seat vibration. *Journal of Biomechanics*, 21(3):199–206, 1988.

[101] G. S. Paddan and M. J. Griffin. Effect of seating on exposures to whole-body vibration in vehicles. *Journal of Sound and Vibration*, 253(1):215–241, 2002.

[102] K. T. Palmer, M. J. Griffin, H. Bendall, B. Pannett, and D. Coggon. Prevalence and pattern of occupational exposure to whole body vibration in great britain: findings from a national survey. *Occupational and Environmental Medicine*, 57:229–236, 2000.

[103] N. G. Pantelelis and A. E. Kanarachos. A simple and effective active seat suspension for agricultural vehicles. In *Proceedings of IFAC Control Applications and Ergonomics in Agriculture, Athens, Greece*, 15-17 June 1998.

[104] J. Périsse and L. Jézéquel. An original feedback control with a reversible electromechnical actuator used as an active isolation system for a seat suspension. part i: Theoretical study. *Vehicle System Dynamics*, 34:305–331, 2000.

[105] J. Périsse and L. Jézéquel. An original feedback control with a reversible electromechnical actuator used as an active isolation system for a seat suspension. part ii: Experimental study. *Vehicle System Dynamics*, 34:381–399, 2000.

[106] R. Pintelon and J. Schoukens. *System identification: A frequency domain approach*. IEEE Press, New York, NY, 2001.

[107] J. D. Pinter. *Global Optimization in Action*. Kluwer Academic Publishers, Dordrecht, 1996.

[108] M. H. Pope and T. H. Hansson. Vibration of the spine and low back pain. *Clinical Orthopaedics and Related Research*, 279:49–59, 1992.

[109] M. H. Pope, M. Magnusson, and D. G. Wilder. Low back pain and whole body vibration. *Clinical orthopaedics and related research*, 354:241–248, 1998.

[110] Y. Qiu and M. J. Griffin. Transmission of fore-aft vibration to a car seat using field tests and laboratory simulation. *Journal of Sound and Vibration*, 264:135–155, 2003.

[111] G. Quaglia and M. Sorli. Air suspension dimensionless analysis and design procedure. *Vehicle System Dynamics*, 35(6):443–475, 2001.

[112] S. Rakheja, Z. Q. Wang, and P.-E. Boileau. Ride performance analysis of a torsio-elastic linkage suspension for log skidders. In *Proceedings of United Kingdom Group Meeting on Human Response to Vibration, MIRA, UK*, 18-20 September 1996.

[113] R. Salomon. Evolutionary algorithms and gradient search: similarities and differences. *IEEE Transactions on evolutionary computation*, 2(2):45–55, 1998.

[114] D. Sammier, O. Sername, and L. Dugard. Skyhook and H∞ control of semi-active suspensions: Some practical aspects. *Vehicle System Dynamics*, 39(4):279–308, 2003.

[115] A. J. Scarlett, J. S. Price, D. A. Semple, and R. M. Stayner. *Whole-body vibration on agricultural vehicles: evaluation of emission and estimated exposure levels*. Health & Safety Executive, Sudbury, Suffolk, 2005.

[116] A. J. Scarlett, J. S. Price, and R. M. Stayner. *Whole-body vibration: Initial evaluation of emissions originating from modern agricultural tractors.* Health & Safety Executive, Sudbury, Suffolk, 2002.

[117] A. J. Scarlett, J. S. Price, and R. M. Stayner. Whole-body vibration: Evaluation of emission and exposure levels arising from agricultural tractors. *Journal of Terramechanics*, 44:65–73, 2007.

[118] J. Schoukens, P. Guillaume, and R. Pintelon. *Design of broadband excitation signals*, pages 126–159. Englewood Cliffs, NJ: Prentice-Hall, 1993.

[119] J. Schrottmaier and M. Nadlinger. Investigation and optimisation of the vibration characteristics of tractors with front-axle suspension and cab suspension. In *In Proceedings of 58th VDI-MEG-Tagung Landtechnik, Műnster, Germany*, 10-11 October 2000.

[120] H. Seidel, U. Schuster, G. Menzel, N. N. Kurerov, J. Richter, E. J. Schajpak, R. Blűthner, A. Meister, and P. Ullsperger. Changes in auditory evoked brain potentials during ultra-low frequency whole-body vibration of man or of his visual surround. *European Journal of Applied Physiology*, 61:356–361, 1990.

[121] SIMULINK. *Toolbox for Matlab.* Copyright © by The MathWorks Inc., Version 4.1, 2001.

[122] C. C. Smith, D. Y. McGehee, and A. J. Healey. The prediction of passenger riding comfort from acceleration data. *Transactions of the ASME*, 100:34–41, 1978.

[123] D. A. Stewart. A platform with six degrees of freedom. *Proc. of inst. Mech. Eng.*, 180(1):371–386, 1965.

[124] J. Swevers. *Identification of mechatronic systems, Lecture notes.* Division of Production Engineering, Machine Design an Automation, K.U.Leuven, Belgium, 1996.

[125] J. Swevers, C. Lauwerys, B. Vandersmissen, M. Maes, K. Reybrouck, and P. Sas. A model-free control structure for the on-line tuning of the semi-active suspension of a passenger car. *Mechanical Systems and Signal Processing*, 21:1422–1436, 2007.

[126] A. G. Thompson and B. R. Davis. Technical note: Force control in electrohydraulic active suspensions revisited. *Vehicle System Dynamics*, 35(3):217–222, 2001.

[127] W. T. Thomson. *Theory of vibration with applications*. Stanley Thornes (Publishers) Ltd, Cheltenham, 4th edition, 1998.

[128] P. E. Uys, P. S. Els, and M. Thoresson. Suspension settings for optimal ride comfort of off-road vehicles travelling on roads with different roughness and speeds. *Journal of Terramechnics*, 44:163–175, 2007.

[129] D. Vaes, K. Engelen, J. Anthonis, J. Swevers, and P. Sas. Multivariable feedback desing to improve tracking performance on tractor vibration test rig. *Mechanical Systems and Signal Processing*, 21:1051–1075, 2007.

[130] M. Valášek, W. Kortűm, Z. Šika, L. Magdolen, and O. Vaculín. Development of semi-active road-friendly truck suspensions. *Control Engineering Practice*, 6:735–744, 1998.

[131] W. Vermote. *Sound and mechanical vibrations (in Dutch)*. Katholieke Industriele Hogeschool West-Vlaanderen, Oostende, 1994.

[132] T. Van der Waeteren. *Mechnical vibrations (in Dutch)*. Katholieke Universiteit Leuven, 1969.

[133] VTT. *VTT Symposium 209: Modelling and simulation of multitechnological machine systems*, chapter Simulation based design of mobile machine vibraton control and active cabin suspension prototype, pages 121–138. VTT, Espoo, Finland, 2001.

[134] D. G. Wilder, M. H. Pope, and M. Magnusson. Mechanical stress reduction during seated jolt/vibration exposure. *Seminars in Perinatology*, 20(1):54–60, 1996.

[135] J. D. Wu and R. J. Chen. Application of an active controller for reducing small-amplitude vertical vibration in a vehicle seat. *Journal of Sound and Vibration*, 274:939–951, 2004.

[136] X. Wu and M. J. Griffin. The influence of end-stop buffer characteristics on the severity of suspension seat end-stop impacts. *Journal of Sound and Vibration*, 215(4):989–996, 1998.

[137] C. Yue, T. Butsuen, and J. K. Hedrick. Alternative control laws for automotive active suspensions. *Transactions of the ASME*, 111:286–291, 1989.

[138] ZF Sachs AG, Ernst-Sachs-Straße 62, 97424 Schweinfurt. *Suspension Technology for Commercial Vehicles*, 2002.

Appendix A

Global Optimization

This appendix gives a general description of the methods available for global search. Afterwards it explains more thoroughly the DIRECT method used in chapter 6.

A.1 Introduction

During the optimization of parameters in the model of the passive suspension systems, optimization techniques had to be used that could optimize the several parameters bound by simple limits. The functions that had to be minimized were based on either the objective comfort values effRMS and VDV or the FRF of the system. In several cases this cost function resembled figure 6.2, where the large amount of local minima makes searching the space for the absolute minimum difficult. Standard derivative based optimization techniques are prone to getting stuck in those local minima [98].

One way of solving such 'noisy' functions, would be varying each parameter in its range and computing the function value in a large amount of points, after which a filtering technique can denoise the function. In most cases the time for solving a function over the total domain takes too much time and the denoised function still has multiple minima. In this case the use of global optimization techniques is necessary.

A.2 Overview

The internet page http://www.cs.sandia.gov/opt/survey and the book of Pinter [107] give an overview of the global optimization techniques with their benefits, drawbacks and application area. All the techniques are used for solving problems of the following form:

$$\min f(x), \tag{A.1}$$

$$\begin{array}{ll} \text{subject to} & x \in [l,u], \\ \text{with} & [l,u] := \{x \in \mathbb{R}^n \mid l_i \leq x_i \leq u_i, i = 1, \cdots, n. \end{array}$$

In here f denotes the function to be minimized and x is a parameter or variable vector to be optimized with n parameters x_i. The search space is limited by the real vectors l and u. There exist a big variety of methods to solve this problem but the algorithms for solving global minimization problems can be classified into two main groups: heuristic methods that find the global minimum with a high probability and methods that guarantee to find a global optimum with a required accuracy [73].

A.2.1 Heuristic methods

A.2.1.1 Tabu search

This search method is based on the random choice of points in the search space. Moves are only made in directions which decrease the function value. In this way the method locates a local minimum. The movements are recorded in one or more Tabu lists. In a next iteration this local minimum is avoided by accepting poor solutions if it is to avoid a path already investigated.

At initialization the goal is to make a rough examination of the solution space, known as 'diversification', but as candidate locations are identified, the search is more focused to produce local solutions in a process of 'intensification'.

This method can be used for combinatorial optimization problems like integer programming problems and the travelling salesman, but can also be used for solving continuous functions.

A.2.1.2 Statistical algorithms

The basic idea of this method is that a statistical function can model the behavior of a particular objective function. If this is true the statistical function can be used to bias the selection of new sample points instead of choosing the points randomly. The results of these points can be used to update the parameters of the statistical function.

One of the challenging things of this method is the verification that the statistical model is appropriate for the function one wants to optimize. The method has its applications but is very complex to implement.

A.2.1.3 Evolutionary algorithms

Evolutionary algorithms (EAs) are derivative-free stochastic optimization methods based on the concepts of natural selection and evolutionary processes. EAs encode each point of the solution space into a binary bit string called a chromosome and each point is associated with a 'fitness' value which is usually equal to the objective function evaluated at the point. Instead of a single point, EAs keep a set of points as a population (gene pool) which is then evolved repeatedly toward a better overall fitness value. In each generation the EA constructs a new population using genetic operators such as crossover and mutation. Members with higher fitness values are more likely to survive and to participate in mating (crossover) operations. After a number of generations, the population contains members with better fitness values analogous to Darwinian models of evolution by random mutation and natural selection. EAs are sometimes referred to as methods of population-based optimization that improve performance by upgrading entire populations rather than individual members [77].

One of the strengths of EAs is that they perform well on 'noisy' functions. They don't get stuck in a local minima. EAs are being used both for continuous and discrete functions.

A.2.1.4 Clustering

The danger of multi-start methods is that many starting points may lead to the same local minimum. This gives rise to an inefficient global search. Using a clustering method helps to avoid this pitfall. Clustering method sample points in the search domain and group them around

the local minima. If the groups are identified successfully, the groups can be represented by one individual so redundant local searches can be avoided.

The technique is used for low dimensional functions with an inexpensive object function. It is useful in doing a preliminary investigation of the solution space before using e.g. EAs.

A.2.1.5 Simulated annealing

The principle behind simulated annealing (SA) is analogous to what happens when metals are cooled at a controlled rate. The slowly falling temperature allows the atoms in the molten metal to line themselves up and form a regular crystalline structure that has high density and low energy. But if temperature goes down too quickly the atoms do not have time to orient themselves into a regular structure and the result is a more amorphous material with higher energy.

In SA, the value of an objective function that we want to minimize, is analogous to the energy in a thermodynamic system. At high temperatures SA allows function evaluations at faraway points and it is likely to accept a new point with higher energy. This corresponds to the situation in which high-mobility atoms are trying to orient themselves with other nonlocal atoms and the energy state can occasionally go up. At low temperatures, SA evaluates the objective function only at local points and the likelihood of it accepting a new point with higher energy is much lower. This is analogous to the situation in which the low-mobility atoms can only orient themselves with local atoms and the energy state is not likely to go up again. The most important part of SA is the annealing schedule or cooling schedule, which specifies how rapidly the temperature is lowered from high to low values. This is usually application specific and requires some experimentation [77].

This type of optimization is suitable both in the continuous case as in the discrete one. A variant is called tree annealing and is more suitable for continuous functions.

A.2.2 Deterministic methods

A.2.2.1 Branch and Bound

If a function $f(x)$ has to be minimized over a certain feasible region, the Branch and Bound technique can be applied if one has the means

to compute a lower bound, an upper bound and there is a means to divide the feasible region up into smaller subproblems. The method starts by computing upper and lower bounds for the whole feasible region (the root problem). If the bounds match, the procedure terminates. Otherwise the region is divided in two or more strict subregions that partition the original region. The subproblems become children of the root. If a subproblem renders an optimal solution, which is not necessarily the global minimum, this solution is used to prune the tree of problems of regions that can't render the global minimum (if the lower bound on a region is higher than the optimal solution, it doesn't have to be investigated any more). The search proceeds until all the subregions in the tree have been pruned or solved, or until there is some specified threshold between the best solution found and the lower bounds on all unsolved subproblems.

All the other techniques in this section are closely related to the Branch and Bound technique.

A.2.2.2 Mixed-integer programming

The general structure of a mixed-integer program (MIP) is:

$$\min c^T x, \tag{A.2}$$

$$\begin{aligned} \text{subject to} \quad & A_1 x = b_1, \\ & A_2 x \leq b_2, \\ & l_i \leq x_i \leq u_i \text{ for } i = 1 \cdots n, \\ & x_j \text{ integer for all } j \in D \subset \{1 \cdots n\}, \\ & \text{where } A_1 \in \mathbb{R}^{m_1 \times n}, A_2 \in \mathbb{R}^{m_2 \times n}, m_1 + m_2 = m. \end{aligned}$$

Here A_1, A_2 and, b_1, b_2 and c denote respectively coefficient matrices and vectors. The T in the function to be minimized stands for transpose. j parameters can only have integer values and the minimization takes place with respect to m_1 equalities and m_2 inequalities. If all the variables can be rational ($D = \emptyset$), this is a linear programming problem which can be solved in polynomial time. However when some or all of the variables must be integer, called mixed or pure integer programming, the problem becomes NP-complete.

Most widely used method for solving integer programs is branch and bound. The problem is solved by creating subproblems by restricting

the range of the integer variables. Lower bounds are provided by the linear programming relaxation of the problem: keep the objective function and all constraints but relax the integrality restrictions to derive a linear program.

Also related techniques like Branch and Cut, Branch and Price are used, but they are closely related to the Branch and Bound technique.

Mixed integer programs can be used to formulate just about any discrete optimization problem: scheduling, vehicle routing, production planning, etc.

A.2.2.3 Mixed-integer nonlinear programming

The general form of a Mixed Integer Nonlinear Program (MINLP) is:

$$Z = \min C(y, x), \tag{A.3}$$

$$\begin{aligned} \text{subject to} \quad & h(y, x) = 0, \\ & g(y, x) < 0, \\ & \text{with } y \in \{0, 1\}^m, x \in \mathbb{R}^n. \end{aligned}$$

Engineering design problems often are MINLP problems, since they involve choosing a configuration, which component will be used and which will be omitted (binary y), but also a design of the components and the optimization of design parameters (continuous x, perhaps nonlinear). Again the optimization takes place with respect to certain equalities h and inequalities g. The solution is based on the Branch and Bound technique.

A.2.2.4 Interval methods

Interval techniques are used to compute global information about functions over large regions e.g. strict bounds on function values, Lipschitz constants, etc. Branch and Bound techniques divide the search space up into a collection of boxes for which the lower bound on the objective function is calculated by an interval technique. Interval methods are a sort of a slave to Branch and Bound.

A.3 DIRECT

A.3.1 Introduction

The models in this thesis were all developed using Matlab [92]. Therefore optimization methods were searched which had already an implementation in Matlab. There were two methods available. First the Genetic Algorithm OpTimization toolbox (GAOT) developed by Houch et al. [70] was used, but due to lack of computing power, which can be the case when using Genetic Algorithms [55, 113], this was abandoned quite fast. Instead the glbSolve algorithm was used. It is the Matlab implementation by Björkman and Holmström [12] of DIRECT, a branch and bound algorithm described in a paper by Jones et al. [78]. Direct, *di*viding *rect*angles, stands for a method bases on Lipschitzian Optimization without Lipschitz Constants and this will be explained in the following sections.

A.3.2 Lipschitzian optimization

Direct is an algorithm for finding the global minimum of a multivariate function subject to simple bounds. The algorithm is a modification of the standard Lipschitzian approach. This method assumes that for a function defined on the interval $[l, u]$, there exists a finite bound, K, on the rate of change of the function. K is called the Lipschitz constant and satisfies the following equation:

$$\mid f(x) - f(x') \mid \leq K \mid x - x' \mid, \text{ for all } x, x' \in [l, u]. \tag{A.4}$$

This assumption can be used to compute a lower bound on the function in any closed interval whose endpoints have been evaluated. Figure A.1 illustrates this.

Substituting a and b for x' in equation A.4 renders the inequalities A.5 and A.6 which show up in figure A.1 as lines.

$$f(x) \geq f(a) - K(x - a). \tag{A.5}$$

$$f(x) \geq f(b) + K(x - b). \tag{A.6}$$

The intersection, given by equations A.7 and A.8, renders the lower bound for the function in the interval.

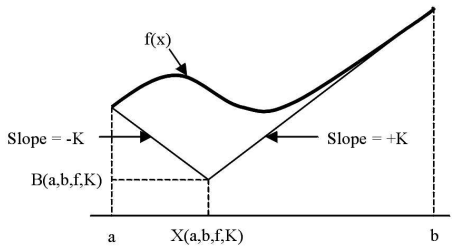

Figure A.1: Technique for bounding the function

$$X(a,b,f,K) = (a+b)/2 + [f(a) - f(b)]/(2K). \tag{A.7}$$

$$B(a,b,f,K) = [f(a) + f(b)]/2 - K(b-a)/2. \tag{A.8}$$

This point serves also as splitting point. After evaluation of the function in $X(a,b,f,K)$, a lower bound for the two new intervals can be computed. The lowest B-value is used as splitting point and the procedure of finding lower bounds starts again. The algorithm stops if the new lower bound is within some pre-specified tolerance of the current best solution. The procedure can be seen in figure A.2

Each lower bound is the sum of two terms $[f(a) + f(b)]/2$ and $-K(b-a)/2$. The first term is lower when the function values of the endpoints are low, thus this term leads to select intervals where previous function evaluations have been good and promotes in this way local search. The second term is lower, the bigger the interval is. This leads to exploring uncovered areas, so to global search. The Lipschitz constant K serves as a relative weight on global versus local search.

The description of this method points out the disadvantages and the problems. First of all, how is it possible to specify the Lipschitz constant for e.g. a complicated function? Secondly, K must be an upper bound on the rate of change of the function, so it will be generally quite high, resulting in slow convergence. A third problem is the computational complexity of the method. To get started one must evaluate the function in the vertices. One dimensional problems don't

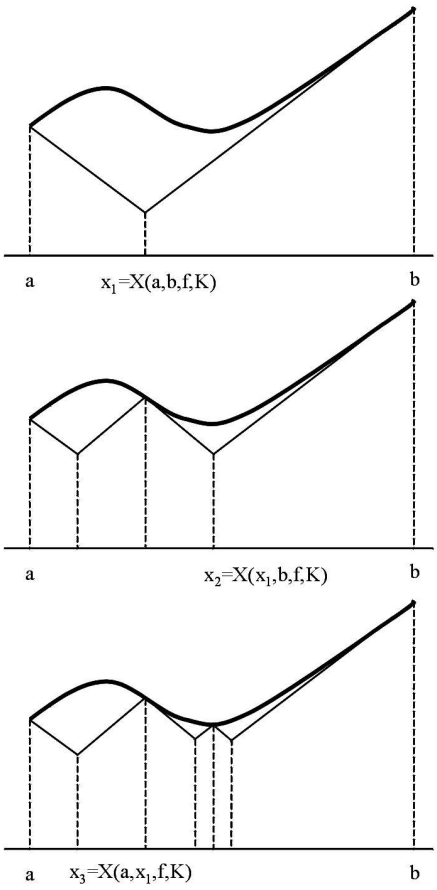

FIGURE A.2: Procedure for finding the optimum

give difficulties, but searching in an n dimensional space implies 2^n function evaluations to initialize the method. For selecting a new splitting point, one has to solve several systems of n equations with $n+1$ unknowns.

A.3.3 DIRECT algorithm

To overcome these difficulties, the DIRECT algorithm was developed. The method evaluates the function at the center of a new interval instead of at the vertices, so initialization is done by evaluating one point.

The calculation of the lower bound changes. It uses the center $c = (a + b)/2$. Setting x' equal to c in equation A.4, $f(x)$ must satisfy the following inequalities:

$$f(x) \geq f(c) + K(x - c), \text{ for } x \leq c, \tag{A.9}$$

$$f(x) \geq f(c) - K(x - c), \text{ for } x \geq c. \tag{A.10}$$

This leads to a lower bound of:

$$\text{lower bound } = f(c) - K(b - a)/2, \tag{A.11}$$

Figure A.3 shows the lines represented by the two equations A.9 and A.10 and the lower bound, equation A.11.

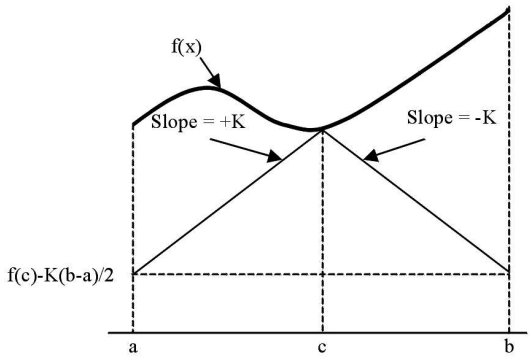

Figure A.3: DIRECT version of finding a lower bound

To maintain the property of using the center of the intervals, the interval is divided into thirds. The original center becomes the center of a smaller interval. This solves the problem of complexity.

To solve the problem of the Lipschitz constant, suppose as starting point a search space partitioned up in the intervals $[a_i, b_i]$, i=1,. . . ,m.

A decision has to be made which interval(s) in the search space have to be sampled further.

In figure A.4 each dot has as vertical coordinate $f(c_i)$ and as horizontal $(b_i - a_i)/2$. The horizontal coordinate captures the goodness of the global search, that is, goodness based on the amount of unexplored territory in the interval, while $f(c_i)$ captures the goodness with respect to the local search.

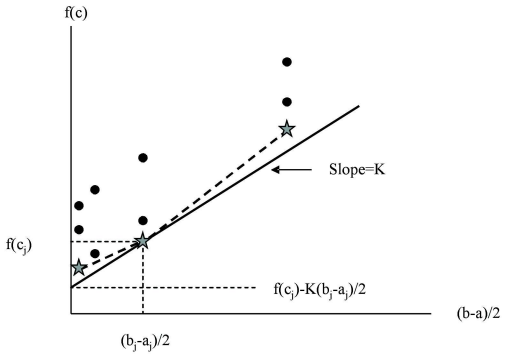

FIGURE A.4: Selection of intervals which might contain the global minimum

In figure A.4 it is very simple to find the lower bound for a certain Lipschitz constant K. Plot a line with slope K in the figure and the lower bound is the intersection with the Y-axis. If the K is large, the selection is tending to large intervals. If K is small, the emphasis lays on intervals with low $f(c_i)$. So K once again acts as a weighting parameter between the global and local search.

Instead of choosing one Lipschitz value, the method uses all available values for K and splits all those intervals which have the lowest bound for a certain K. Those intervals are indicated by stars in figure A.4.

This is the strength of the method. A Lipschitz constant doesn't have to be specified and the method itself takes care of the weight between local and global search. In the paper [78] it is proven that the DIRECT method guarantees to converge to the global optimum if the objective function is continuous in the neighborhood of the optimum.

A.4 Conclusion

This appendix gives an overview of methods of global optimization and describes in-depth the ,in Matlab implemented, bound and branch technique called DIRECT. This technique is successfully used in the thesis to optimize the free parameters of the developed suspension system.

Appendix B

Semi-Active Suspension

This appendix shows the effect of using semi-active control laws in the design of the cab suspension system. This appendix has not the intention to fully develop a semi-active cab suspension, but wants to show the potential benefits semi-active control laws can provide in this case.

B.1 Introduction

A classical quarter car passive suspension always has to negotiate a delicate equilibrium between improving the comfort by reducing the vibrations the passengers are exposed to and keeping good road holding capabilities of the car by minimizing the variation of forces in the tire as mentioned earlier in chapter 2. Semi-active suspensions present a means to solve or at least reduce this conflict [51]. In the design of the cabin suspension this conflict is not present. Nevertheless the effect of using a semi-active approach is investigated in this appendix.

Semi-active suspensions, as their name implies, fill the gap between purely passive and purely active suspensions. A conventional passive parallel spring-damper suspension provides a damping force proportional to the relative velocity between the isolated mass and the moving base. Active systems use force generators to reduce the vibrations of the mass. These force generators are generally complex, inefficient and limited in frequency response. With their necessary power supplies, they tend to be much more expensive, bulky, massive and delicate than passive elements [79].

This lead to the consideration of semi-active dampers. The idea is to modulate the dissipation in a basically passive damper as a function of sensed variables such as mass velocities. The amount of power needed in this systems is restricted to the energy needed to change the properties of the passive damper. Special dampers like electro- and magneto-rheological types are very apt to perform as semi-active dampers and can therefore be found in many vibration control applications [21, 94].

From a performance point of view, semi-active suspension systems are an improvement over passive solutions but cannot completely imitate the behavior of active suspensions due to the lack of an external energy source [48]. In this way they represent a compromise between performance improvement and simplicity of implementation [71]. This, together with economic factors, make semi-active suspension favored over fully active ones [42]. Therefore it is no surprise that since its introduction in [80], the semi-active concept has been applied to a broad class of vibration isolation problems [90, 130].

B.2 Design of the semi-active suspension

B.2.1 Suspension model

The semi-active suspension in this appendix is build around the base motion quarter-cabin model of the hydro-pneumatic SISO suspension, developed in chapter 4. Within this model several parameters are variable: internal pressures, nitrogen volumes, dimensions (stroke, diameter of rod and cylinder) of the cylinder and the opening of the valve. These parameters, with exception of the cylinder dimensions, were optimized in chapter 6 to design the optimum passive suspension system with respect to comfort improvement.

This hydro-pneumatic suspension system can very easily be converted from passive to semi-active. For the model this means adding a semi-active control law according to which the valve opening is changed. In this way the damping in the suspension becomes variable. In practice this would mean using a hydraulic valve that changes its opening according to a semi-active control law.

Not only is conversion to a semi-active system simple with the hydro-pneumatic suspension, the damping the resulting suspension provides can range from a few Ns/m to infinity (when the valve is

closed). The reason for that is that the damping takes place in the hydraulic fluid of the suspension which is under normal circumstances incompressible.

The optimized passive hydro-pneumatic suspensions of chapter 6 will serve as a basis of comparison in this appendix.

B.2.2 Semi-active control laws

Two fairly straightforward semi-active control laws are used for this suspension. Those laws were found in a paper by Ferraresi et al. [48] and are an adaptation of the rules for the semi-active sky-hook found in the paper of Karnopp et al. [80]. Instead of making the damping force proportional to the absolute output velocity of, in this case, the cabin that has to be controlled, the relative velocity between cabin and base also comes into play.

The semi-active damping force is only active when the relative velocity between the base and the cab have the same sign as the absolute velocity of the cab. This, because in the other case (opposite signs) the damping force deteriorates the vibrations. This is also the reason why, when no damping force is demanded, the damping in the system should be as low as possible. This can be taken care off by reducing the number of bends, corners and constrictions in the tubes in which the oil is flowing to a minimum and providing a valve with a big orifice, since it are the energy losses in those instances that create the damping in the suspension.

In the first law the semi-active part of the damping force is proportional to the relative velocity between the input and the output, respectively at the base and at the cabin and proportional to the absolute output velocity of the cabin. The law, semi-active (1), is given by:

$$F_D = \begin{cases} -\beta(\dot{y}-\dot{x}) - \beta_{SA}|\dot{y}|(\dot{y}-\dot{x}) & \text{for } \dot{y}(\dot{y}-\dot{x}) > 0 \\ -\beta(\dot{y}-\dot{x}) & \text{for } \dot{y}(\dot{y}-\dot{x}) < 0 \end{cases} \tag{B.1}$$

in which F_D is the damping force, $\dot{x}$ the input velocity, $\dot{y}$ the output velocity entering the cabin, β the damping constant of the passive part of the damping force and β_{SA} the damping constant of the semi-active part. The value of β depends on the construction of the suspension while β_{SA} depends on the characteristics of the valve.

The second law, semi-active(2), increases the importance of the absolute velocity by squaring it, resulting in:

$$F_D = \begin{cases} -\beta(\dot{y}-\dot{x}) - \beta_{SA}\dot{y}^2(\dot{y}-\dot{x}) & \text{for } \dot{y}(\dot{y}-\dot{x}) > 0 \\ -\beta(\dot{y}-\dot{x}) & \text{for } \dot{y}(\dot{y}-\dot{x}) < 0 \end{cases} \tag{B.2}$$

Both semi-active control laws are applied to the model of the hydropneumatic suspension.

B.2.3 Optimization

To determine the value of β_{SA} in both control laws, the procedure of chapter 6 is used. Instead of optimizing the parameters of the hydropneumatic suspension, the parameter of the control law is optimized. Here it has been done by calculating the β_{SA} that minimized the VDV when in-situ measurements corresponding with conditions IX, XIV and XVIII, respectively harvesting at $4km/h$, transport on unpaved road at $11km/h$ and transport on a paved road at $28km/h$, are applied to the semi-active suspensions.

B.3 Results

The results shown in this appendix are adaptations from papers [28, 30, 29] which describe the use of semi-active control laws in the base motion quarter-cabin suspension. Table B.1 gives a resume of the obtained results.

Looking at the results of the passive suspension one sees clearly that a reduction by almost 80% in VDV is possible on the paved road. Similar reductions can be found looking at the values for the unpaved road and the field. The semi-active control laws improve these results even with a factor 3 and higher. The first semi-active control law is slightly better than the second one. Overemphasizing the absolute velocity is in this case not a benefit.

Calculating the time to reach the daily exposure limit of $9.1m/s^{1.75}$ given in European Regulation (see section 2.1.4), the results are even more spectacular. Without a suspension, this level is reached on the field after 45 minutes, on the unpaved road at approximately 3 hours and on the paved road within 15 minutes. The passive and semi-active suspension change these values to several days of non-stop driving.

input profile	suspension	VDV $[m/s^{1.75}]$
field($4km/h$)	non	4.108
	passive	1.022
	semi-active(1)	0.121
	semi-active(2)	0.128
unpaved road ($11km/h$)	non	3.049
	passive	1.073
	semi-active(1)	0.279
	semi-active(2)	0.381
paved road ($28km/h$)	non	5.606
	passive	1.132
	semi-active(1)	0.340
	semi-active(2)	0.519

TABLE B.1: Calculated Vibration Dose Values for different road profiles using different suspension systems

Some remarks are in place concerning these results. The values are obtained for a model of a suspension system. For the passive system, effort has been put in the modelling of the suspension therefore these results will get close to the practical achievable results. For the semi-active suspension however, no model of a valve has been introduced. This means that the bandwidth of the valve is assumed to be infinite, with immediate change of damping in the system upon demand. Since this speed of action is crucial to get rid of damping forces that enlarge the vibrations, it remains to be seen if a practical realization of these semi-active suspensions will improve the vibrations well enough to be an economical sound alternative for the passive suspension system.

Figure B.1 gives a visual impression of the potential of these suspension systems. The maximal accelerations experienced on a paved road shift from above $10m/s^2$ when no suspension is used, over $5m/s^2$ for the passive suspension to below $0.5m/s^2$ for the first semi-active suspension system.

B.4 Conclusion

This appendix discussed the use of semi-active control laws in the design of a cab suspension for a combine harvester. On a model of a

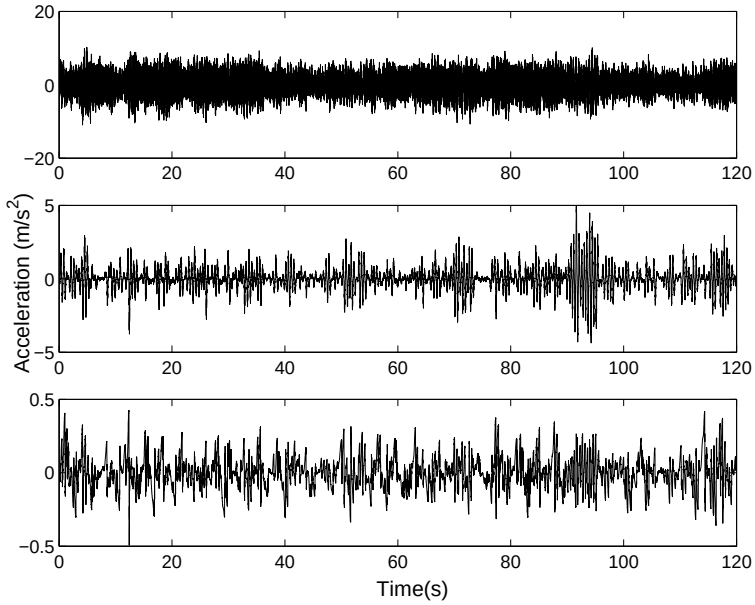

Figure B.1: Simulation of the accelerations on the road using: no suspension (top figure), a passive suspension (middle figure), the first semi-active suspension (bottom figure)

hydro-pneumatic suspension, reduction of Vibration Dose Values up to 90% were observed. This substantial reduction proves that a semi-active cab suspension can be used to improve the vibrational comfort conditions of the operator of this and other agricultural machines.